

Ultrasonography of the Upper Extremity: Elbow

Ferdinando Draghi

 Springer

Ultrasonography of the Upper Extremity: Elbow

Ferdinando Draghi

Ultrasonography of the Upper Extremity: Elbow

 Springer

Ferdinando Draghi
University Hospital
Foundation IRCCS, Policlinico San
Matteo University Hospital
Pavia
Italy

ISBN 978-3-319-77340-7 ISBN 978-3-319-77341-4 (eBook)
<https://doi.org/10.1007/978-3-319-77341-4>

Library of Congress Control Number: 2018939148

© Springer International Publishing AG, part of Springer Nature 2018

This work is subject to copyright. All rights are reserved by the Publisher, whether the whole or part of the material is concerned, specifically the rights of translation, reprinting, reuse of illustrations, recitation, broadcasting, reproduction on microfilms or in any other physical way, and transmission or information storage and retrieval, electronic adaptation, computer software, or by similar or dissimilar methodology now known or hereafter developed.

The use of general descriptive names, registered names, trademarks, service marks, etc. in this publication does not imply, even in the absence of a specific statement, that such names are exempt from the relevant protective laws and regulations and therefore free for general use.

The publisher, the authors and the editors are safe to assume that the advice and information in this book are believed to be true and accurate at the date of publication. Neither the publisher nor the authors or the editors give a warranty, express or implied, with respect to the material contained herein or for any errors or omissions that may have been made. The publisher remains neutral with regard to jurisdictional claims in published maps and institutional affiliations.

Printed on acid-free paper

This Springer imprint is published by the registered company Springer International Publishing AG part of Springer Nature
The registered company address is: Gewerbestrasse 11, 6330 Cham, Switzerland

Preface

This volume *Ultrasonography of the Upper Extremity: Elbow* represents a continuation, with the same intentions, of *Ultrasonography of the Upper Extremity: Hand and Wrist*. I decided, in fact, to create this second volume because constant and rapid technological progress has led to incredible progress in the use of ultrasound for the diagnosis of diseases of the musculoskeletal system, particularly of some areas such as the elbow. The changing science has forced those who practice osteoarticular ultrasound to rapidly increase their knowledge. I then tried to write a monograph useful for people who are just beginning to learn about the topic as well as for people who already have experience in the area, in an attempt to make a complex topic—that is the ultrasound of the elbow—easier to understand.

The monograph consists of two parts that are each four chapters in length: a general part (introduction, anatomy, examination techniques and ultrasound appearance and pathology) and a second part that describes the study of elbow ultrasound based on topography (the anterior aspect: muscle and distal bicep tendon, brachial muscle and tendon, bicipitoradial and interosseous bursae, median nerve, radial nerve and coronoid recess; the lateral aspect: common extensor tendon and lateral collateral ligament; the medial aspect: common flexor tendon, medial collateral ligament and ulnar nerve; the posterior aspect: triceps muscle and tendon, olecranon bursa and synovial recess).

The first part, which is aimed primarily at people who are beginning to learn about the topic, includes schematic anatomical diagrams, ultrasound images compared with magnetic resonance images (MRI is more panoramic and, therefore, easier to understand) and images of models to clarify the correspondence between anatomical sites and ultrasound images. The fourth chapter (pathology) addresses pathologies according to the structures involved, tendons, muscles, nerves, synovium and bone, and it highlights the advantages and limitations of ultrasound compared to other diagnostic imaging, particularly traditional radiology and MRI.

The second part is dedicated to experts in osteoarticular ultrasound. It describes the various pathologies of the districts of the elbow, as well as specific aspects such as the evaluation of therapeutic results of pathologies of the tendons and nerves.

Even for this second monograph, I tried to focus on creating text that is of practical value. I hope I have succeeded and that the monograph is useful to readers. Enjoy the reading.

Pavia, Italy

Ferdinando Draghi

Contents

1 Introduction	1
References	7
2 Anatomy	9
References	15
3 Examination Techniques and Ultrasound Appearance	17
References	26
4 Pathology	29
References	39
5 Anterior Elbow	41
References	46
6 Lateral Elbow	47
References	51
7 Medial Elbow	53
References	58
8 Posterior Elbow	61
References	70
Index	73
Author Index	77

Content Overview

Elbow joints

- Humero-radial joint
- Humero-ulnar joint
- Proximal radio-ulnar joint

Joint capsule

Joint synovium

Joint recesses

Elbow fat pads

Collateral ligament

- Medial collateral ligament
- Lateral collateral ligament

Elbow muscles

- Anterior group
- Lateral group
- Medial group
- Posterior group

Elbow bursae

- Olecranon bursa
- Bicipitoradial bursa

Elbow nerves

- Ulnar nerve
- Median nerve
- Radial nerve

The elbow consists of three different joints: the humero-radial (between the radial head and the capitellum of the humerus) (Fig. 1.1a, b), the humero-ulnar (between the ulnar trochlear notch

and the trochlea of the humerus) (Fig. 1.1c, d), and the proximal radio-ulnar joint (Fig. 1.1e, f). Combined, these articulations create a trochleoginglymoid joint with a range of motion of approximately 0° of extension and 140° of flexion; supination and pronation are both approximately 80°.

These three joints share a common capsule and a common joint space [1–5]. The joint space has two main recesses, the anterior and the posterior, also known as the coronoid and olecranon recesses (Fig. 1.2). With elbow in flexion fluid is collected posteriorly and, only when in larger quantities, anteriorly; the identification of 1–3 mL of fluid is possible with sonography, posteriorly with the elbow flexed.

Three fat pads are present in the elbow, interposed between the joint capsule and the synovium; therefore, intracapsular and extrasynovial (Fig. 1.3) [6, 7].

The anterior fat pads are the summation of two fat masses. During extension, this rests in the radial and coronoid fossae, applied close to bone by the overlying brachialis muscle, while it is highly mobile during flexion.

The posterior fat pad is highly mobile during extension, while it rests in the olecranon fossa during flexion, applied close to the bone by the overlying triceps tendon. Distension of the synovium elevates the fat pads (Fig. 1.4), providing the basis for the fat pad sign [8].

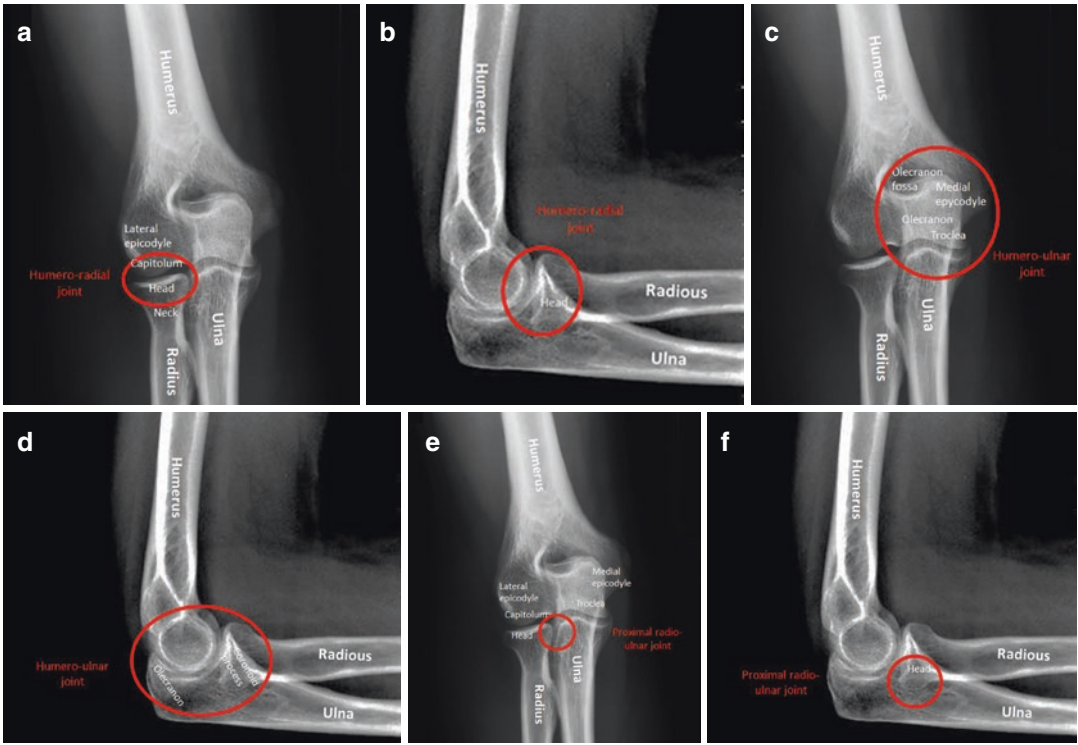


Fig. 1.1 Schematic diagram of the elbow joint. This joint consists of three different joints: humero-radial, between the radial head and the capitellum of the humerus (a, b),

humero-ulnar, between the ulnar trochlear notch and the trochlea of the humerus (c, d), and the proximal radio-ulnar joint (e, f)

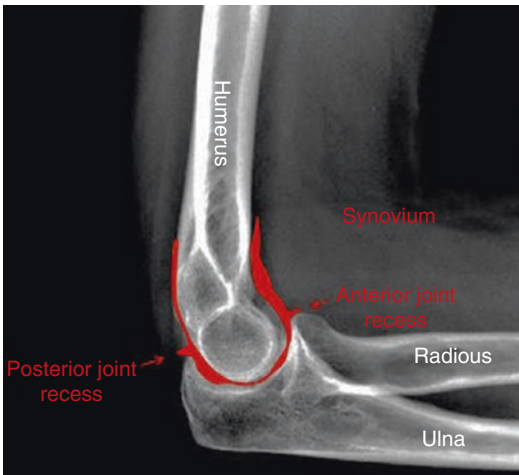


Fig. 1.2 Schematic diagram of the elbow synovium. The three elbow joints share a common synovium, with two main recesses the anterior and the posterior, also known as coronoid and olecranon recesses

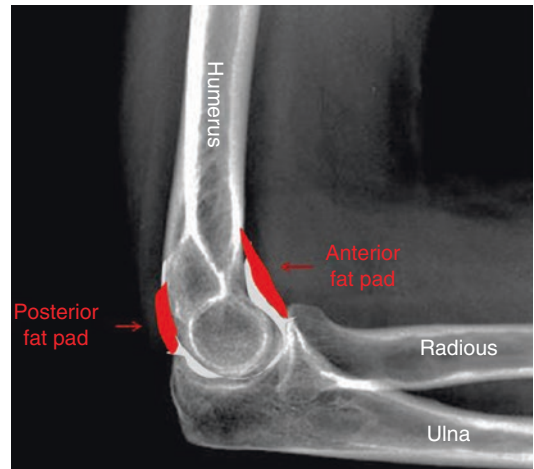


Fig. 1.3 Schematic diagram of the elbow fat pads. Between the articular capsule and synovium there are three fat pads, two anterior and one posterior. The summation of the two anterior fat masses forms the anterior fat pad. Their function of the fat pads is to fluidify elbow movement

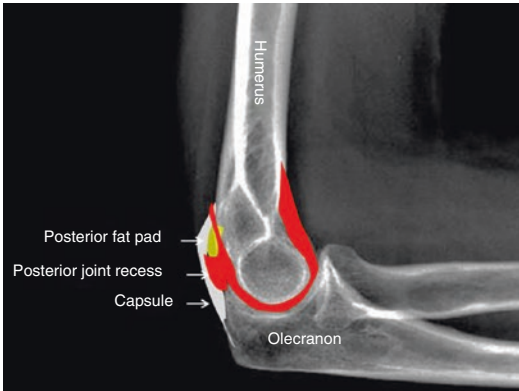


Fig. 1.4 Schematic diagram of the elbow effusion with fat pad dislocation. When effusion is present, the fat pads are displaced superiorly, particularly the posterior

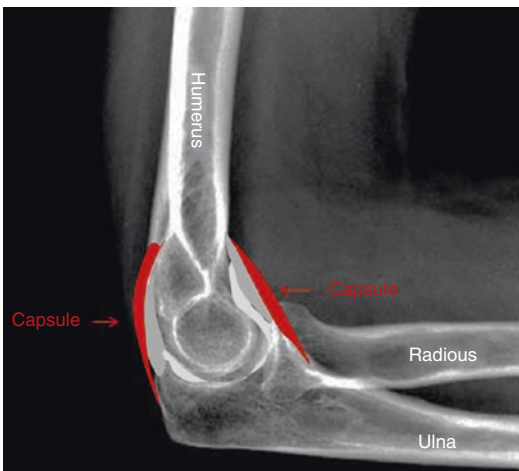


Fig. 1.5 Schematic diagram of the joint capsule. The joint capsule surrounds the synovium and fat pads. The anterior capsule inserts proximally above the coronoid and radial fossas, distally in the anterior margin of the coronoid process and in the annular ligament laterally. The posterior capsule inserts proximally above the olecranon fossa and distally at the annular ligament and the olecranon

The joint capsule surrounds all three elbow joints [1, 2]. The anterior capsule inserts proximally above the coronoid and radial fossas, distally in the anterior margin of the coronoid process and laterally in the annular ligament. The posterior capsule inserts proximally above the olecranon fossa, and distally at the annular ligament and the olecranon (Fig. 1.5).

The medial and lateral collateral ligament complexes are primary elbow stabilizers (Table 1.1) [9–12].

Table 1.1 Static and dynamic constraints of the elbow

Static constraint (passive elbow stabilizers)	Osteoarticular anatomy
	Medial and lateral collateral ligament complexes
	Capsule
Dynamic constraint (active elbow stabilizers)	Muscles

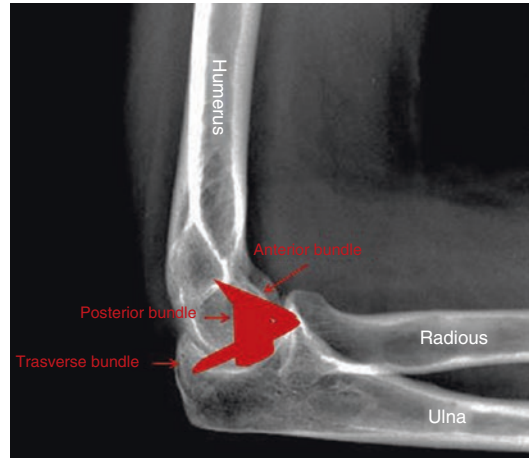


Fig. 1.6 Schematic diagram of medial collateral ligament. The medial collateral ligament complex consists of three bundles: anterior, posterior, and transverse. The anterior bundle is the most significant component being the main stabilizer to valgus stress of the elbow. The transverse bundle offers little contribution to elbow stability due to its origin and insertion, both on the ulna

The medial collateral ligament complex consists of three bundles: anterior, posterior, and transverse (Fig. 1.6). The anterior bundle is the most significant component, being the main stabilizer to valgus stress of the elbow. Its origin is at the anterior–inferior medial epicondyle and inserts into the sublime tubercle of the coronoid process. The anterior band is taut in extension and relaxes in flexion.

The posterior band originates in the posterior and distal aspects of the medial epicondyle and inserts into the medial olecranon.

The posterior band is taut at intermediate positions and relaxed in extension.

The transverse bundle origin is on the tip of the olecranon and it inserts into the coronoid process. The transverse bundle offers little contribution to elbow stability due to its origin and insertion, both on the ulna.

The lateral collateral ligament complex (Fig. 1.7) consists of three components: the radial collateral ligament, the lateral ulnar collateral ligament, and the annular ligament; an accessory collateral ligament is also described.

The radial collateral ligament “proper” extends from the inferior aspect of the lateral epicondyle and inserts with the fibers of the annular ligament.

The lateral ulnar collateral ligament originates more posteriorly, extending to the supinator crest of the ulna. The lateral ulnar collateral ligament plays a major role in stabilizing against varus stress.

The annular ligament encircles the radial head, attaching to the radial notch of the ulna. It serves to maintain radial head articulation with the ulna. The accessory lateral collateral ligament is variably present.

Four muscle compartments surround the elbow joint (Table 1.2): anterior (Fig. 1.8a), lateral (Fig. 1.8a), medial (Fig. 1.8a), and posterior (Fig. 1.8b) [5].

The anterior flexor group consists of the brachialis and biceps brachii muscles.

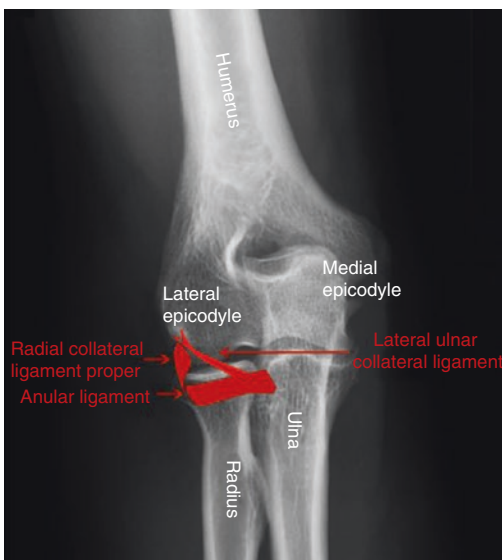


Fig. 1.7 Schematic diagram of the lateral collateral ligament. The lateral collateral ligament complex consists of three components: the radial collateral ligament, the lateral ulnar collateral ligament, and the annular ligament. The lateral ulnar collateral ligament has the major role in constraining varus stress

Table 1.2 Function of the elbow muscles

Muscle	Function
Biceps brachii	Elbow flexion Forearm supination
Brachialis	Elbow flexion
Pronator teres	Elbow flexion Forearm pronation
Palmaris longus, flexor carpi radialis, flexor digitorum superficialis, flexor carpi ulnaris	Elbow joint stabilization
Flexor digitorum profundus	Elbow joint stabilization
Triceps brachii	Elbow extension
Anconeus	Elbow extension
Brachioradialis	Elbow flexion
Extensor carpi radialis brevis, extensor digitorum communis, extensor digiti minimi, extensor carpi ulnaris	Elbow joint stabilization
Extensor carpi radialis longus	Elbow joint stabilization
Supinator	Elbow flexion Forearm supination

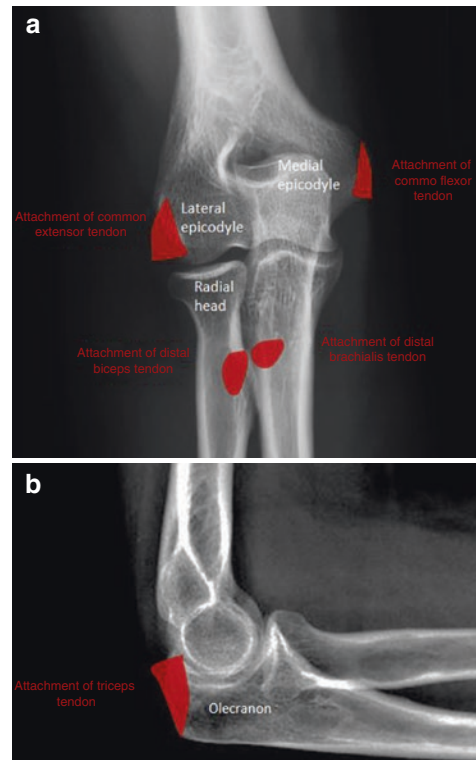


Fig. 1.8 Schematic diagram of muscle. Four muscle compartments surround the elbow joint: anterior, lateral, medial, and posterior. The anterior flexor group consists of the brachialis and biceps brachii muscles (a). The lateral muscle group includes the extensors of the wrist and of the hand (a). The medial muscle group includes the flexor muscles (a), and the posterior includes the triceps (b)

The lateral muscle group includes the extensors of the wrist and hand, as well as the supinator and brachioradialis muscles. The common extensor tendon consists of tendon fibers from the extensor carpi radialis brevis, extensor digitorum, extensor digiti minimi, and extensor carpi ulnaris.

Medially, the flexor muscles group consists of flexor carpi radialis, palmaris longus, flexor carpi ulnaris, flexor digitorum superficialis, and pronator teres muscles.

The posterior extensor muscle group consists of the triceps and anconeus muscles.

There are several bursae present at the elbow joint. A bursa is an extra-articular structure that functions to decrease friction between tendons, bone, skin, etc. [13]. Bursae can be classified as native and non-native (adventitious) bursae [14]. In the elbow, the most frequently affected by disease are the olecranon and the bicipitoradial bursae.

The olecranon bursa (Fig. 1.9a) is located between the olecranon process and the subcutaneous tissues [14–20].

The bicipitoradial bursa is located at the distal biceps insertion into the radial tuberosity. This bursa is subtendinous in position, lying between the biceps insertion and the underlying radius (Fig. 1.9b) [21–25].

At the elbow joint, the main nerve trunks, ulnar, median, and radial nerves, are all in a superficial position [25, 26] and the superficial seat explains why traumatic lesions of the nerves in the elbow are frequent [3, 27–30].

The ulnar nerve (Fig. 1.10) traverses the elbow along a groove on the postero-medial aspect of

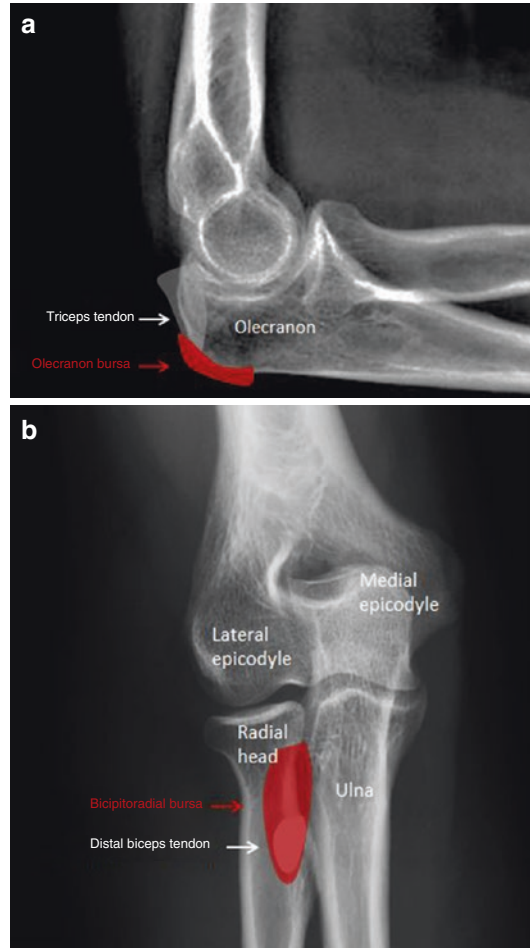


Fig. 1.9 Schematic diagram of the main elbow bursae. The olecranon bursa (a) is located between the olecranon process and the subcutaneous tissues. The bicipitoradial bursa (b) is located at the distal biceps insertion onto the radial tuberosity



Fig. 1.10 Schematic diagram of the ulnar nerve in the elbow. The ulnar nerve traverses the elbow along a groove on the postero-medial aspect of the humerus (cubital tunnel), at the level of the medial epicondyle. The Osborne's ligament forms the ceiling of the cubital tunnel

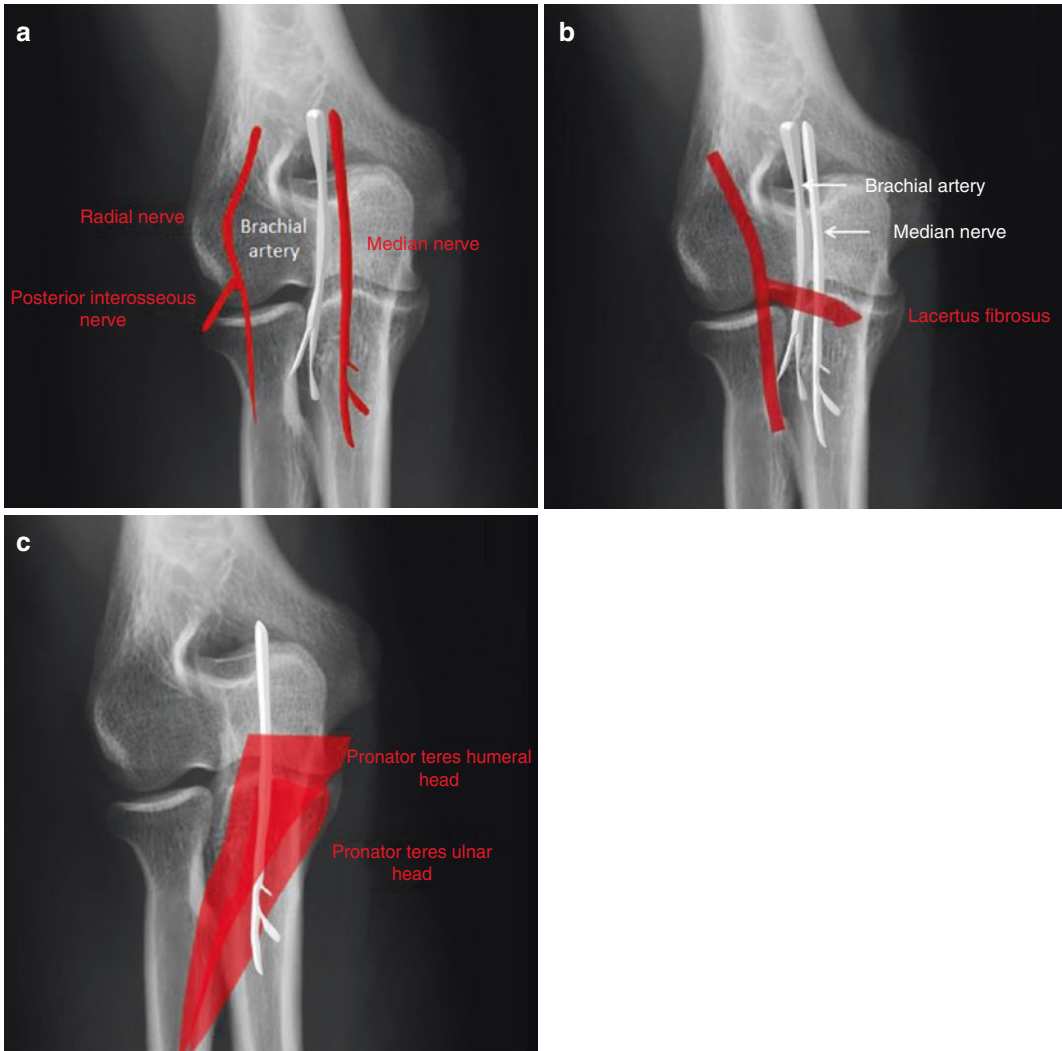


Fig. 1.11 Schematic diagram of median nerve in the elbow. The median nerve, in the antecubital fossa, is medial to the brachial artery (a), beneath the bicipital apo-

neurosis (b), prior to its distal course between the heads of the pronator teres muscle (c)

the humerus, at the level of the medial epicondyle, the so-called cubital tunnel. The cubital tunnel is delimited by the olecranon and the medial epicondyle and bridged by the cubital tunnel retinaculum (Osborne's ligament).

The median nerve (Fig. 1.11) is anteriorly in the antecubital fossa, medial to the brachial artery, beneath the bicipital aponeurosis, prior to its distal course between the heads of the pronator teres muscle.

The radial nerve (Fig. 1.12) lies in a groove between the brachialis and the brachioradialis muscles proximally and extensor carpi radialis distally, then divides into the superficial and the posterior interosseous branches. The posterior interosseous nerve lies between the superficial and deep portions of the supinator muscle.



Fig. 1.12 Schematic diagram of radial nerve in the elbow. The radial nerve lies in the elbow and divides into the superficial and the posterior interosseous branches. The posterior interosseous nerve lies between the superficial and deep portions of the supinator muscle

References

- Konin GP, Nazarian LN, Walz DM. US of the elbow: indications, technique, normal anatomy, and pathologic conditions. *Radiographics*. 2013;33(4):E125–47.
- Radunovic G, Vlad V, Micu MC, Nestorova R, Petranova T, Porta F, Iagnocco A. Ultrasound assessment of the elbow. *Med Ultrason*. 2012;14(2):141–6.
- Draghi F, Danesino GM, de Gautard R, Bianchi S. Ultrasound of the elbow: examination techniques and US appearance of the normal and pathologic joint. *J Ultrasound*. 2007;10(2):76–84.
- Tran N, Chow K. Ultrasonography of the elbow. *Semin Musculoskelet Radiol*. 2007;11(2):105–16.
- Finlay K, Ferri M, Friedman L. Ultrasound of the elbow. *Skelet Radiol*. 2004;33(2):63–79.
- Hamada D, Matsuura T, Sugiura K, Higuchi T, Suzue N, Goto T, Tsutsui T, Wada K, Fukuta S, Sairyu K. An unusual cause of posterior elbow impingement: detachment of a hypertrophied posterior fat pad. *Case Rep Orthop*. 2015;2015:121646.
- Draghi F, Ferrozzi G, Urciuoli L, Bortolotto C, Bianchi S. Hoffa's fat pad abnormalities, knee pain and magnetic resonance imaging in daily practice. *Insights Imaging*. 2016;7(3):373–83.
- Thornton R, Riley GM, Steinbach LS. Magnetic resonance is highly mobile imaging of sports injuries of the elbow. *Top Magn Reson Imaging*. 2003;14(1):69–86.
- Daniels DL, Mallisee TA, Erickson SJ, Boynton MD, Carrera GF. The elbow joint: osseous and ligamentous structures. *Radiographics*. 1998;18(1):229–36.
- Reichel LM, Milam GS, Sitton SE, Curry MC, Mehlhoff TL. Elbow lateral collateral ligament injuries. *Hand Surg Am*. 2013;38(1):184–201. quiz 201
- Borges NC, Weissengruber GE, Huber J, Kofler J. Ultrasonographic examination of the elbow region in calves and cows--normal appearance. *Berl Munch Tierarztl Wochenschr*. 2015;128(9-10):416–24.
- Yoshida M, Goto H, Takenaga T, Tsuchiya A, Sugimoto K, Musahl V, Fu F, Otsuka T. Anterior and posterior bands of the anterior bundle in the elbow ulnar collateral ligament: ultrasound anatomy. *J Shoulder Elb Surg*. 2017;26(10):1803–9.
- Ruangchaijatuporn T, Gaetke-Udager K, Jacobson JA, Yablon CM, Morag Y. Ultrasound evaluation of bursae: anatomy and pathological appearances. *Skelet Radiol*. 2017;46(4):445–62.
- Draghi F, Corti R, Urciuoli L, Alessandrino F, Rotondo A. Knee bursitis: a sonographic evaluation. *J Ultrasound*. 2015;18(3):251–7.
- Blankstein A, Ganel A, Givon U, Mirovski Y, Chechick A. Ultrasonographic findings in patients with olecranon bursitis. *Ultraschall Med*. 2006;27(6):568–71.
- Blackwell JR, Hay BA, Bolt AM, Hay SM. Olecranon bursitis: a systematic overview. *Should Elb*. 2014;6(3):182–90.
- Reilly D, Kamineni S. Olecranon bursitis. *J Shoulder Elb Surg*. 2016;25(1):158–67.
- Floemer F, Morrison WB, Bongartz G, Ledermann HP. MRI characteristics of olecranon bursitis. *Am J Roentgenol*. 2004;183(1):29–34.
- Del Buono A, Franceschi F, Palumbo A, Denaro V, Maffulli N. Diagnosis and management of olecranon bursitis. *Surgeon*. 2012;10(5):297–300.
- Patel J, Girishkumar, Mruthyunjaya, Rupakumar CS. Bilateral olecranon bursitis - a rare clinical presentation of calcium pyrophosphate crystal deposition disease. *J Orthop Case Rep*. 2014;4(1):3–6. <https://doi.org/10.13107/jocr.2250-0685.137>.
- Skaf AY, Boutin RD, Dantas RW, Hooper AW, Muhle C, Chou DS, Lektrakul N, Trudell DJ, Haghghi P, Resnick DL. Bicipitoradial bursitis: MR imaging findings in eight patients and anatomic data from contrast material opacification of bursae followed by routine radiography and MR imaging in cadavers. *Radiology*. 1999;212(1):111–6.
- Draghi F, Gregoli B, Sileo C. Sonography of the bicipitoradial bursa: a short pictorial essay. *J Ultrasound*. 2012;15(1):39–41.
- Lui TH, Sit YK, Pan XH. Endoscopic resection of the bicipitoradial bursa. *Sports Med Arthrosc*. 2016;24(1):7–10.
- Bak B. Bicipitoradial bursitis. *Ugeskr Laeger*. 2008;170(40):3123–4.
- Chew ML, Giuffrè BM. Disorders of the distal biceps brachii tendon. *Radiographics*. 2005;25(5):1227–37.

26. Husarik DB, Saupe N, Pfirrmann CW, Jost B, Hodler J, Zanetti M. Elbow nerves: MR findings in 60 asymptomatic subjects--normal anatomy, variants, and pitfalls. *Radiology*. 2009;252(1):148–56. <https://doi.org/10.1148/radiol.2521081614>.
27. Gregoli B, Bortolotto C, Draghi F. Elbow nerves: normal sonographic anatomy and identification of the structures potentially associated with nerve compression. A short pictorial-video article. *J Ultrasound*. 2013;16(3):119–21.
28. Alessandrino F, Pagani C, Draghi F. In-continuity neuroma of the median nerve at the elbow. *J Ultrasound*. 2014;17(3):229–31.
29. Padua L, Di Pasquale A, Liotta G, Granata G, Pazzaglia C, Erra C, Briani C, Coraci D, De Franco P, Antonini G, Martinoli C. Ultrasound as a useful tool in the diagnosis and management of traumatic nerve lesions. *Clin Neurophysiol*. 2013;124(6):1237–43.
30. Bianchi S, Draghi F, Beggs I. Ultrasound of the peripheral nerves. In: *Clinical ultrasound*, vol. 2. Philadelphia: Elsevier; 2011. p. 1158–67.

Content Overview

Articular bones

- Humerus
- Ulna
- Radius

Articular cartilage

Joint synovium

Joint capsule

Elbow fat pads

Collateral ligament

- Medial collateral ligament
- Lateral collateral ligament

Elbow muscles

- Anterior group
- Lateral group
- Medial group
- Posterior group

Elbow bursae

- Olecranon bursa
- Bicipitoradial bursa

Elbow nerves

- Ulnar nerve
- Median nerve
- Radial nerve

The elbow can be simplified to a joint between the distal humerus and proximal ulna and radius [1, 2] (Figs. 2.1 and 2.2). The articular surfaces of the humerus are formed of two components: the trochlea and the capitellum, which articulate with

the ulna and radius, respectively (Fig. 2.1). The trochlea articulates with the ulna and is covered by articular cartilage over an arc of 300°. The radial head articulates with both the radial notch of the ulna and the capitulum of the humerus. Articular cartilage covers the concave surface of the radial head and an arc of 280° of the rim. The proximal ulna consists of the olecranon and the anterior surface of the ulnar notch (Fig. 2.2). The notch is covered by articular cartilage, except for the mid portion, which is usually covered by fatty tissue. The distal end of the ulnar notch is the coronoid process.

Just proximal to the condyles, there are three fossae uncovered from articular cartilage: anteriorly, the coronoid and radial, which accommodate the coronoid process of the ulna and radial head, respectively, during elbow flexion, and posteriorly, the olecranon fossa, which accommodates the olecranon in full elbow extension.

The synovial cavities of the elbow joint are in free communication with each other (Fig. 2.2), extending down the proximal neck of the radius, below the annular ligament [3].

The normal joint capsule is a compact linear structure, with normal thickness in the adult population approaching 2 mm. The anterior capsule inserts proximally above the coronoid and radial fossas, distally in the anterior margin of the coronoid process and in the annular ligament laterally. The posterior capsule inserts proximally

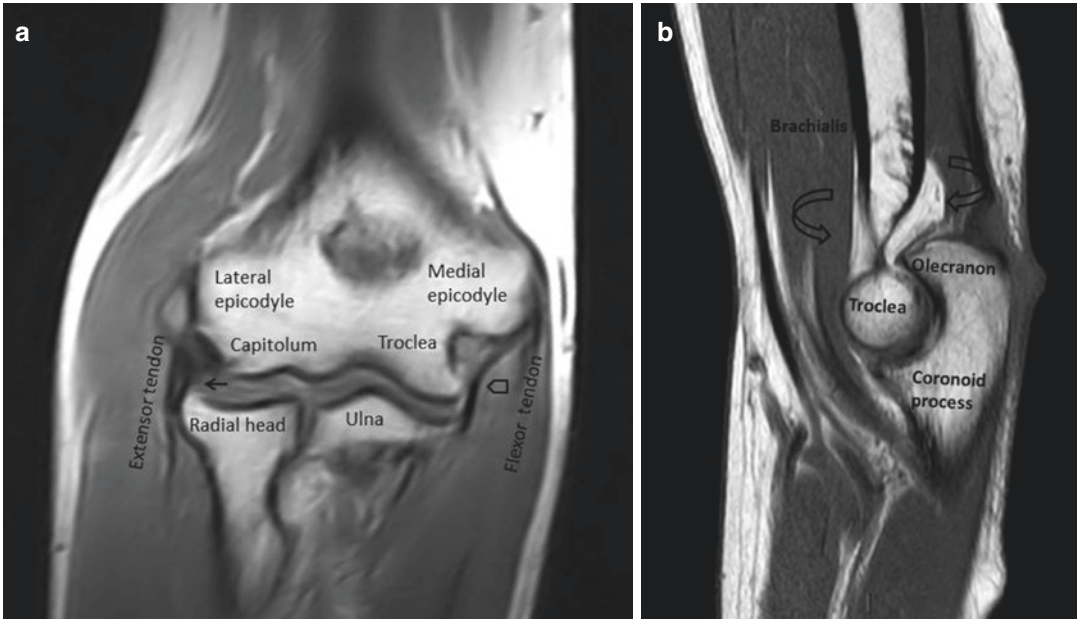


Fig. 2.1 Normal elbow anatomy. T1-weighted oblique-coronal (a) and sagittal (b) MR images. The elbow can be simplified to a joint between the distal humerus and the proximal ulna and radius. The articular surfaces of the humerus are formed of two components, the trochlea and

the capitellum, which articulate with the ulna and radius, respectively. Arrow: radial collateral ligament, void arrow: anterior band of the ulnar collateral ligament, curved arrows: fat pads

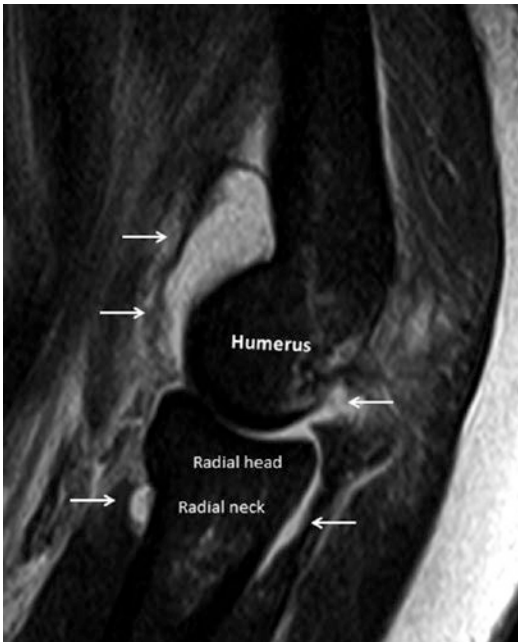


Fig. 2.2 Joint synovium. Sagittal MRI fat-suppressed PD image. The synovial cavities (arrows) of the elbow are in free communication with each other, extending down the proximal neck of the radius, below the annular ligament

above the olecranon fossa and distally at the annular ligament and the olecranon [2, 4, 5].

Three fat pads are present in the elbow, interposed between the joint capsule and the synovium; therefore, these are known as intra-capsular and extrasynovial [6] (Fig. 2.1).

The medial and lateral collateral ligament complexes (Fig. 2.1) are primary elbow stabilizers [7, 8]. The medial collateral ligament complex consists of three bundles with different points of origin and insertion forming a triangular shape: the anterior, posterior, and transverse. The anterior bundle origin is anterior–inferior to the medial epicondyle and inserts onto the sublime tubercle of the coronoid process. The posterior band origin is on the posterior and distal aspects of the medial epicondyle, and it inserts onto the medial olecranon. The transverse bundle originates on the tip of the olecranon and inserts onto the coronoid process. The lateral collateral ligament complex consists of three components, the radial collateral ligament (Fig. 2.1), lateral ulnar collateral ligament

(Fig. 2.4), and annular ligament (Fig. 2.5). The radial collateral ligament “proper” extends from the inferior aspect of the lateral epicondyle and inserts with the fibers of the annular ligament. The lateral ulnar collateral ligament originates more posteriorly, extending to the supinator crest of the ulna. The annular ligament encircles the radial head, attaching to the radial notch of the ulna. An accessory lateral collateral ligament is variably present.

The muscles and tendons may be categorized into four groups: anterior, lateral, medial, and posterior (Table 2.1) (Fig. 2.3).

The anterior compartment includes the biceps brachii and brachialis muscles.

The biceps muscle is located superficial to the brachialis muscle and lateral to the brachial artery and median nerve. Its tendon has an oblique course and 90° rotation, to insert on the radial tuberosity. Recent studies show that the tendon is always formed of two components, joined by a common paratenon and a lax endotenon septum, which corresponds to the long head and the short head of the muscle [9–11].

An aponeurosis, the lacertus fibrosus, emerges from the myotendinous junction of biceps brachii muscle, bridging the brachial artery and the median nerve; this descends medially to insert onto the deep fascia of the forearm [12].

The brachialis muscle is located deep in the biceps brachii muscle and inserts onto the anterior surface of the coronoid process of the ulna. The insertion may be purely muscular, tendinous, or mixed. The brachialis muscle has been described as having two separate heads: superficial and deep. The attachment of the superficial is more distal than that of the deep, although the two heads attach as a single contiguous structure in a blended manner [13].

The lateral muscle group is made up of the extensor of the wrist and finger as well as the supinator and brachioradialis muscles.

The common extensor tendon comprises the extensor carpi radialis brevis, the extensor digitorum, the extensor digiti minimi, and the extensor carpi ulnaris muscle, which attach at the lateral epicondyle of the humerus. The common extensor tendon is flattened; the individual input of tendon fibers is impossible to distinguish by ultrasound, but the extensor carpi radialis brevis makes up the most of deep portion, and the extensor digitorum comprises the surface layer at the front of the lateral epicondyle of the humerus.

The supinator muscle arises from the humerus, elbow lateral collateral ligament and ulna to insert onto the radius as two layers: superficial and deep [14, 15]. The two layers are separated

Table 2.1 Musculature of the elbow

Muscle	Elbow insertion
Biceps brachii	Radial tuberosity and fascia of forearm via bicipital aponeurosis
Brachialis	Coronoid process and tuberosity of ulna
Pronator teres	Lateral surface of radius
Palmaris longus, flexor carpi radialis, flexor digitorum superficialis, flexor carpi ulnaris	Medial epicondyle of humerus
Flexor digitorum profundus	Medial and anterior surfaces of ulna and interosseous membrane
Triceps brachii	Olecranon and fascia of forearm
Anconeus	Lateral epicondyle
Brachioradialis	Lateral supracondylar ridge of humerus
Extensor carpi radialis brevis, extensor digitorum communis, extensor digiti minimi, extensor carpi ulnaris	Lateral epicondyle of humerus
Extensor carpi radialis longus	Lateral supracondylar ridge of humerus
Supinator	Lateral epicondyle, radial collateral and annular ligaments, supinator crest of ulna

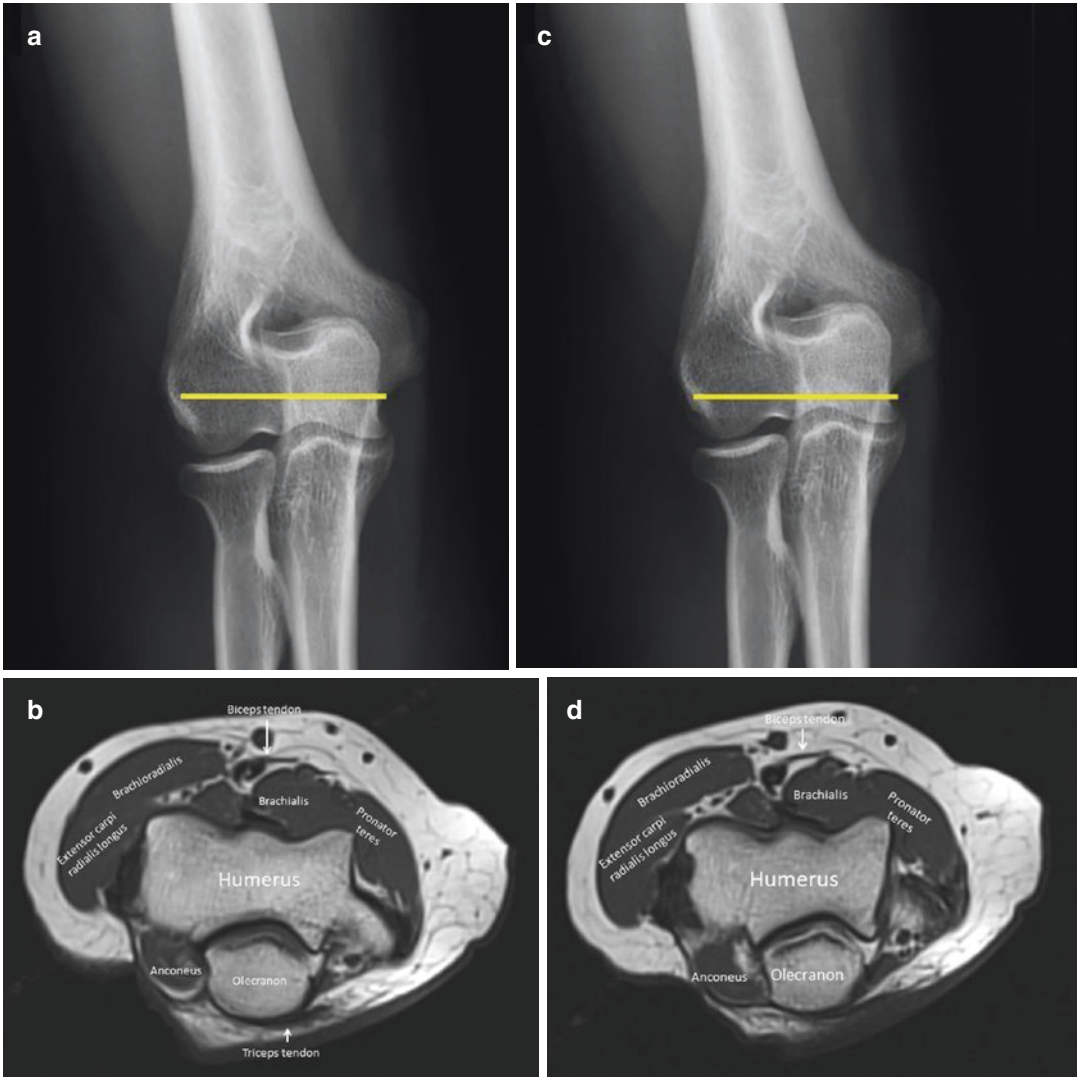


Fig. 2.3 Normal elbow anatomy: muscle. From proximal to distal placement of the images: **a, c, e**, T1-weighted T1 axial MR images; **b, d, f**. The muscles and tendons may be categorized into four groups: anterior, lateral, medial, and posterior. The anterior compartment includes the biceps brachii and brachialis muscles. The lateral muscle group

is made up of extensor of the wrist and finger as well as the supinator and brachioradialis muscles. The medial muscle group comprises the pronator teres and the wrist flexor muscles. The posterior muscle compartment consists of the triceps and anconeus muscles

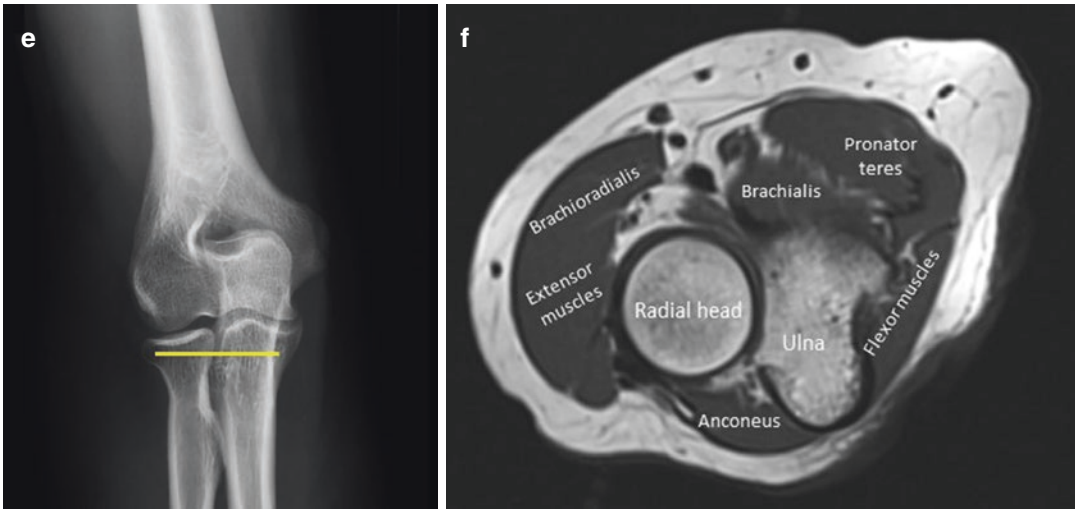


Fig. 2.3 (continued)

by an interstice, which the deep branch of the radial nerve runs between. The most proximal part of the superficial layer of the supinator muscle is always muscular in newborn full-term fetuses [16, 17]. It was suggested that the most superior part of the superficial layer, a fibrous arch known as the arcade of Frohse, is probably formed in adults due to repeated rotation movements. In some pathological circumstances, the deep branch of the radial nerve can be compressed, leading to an entrapment syndrome called radial tunnel syndrome.

The medial muscle group comprises the pronator teres and the wrist flexor muscles.

The common flexor tendon attaches at the medial epicondyle of the humerus. It is the fusion of the tendons of flexor carpi radialis, flexor digitorum superficialis, palmaris longus, and flexor carpi ulnaris. The common flexor tendon is broader and shorter than the common extensor tendon, and is visibly separated from adjacent local structures [18].

The pronator teres, located at the anteromedial side of the elbow and proximal forearm, is composed of a humeral head and an ulnar head. The larger humeral head is located superficially; the ulnar head is deeper and smaller. The two heads fuse distally to form a muscular body, which inserts onto the lateral side of the radius. At the

elbow, the median nerve generally runs between the two bellies of the pronator teres [19].

The posterior muscle compartment consists of the triceps and anconeus muscles.

The triceps musculo-tendinous unit consists of three parts: the long head, the lateral head, and the medial head; the origin of each head is different. The distal triceps tendon attaches at the postero-superior part of the olecranon process. MR-atomic studies have demonstrated a bipartite appearance (deep and superficial) of the triceps tendon insertion. The medial head appeared to have a separate insertion from the common tendon (long and lateral heads). The insertion of the medial head is deeper and mainly muscular at its insertion [20, 21]. Variations in the triceps brachii muscle are rare.

The anconeus muscle sweeps obliquely between the lateral epicondyle and olecranon. Along the posteromedial elbow, an anconeus epitrochlearis muscle—defined as an accessory muscle that traverses the top of the cubital tunnel—is found in 25% of all individuals.

There are several bursae present at the elbow joint [22]; the clinically most important are the olecranon and the bicipitoradial. The olecranon bursa [23, 24] is located between the olecranon process and the subcutaneous tissues. The bicipitoradial bursa is located at the distal biceps inser-

tion onto the radial tuberosity lying between the biceps insertion and the underlying radius [25].

At the elbow joint, the ulnar (Fig. 2.4), median (Fig. 2.5), and radial nerves (Fig. 2.6) are in a superficial position [26–29]. The ulnar nerve traverses along a groove on the posteromedial aspect of the humerus, at the level of the medial epicondyle, bridged by the cubital tunnel retinaculum (Osborne's ligament) (Fig. 2.4) [30].

The median nerve is anteriorly in the antecubital fossa, medial to the brachial artery (Fig. 2.5), beneath the bicipital aponeurosis, prior to its distal course between the heads of the pronator teres muscle [19]. The radial nerve (Fig. 2.6) lies in a groove between the brachialis and the brachioradialis muscles proximally and extensor carpi

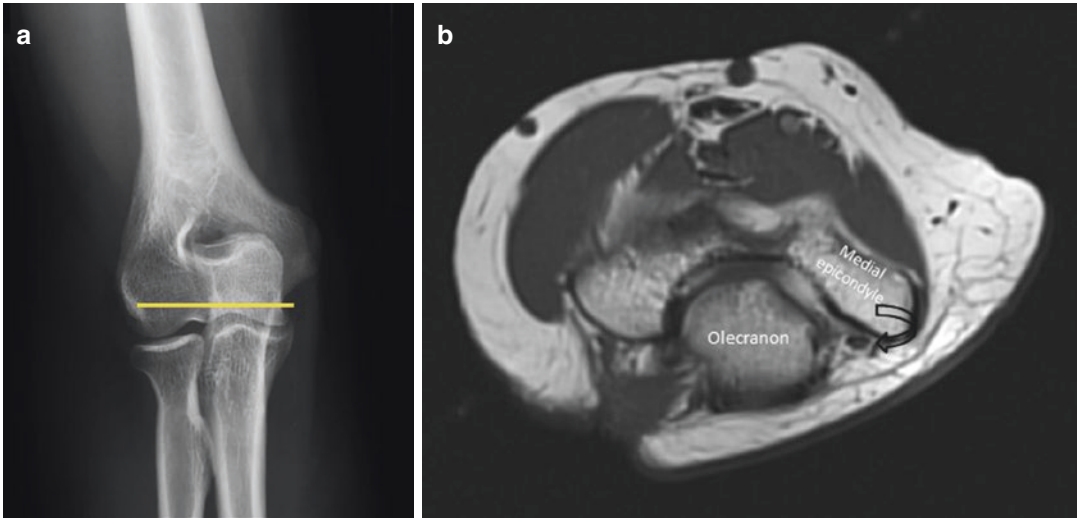


Fig. 2.4 Ulnar nerve. (a) Placement of the images, (b) weighted T1 axial MR images. The ulnar nerve (curved arrow) in the elbow courses in a subcutaneous location

through the condylar groove, delimited by the olecranon and the medial epicondyle and bridged by the cubital tunnel retinaculum (Osborne's ligament)

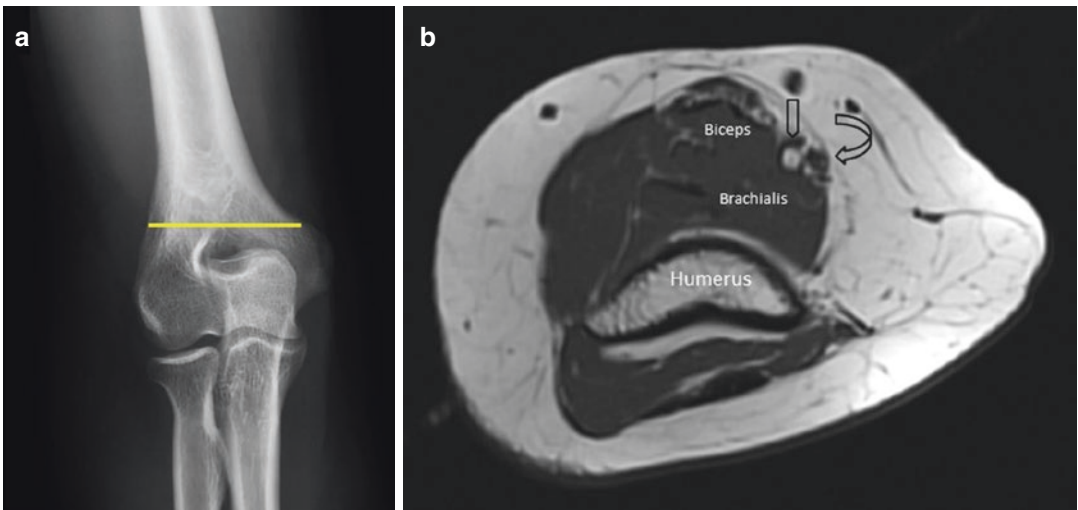


Fig. 2.5 Median nerve. (a) Placement of the images, (b) weighted T1 axial MR images. The median nerve (curved arrow) is in an anterior position medial to the brachial

artery (void arrow), beneath the bicipital aponeurosis, prior to its distal course between the heads of the pronator teres muscle

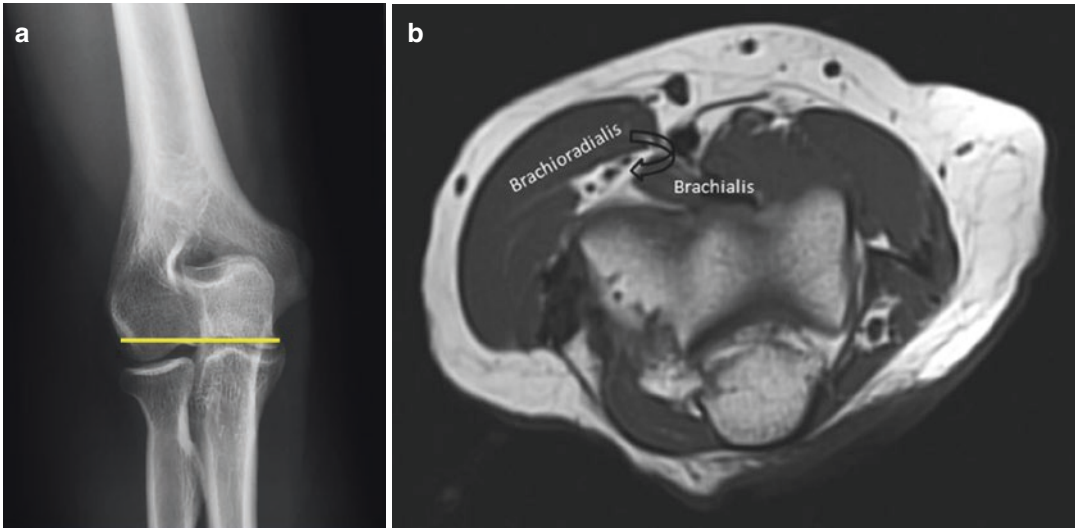


Fig. 2.6 Radial nerve. (a) Placement of the images, (b) weighted T1 axial MR images. The radial nerve (curved arrow) lies between the brachialis and the brachioradialis

muscles proximally, then divides into the superficial and posterior interosseous branches

radialis distally. Then, it divides into the superficial and the posterior interosseous branches. The posterior interosseous nerve lies between the superficial and deep portions of the supinator muscle [14].

References

1. Francesc Malagelada D, Dalmau-Pastor M, Vega J, Golanó P. Elbow anatomy. In: Doral MN, Karlsson J, editors. Sports injuries. Heidelberg: Springer; 2015. https://doi.org/10.1007/978-3-642-36569-0_38.
2. Draghi F, Danesino GM, de Gautard R, Bianchi S. Ultrasound of the elbow: examination techniques and US appearance of the normal and pathologic joint. *J Ultrasound*. 2007;10(2):76–84.
3. Alcid JG, Ahmad CS, Lee TQ. Elbow anatomy and structural biomechanics. *Clin Sports Med*. 2004;23(4):503–17.
4. Konin GP, Nazarian LN, Walz DM. US of the elbow: indications, technique, normal anatomy, and pathologic conditions. *Radiographics*. 2013;33(4):E125–47.
5. Radunovic G, Vlad V, Micu MC, Nestorova R, Petranova T, Porta F, Iagnocco A. Ultrasound assessment of the elbow. *Med Ultrason*. 2012;14(2):141–6.
6. Hamada D, Matsuura T, Sugiura K, Higuchi T, Suzue N, Goto T, Tsutsui T, Wada K, Fukuta S, Sairyu K. An unusual cause of posterior elbow impingement: detachment of a hypertrophied posterior fat pad. *Case Rep Orthop*. 2015;2015:121646.
7. Daniels DL, Mallisee TA, Erickson SJ, Boynton MD, Carrera GF. The elbow joint: osseous and ligamentous structures. *Radiographics*. 1998;18(1):229–36.
8. Reichel LM, Milam GS, Sittton SE, Curry MC, Mehlhoff TL. Elbow lateral collateral ligament injuries. *Hand Surg Am*. 2013;38(1):184–201.
9. Blasi M, de la Fuente J, Martinoli C, Blasi J, Pérez-Bellmunt A, Domingo T, Miguel-Pérez M. Multidisciplinary approach to the persistent double distal tendon of the biceps brachii. *Surg Radiol Anat*. 2014;36(1):17–24.
10. Tagliafico A, Michaud J, Capaccio E, Derchi LE, Martinoli C. Ultrasound demonstration of distal biceps tendon bifurcation: normal and abnormal findings. *Eur Radiol*. 2010;20(1):202–8.
11. Sanal HT, Chen L, Negrao P, Haghghi P, Trudell DJ, Resnick DL. Distal attachment of the brachialis muscle: anatomic and MRI study in cadavers. *Am J Roentgenol*. 2009;192(2):468–72.
12. Korschake M, Stofferin H, Moriggl B. Ultrasound visualization of an underestimated structure: the bicapital aponeurosis. *Surg Radiol Anat*. 2017;39(12):1317–22. <https://doi.org/10.1007/s00276-017-1885-0>.
13. Tagliafico A, Michaud J, Perez MM, Martinoli C. Ultrasound of distal brachialis tendon attachment: normal and abnormal findings. *Br J Radiol*. 2013;86(1025):20130004.
14. Berton C, Wavreille G, Lecomte F, Miletic B, Kim HJ, Fontaine C. The supinator muscle: anatomical bases for deep branch of the radial nerve entrapment. *Surg Radiol Anat*. 2013;35(3):217–24.
15. Ozturk A, Kutlu C, Taskara N, Kale AC, Bayraktar B, Cecen A. Anatomic and morphometric study of

- the arcade of Frohse in cadavers. *Surg Radiol Anat.* 2005;27(3):171–5.
16. Spinner M. The arcade of Frohse and its relationship to posterior interosseous nerve paralysis. *J Bone Joint Surg Br.* 1968;50(4):809–12.
 17. Tatar I, Kocabiyyik N, Gayretli O, Ozan H. The course and branching pattern of the deep branch of the radial nerve in relation to the supinator muscle in fetus elbow. *Surg Radiol Anat.* 2008;31(8):591–6.
 18. Martinoli C, Bianchi S, Giovagnorio F, Pugliese F. Ultrasound of the elbow. *Skelet Radiol.* 2001;30:605–14.
 19. Créteur V, Madani A, Sattari A, Bianchi S. Sonography of the pronator teres: normal and pathologic appearances. *J Ultrasound Med.* 2017;36(12):2585–97. <https://doi.org/10.1002/jum.14306>.
 20. Belentani C, Pastore D, Wangwinyuvirat M, Dirim B, Trudell DJ, Haghighi P, Resnick D. Triceps brachii tendon: anatomic-MR imaging study in cadavers with histologic correlation. *Skelet Radiol.* 2009;38(2):171–5.
 21. Tagliafico AS, Bignotti B, Martinoli C. Elbow US: anatomy, variants, and scanning technique. *Radiology.* 2015;275(3):636–50.
 22. Ruangchaijatuporn T, Gaetke-Udager K, Jacobson JA, Yablon CM, Morag Y. Ultrasound evaluation of bursae: anatomy and pathological appearances. *Skelet Radiol.* 2017;46(4):445–62.
 23. Blankstein A, Ganel A, Givon U, Mirovski Y, Chechick A. Ultrasonographic findings in patients with olecranon bursitis. *Ultraschall Med.* 2006;27(6):568–71.
 24. Blackwell JR, Hay BA, Bolt AM, Hay SM. Olecranon bursitis: a systematic overview. *Should Elb.* 2014;6(3):182–90.
 25. Draghi F, Gregoli B, Sileo C. Sonography of the bicipitoradial bursa: a short pictorial essay. *J Ultrasound.* 2012;15(1):39–41.
 26. Husarik DB, Saupé N, Pfirrmann CW, Jost B, Hodler J, Zanetti M. Elbow nerves: MR findings in 60 asymptomatic subjects—normal anatomy, variants, and pitfalls. *Radiology.* 2009;252(1):148–56.
 27. Gregoli B, Bortolotto C, Draghi F. Elbow nerves: normal sonographic anatomy and identification of the structures potentially associated with nerve compression. A short pictorial-video article. *J Ultrasound.* 2013;16(3):119–21.
 28. Alessandrino F, Pagani C, Draghi F. In-continuity neuroma of the median nerve at the elbow. *J Ultrasound.* 2014;17(3):229–31.
 29. Bianchi S, Draghi F, Beggs I. Ultrasound of the peripheral nerves. In: *Clinical ultrasound*, vol. 2. Philadelphia: Elsevier; 2011. p. 1158–67.
 30. Bianchi S, Martinoli C. Elbow. In: Bianchi S, Martinoli C, editors. *Ultrasound of the musculoskeletal system*. New York: Springer; 2007. p. 349–408.



Examination Techniques and Ultrasound Appearance

3

Content Overview

Anterior elbow

- Biceps muscle and tendon
- Brachialis muscle and tendon
- Median nerve
- Articular cartilage
- Anterior recess
- Anterior fat pads

Lateral elbow

- Common extensor tendon
- Lateral collateral ligament
- Radial nerve
- Radiocapitellar joint

Posterior elbow

- Triceps muscle and tendon
- Anconeus muscle and tendon
- Olecranon bursa
- Posterior joint recess
- Ulnar nerve

Medial elbow

- Common flexor tendon
- Medial collateral ligament
- Pronator teres

Ultrasound examination of the elbow may be performed with the patient seated and the elbow placed on the examination table/bed [1–4].

The exam is generally tailored to the clinical question, however a complete evaluation of the elbow should be considered; in these cases, a useful approach is to divide the elbow into anterior,

lateral, posterior, and medial compartments (Table 3.1).

In general, examination of the anterior elbow may begin with the upper limb resting in an extended and supinated position on the examination table (Fig. 3.1). The key structures to be evaluated include the distal biceps muscle and tendon [5–8], the distal brachialis muscle and tendon [9, 10], the anterior joint recess [11] with the anterior fat pad, the median nerve, the radial nerve [12–14], the brachial artery, and the articular cartilage [1].

The biceps muscle is located superficial to the brachialis muscle and lateral to the brachial artery (Table 3.2) and median nerve [4]. Its tendon is long, approximately 7 cm, with an oblique course from the lateral to the medial and 90° rotation, to insert onto the radial tuberosity. It has been demonstrated that the distal biceps tendon is made of two separate tendons belonging to the short and long head of the biceps muscle. The distal portion of the biceps tendon is covered by an extrasynovial paratenon and by the bicipitoradial bursa.

Different approaches have been proposed to study the distal biceps tendon [1, 7]. The different approaches are complementary and may be performed together. In the anterior approach, the tendon may be found on the short-axis and evaluated from proximal to distal (Fig. 3.1); then, the probe is rotated by 90° so it is possible to place the transducer longitudinally to the insertion of the tendon (Fig. 3.2). Longitudinally, increasing the probe pressure over the tendon reduces the anisotropy. In

Table 3.1 Checklist for elbow ultrasound evaluation

Lateral	Common extensor tendon
	Lateral collateral ligament
	Radial nerve
	Supinator muscle
	Posterior interosseous nerve
Anterior	Distal biceps tendon
	Bicipitoradial bursa
	Brachialis tendon
	Median nerve
	Brachial artery
	Joint recess
	Anterior fat pad
Medial	Common flexor tendon
	Medial collateral ligament
	Pronator teres
Posterior	Distal triceps tendon
	Olecranon bursa
	Ulnar nerve
	Joint recess
	Posterior fat pad

**Fig. 3.1** Anterior elbow. Transducer placement is demonstrated on the upper limb resting in an extended and supinated position on the examination table (a). Sonography shows the distal biceps tendon (curved arrow) located superficial to the brachialis muscle, lateral to brachial artery (void arrow) and median nerve (arrow) (b)**Table 3.2** Landmark

Lateral	Common extensor tendon—lateral epicondyle
	Lateral collateral ligament—common extensor tendon
	Radial nerve—brachialis
	Posterior interosseous nerve—supinator muscle
Anterior	Distal biceps tendon—brachial artery
	Bicipitoradial bursa—distal biceps tendon
	Brachialis tendon—biceps muscle
	Median nerve—brachial artery
	Joint recess—brachialis, Brachioradialis
	Anterior fat pad—brachialis
Medial	Common flexor tendon—medial epicondyle
	Medial collateral ligament—common flexor tendon
	Pronator teres—median nerve
Posterior	Distal triceps tendon—olecranon
	Olecranon bursa—distal triceps tendon
	Ulnar nerve—medial epicondyle
	Joint recess—distal triceps tendon
	Posterior fat pad—distal triceps tendon

the medial approach, the elbow is flexed 90° and the forearm supinated (Fig. 3.3); the probe is placed longitudinally and medially over the distal arm. In this position, the brachial artery, medial to the biceps tendon, may be used as an acoustic window. In the posterior approach (Fig. 3.4), the elbow is flexed and the dorsum of the hand pointing toward the ceiling. The transducer is placed on

a transverse plane over the proximal forearm at the level of the radial tuberosity. The insertion of the distal biceps is visible during pronation and supination movements.

From the lateral aspect of the tendon, an aponeurotic expansion, the lacertus fibrosus [15], extends to the medial deep fascia of the forearm [8]. It covers the median nerve and brachial artery and plays

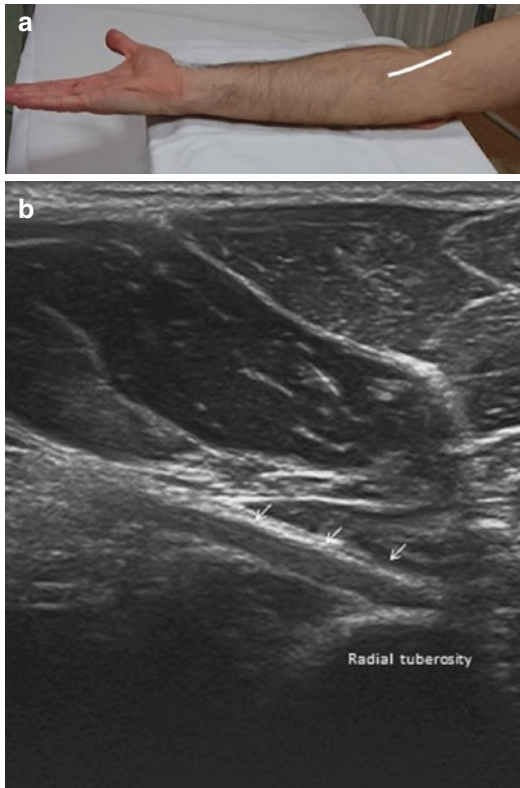


Fig. 3.2 Anterior approach for distal biceps tendon evaluation. Transducer placement (**a**). The distal biceps tendon is highlighted by arrows (**b**). In the anterior approach, the tendon may be found on short-axis and evaluated from proximal to distal; by rotating the probe by 90°, it is possible to place the transducer longitudinally to the insertion of the tendon. Increasing the probe pressure over the tendon reduces the anisotropy

an important role in maintaining the distal biceps tendon in its appropriate position. An anterior approach with transverse planes is generally used to study the lacertus fibrosus. The patient is in a sitting position with the elbow lying on the table, and the lacertus fibrosus is scanned in two planes.

The brachialis muscle (Fig. 3.5) in the elbow is located deep in the biceps muscle. Its tendon inserts onto the ulnar tuberosity. The insertion of the brachialis may be muscular, tendinous, or mixed. Distal attachment of the brachialis is composed of a superficial and a deep head. An anterior approach with the upper limb resting in an extended and supinated position on the exami-

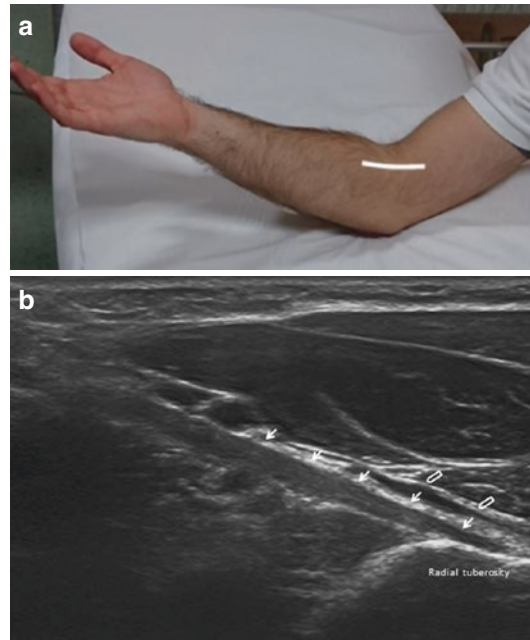


Fig. 3.3 Medial approach for distal biceps tendon evaluation. Transducer placement (**a**). The distal biceps tendon is highlighted by arrows (**a**). The probe is placed longitudinally and medially over the distal arm. In this position, the brachial artery, medial to the biceps tendon, may be used as an acoustic window

nation table is generally used. Transverse and longitudinal planes and pronosupination movements are useful to identify the two separate tendinous components [9, 10].

The median nerve [12–14], in the elbow, runs with the brachial artery, medial to the brachialis muscle. In the cubital fossa, both structures lie medial to the biceps brachii tendon (Fig. 3.1) and underneath the lacertus fibrosus [9]. At this level, the nerve lies medial to the artery and continues between the two heads of the pronator teres muscle. It gives off the anterior interosseous nerve approximately 2–5 cm distal to the medial epicondyle. The median nerve is easily evaluated with ultrasound (Fig. 3.6) on short-axis planes; with the patient in a sitting position and the elbow lying on the table, it has the typical honeycomb appearance.

The evaluation of articular cartilage [1] mainly relies on MR, but anterior transverse ultrasound images over the distal humeral extremity

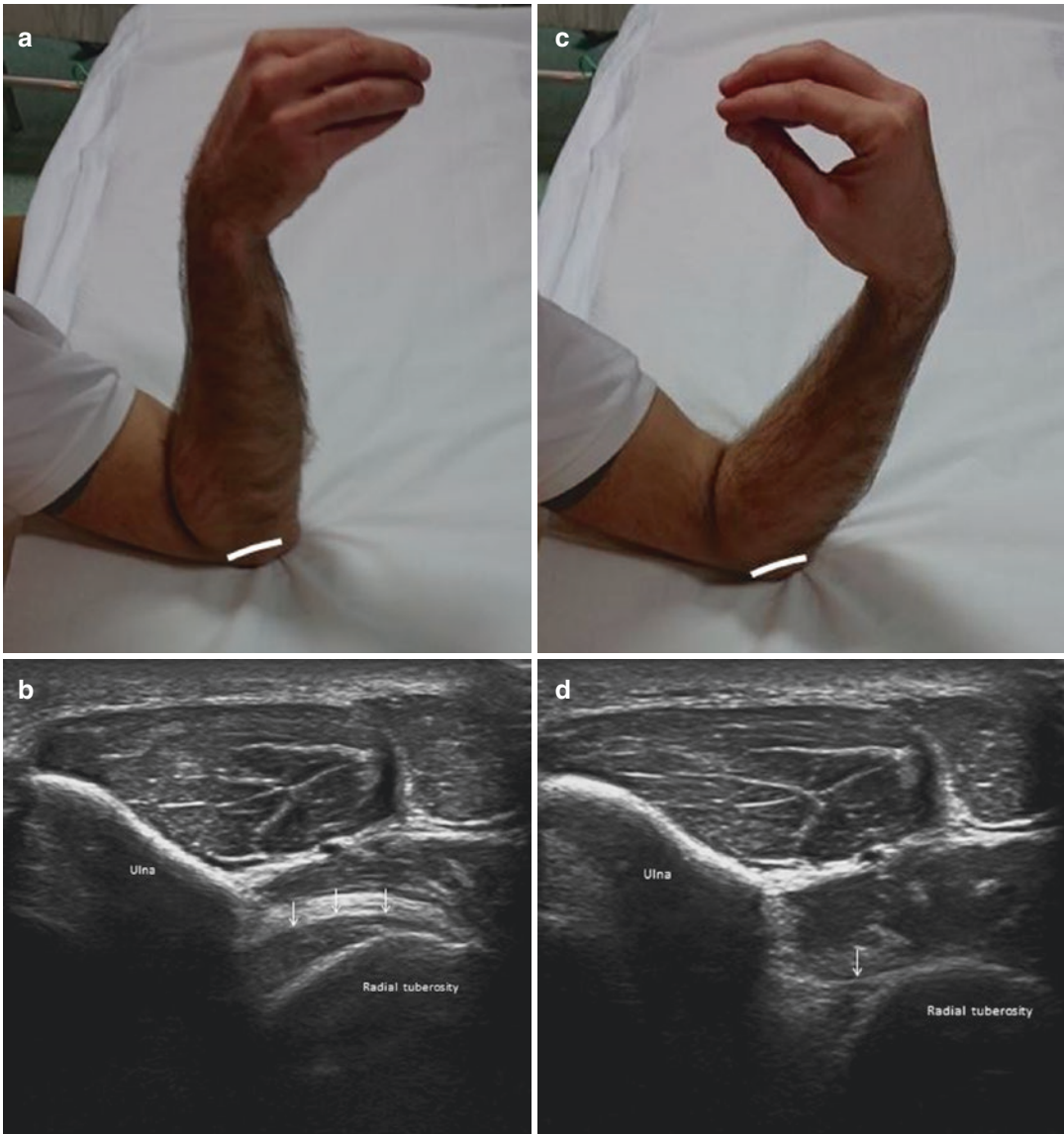


Fig. 3.4 Posterior approach for distal biceps tendon evaluation. Transducer placement (**a**, **c**). The distal biceps is highlighted by arrows (**b**, **d**). The elbow is flexed and the dorsum of the hand is pointing towards the ceiling, in the

so-called cobra position. The transducer is placed on a transverse plane over the proximal forearm at the level of the radial tuberosity. The insertion of the distal biceps is visible during pronation and supination movements

(Fig. 3.7) are able to demonstrate the osteochondral surface of the capitellum and the trochlea. The articular cartilage appears as a hypoechoic band overlying the bone.

The radiocapitellar joint with the radial recess and the coronoid fossa with its respective coronoid recess are generally evaluated with anterior

sagittal images (long-axis). The anterior fat pads are evaluated superficially to the recesses.

The lateral aspect of the elbow is generally examined with the elbow in flexion (Fig. 3.8a) or in the so-called crab position (elbow flexed 90° with the palm resting on the table) (Fig. 3.8b) [16, 17]. The radial head and the lateral epicon-

Fig. 3.5 Brachialis muscle and tendon. An anterior approach with the upper limb resting in an extended and supinated position on the examination table is generally used (**a**). The muscle and the tendon can be found on short-axis and evaluated from proximal to distal; then, by rotating the probe, it is possible to place the transducer longitudinally to the insertion of the tendon and the two separate tendinous components may be identified (**b**)

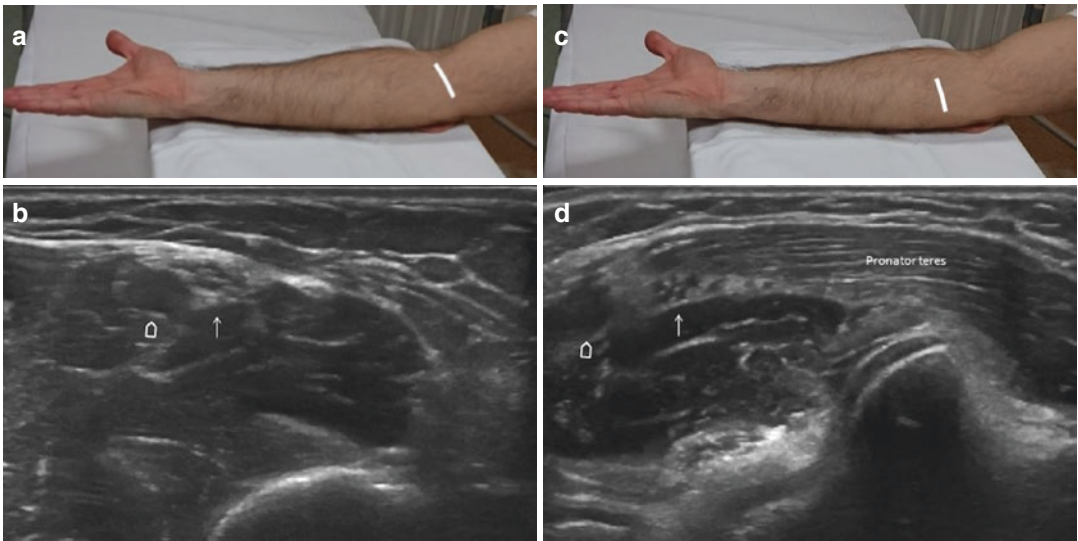
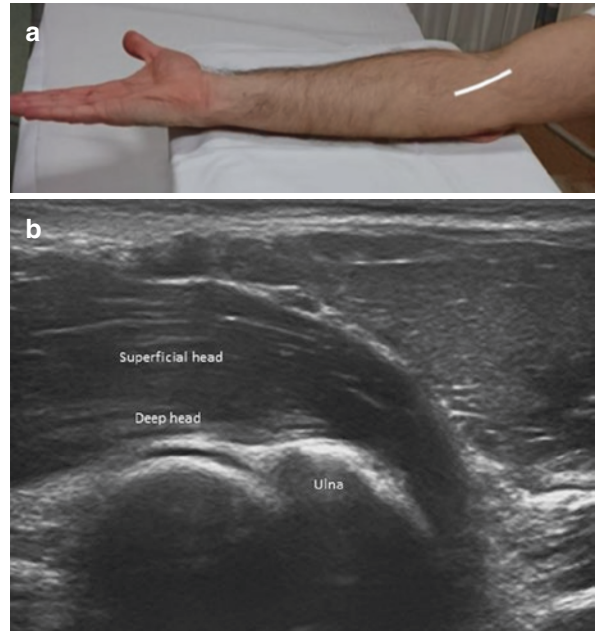


Fig. 3.6 Median nerve. The median nerve is easily evaluated with ultrasound on short-axis planes. In the elbow, it runs with the brachial artery (**a**) transducer placement, (**b**) sonographic image, void arrows—brachial artery, arrow—

median nerve), then continues between the two heads of the pronator teres muscle (**c**) transducer placement, (**d**) sonographic image, void arrows—brachial artery, arrow—median nerve)

dyle may be used as landmarks. In the lateral aspect, the key structures to be evaluated are: the common extensor tendon, the lateral collateral ligament, the radial nerve and part of the radio-capitellar joint.

The common extensor tendon (Fig. 3.8c) arises from the lateral epicondyle. It consists of the tendons of four muscles: extensor carpi radialis brevis, extensor digitorum communis, extensor digiti minimi, and extensor carpi ulnaris. The

Fig. 3.7 Articular cartilage. Transducer placement (a). Ultrasound (b) demonstrates the osteochondral surface consisting of capitellum and trochlea. The articular cartilage appears as a uniform hypoechoic band overlying the subchondral bone

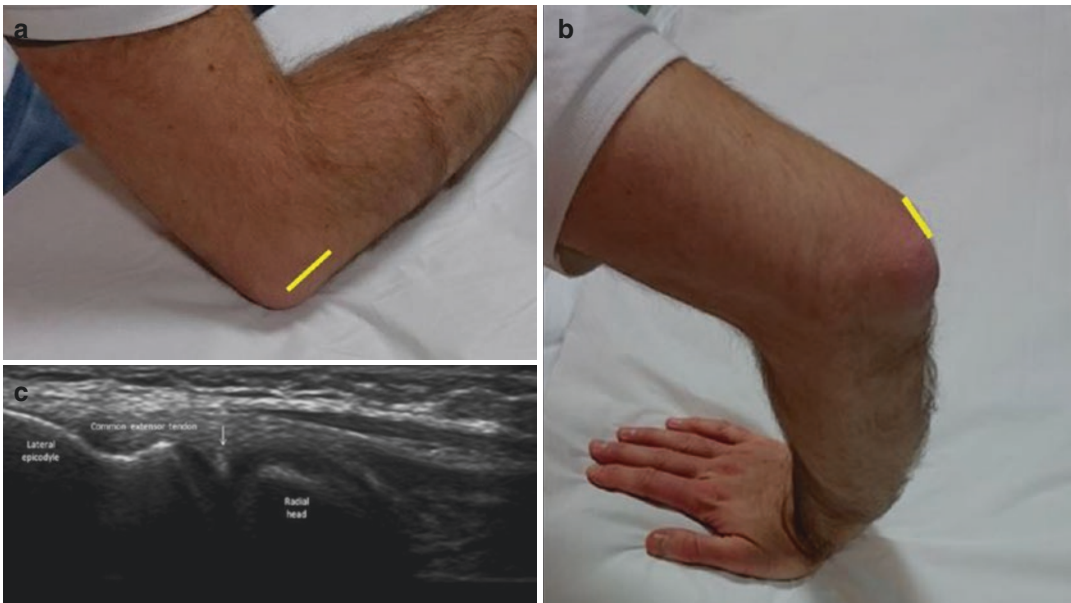
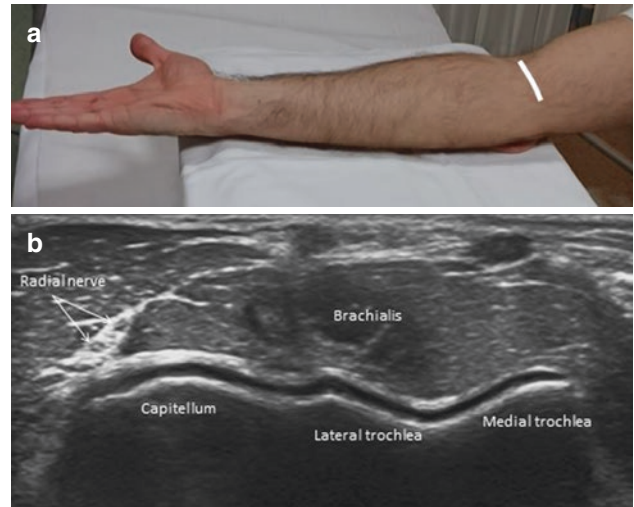


Fig. 3.8 Common extensor tendon. Transducer placement (a, b). Sonographic image (c). The lateral aspect of the elbow is generally examined with the elbow in flexion (a) or in the so-called crab position (elbow flexed 90° with the palm resting on the table) (b). The common extensor

tendon must be evaluated in the long (c) and short axis: the lateral synovial fringe is depicted as a triangular hyperechoic structure between the capitellum and the radial head (arrow). Sonoelastographic image depicts the tendon in red, representing hard tissue (d)

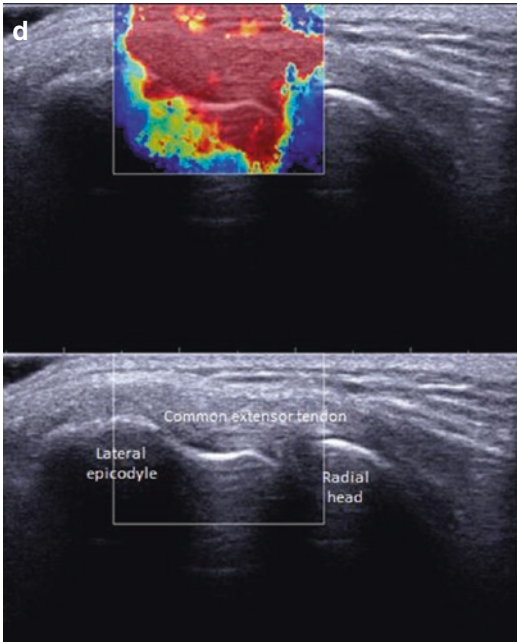


Fig. 3.8 (continued)

extensor carpi radialis brevis is the deepest, and the extensor digitorum is the most superficial. The single contributions from the extensor muscles to the common extensor tendon cannot be identified at ultrasound. The sonoelastographic image depicts the tendon in red, representing hard tissue (Fig. 3.8d).

The common extensor tendon is separated from the joint capsule by the lateral collateral ligamentous. The lateral collateral ligamentous complex consists of: the radial collateral ligament proper (Fig. 3.9), the lateral ulnar collateral ligament, the annular ligament, and sometimes the accessory radial collateral ligament [18–20]. No evidence and consensus exist to evaluate this ligamentous complex by ultrasound.

The lateral synovial fringe (a synovial plica) is depicted as a triangular hyperechoic structure intervening between the capitellum and the radial head (Fig. 3.8c).

The radial nerve is located between the brachialis and the brachioradialis muscles; more distally, the radial nerve divides into the superficial

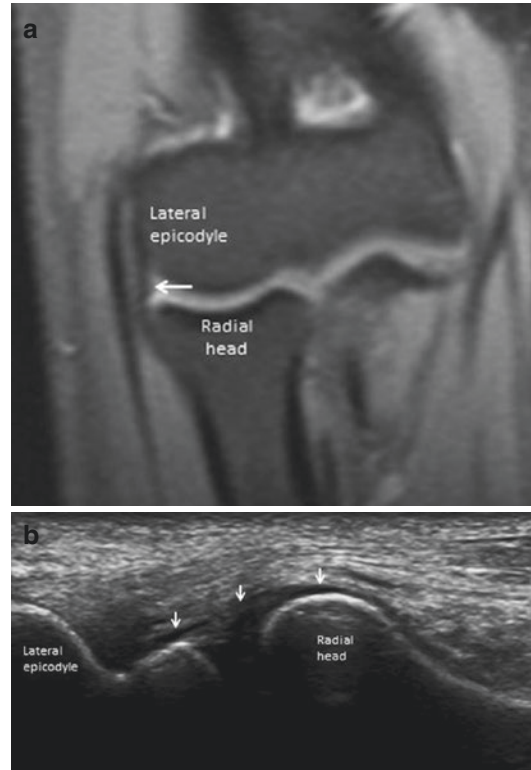


Fig. 3.9 Radial collateral ligament proper. MRI image (a) of the radial collateral ligament proper (arrow) extends from the antero-inferior aspect of the lateral epicondyle to insert into the annular ligament. It is generally examined in the same position as the common extensor tendon and appears hypoechoic (arrows) (b)

cutaneous sensory branch and the posterior interosseous nerve (Fig. 3.10). The posterior interosseous nerve enters the arcade of Frohse, passing between the superficial and deep parts of the supinator muscle [21–23]. Transverse ultrasound images are sufficient to demonstrate the nerve.

The posterior aspect of the elbow is generally examined in the so-called crab position (joint positioned in 90° of flexion, the forearm fully pronated (internally rotated)), and the palm resting on a table (Fig. 3.11). The posterior compartment of the elbow includes the triceps [24–26], the anconeus muscles [27, 28], the olecranon bursa [29–31], the olecranon fossa with the posterior recess [11], and the ulnar nerve [32, 33].

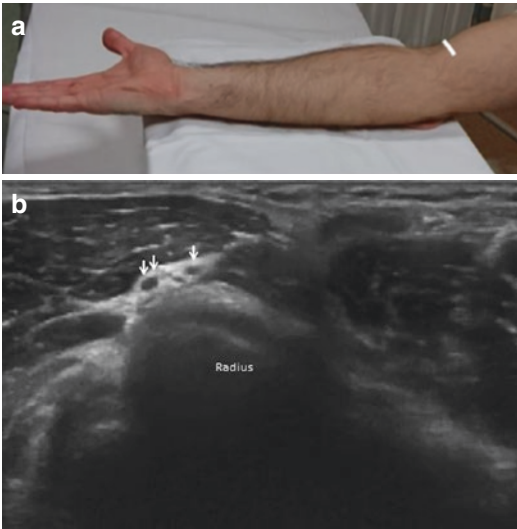


Fig. 3.10 Radial nerve. Transducer placement (a). In the anterior part of elbow (b), the cutaneous sensory branch (arrow) and the posterior interosseous nerve (double arrows), a result of bifurcation of the nerve, can be appreciated with sonography. The two branches are evaluated on short-axis planes

The triceps is made up of three heads, medial, lateral, and long, and is inserted onto the olecranon process of the ulna with a single thick tendon consisting of a superficial portion composed of the lateral and long heads, and a deep portion composed of the medial head [24–26]. Ultrasound examination of the triceps tendon can be performed on transverse and longitudinal planes moving the transducer from the myotendinous junction to the olecranon. Pre-insertional fibers of the tendon may appear hypoechoic owing to the anisotropy artifact.

The anconeus muscle is a small muscle located on the lateral side of the olecranon; it is depicted during the evaluation of the triceps [27, 28, 34]. In some individuals, it is possible to find an accessory muscle located between the posterior aspect of the medial condyle and the medial aspect of the olecranon: the anconeus epitrochlearis muscle. It is depicted during evaluation of the cubital tunnel (Fig. 3.12).

Deep in the triceps, the olecranon fossa and the posterior recess are visible in patients with effusions [11]. The olecranon fossa is identified as a concavity at the distal aspect of the humerus that is filled with the hyperechoic posterior elbow fat pad. The joint may be examined at 45° flexion to move the intra-articular fluid from the anterior synovial space to the olecranon recess.

The ulnar nerve in the elbow courses through the cubital tunnel, a retroepicondylar osseous groove at the postero-medial aspect of the elbow [32, 33]. The cubital tunnel is bordered by the posterior surface of the medial epicondyle and by the olecranon. The posterior bundle of the medial collateral ligament and the retinaculum (Osborne's ligament), respectively, form the floor and ceiling of the cubital tunnel. Stability: due to the particular anatomic location, the ulnar nerve at the elbow is prone to instability. The ultrasound technique to evaluate these conditions can vary; however, this consists initially of an evaluation of the ulnar nerve to look for signs of neuropathy; subsequently, the ulnar nerve is examined during active flexion and extension. The transducer is positioned transversely, with ends over the olecranon and the medial epicondyle.

The medial aspect of the elbow is generally examined with the elbow in extension or in the so-called crab position. The medial epicondyle may be used as a landmark. In the medial aspect, the key structures to be evaluated are: the common flexor tendon [35–37], the medial collateral ligament [19], and the pronator teres [38].

The common flexor tendon (Fig. 3.13) is made, from anterior to posterior, by the flexor carpi radialis, the palmaris longus, the flexor carpi ulnaris, and the flexor digitorum superficialis [35–37]. The tendon is evaluated with a probe placed longitudinally (long axis of the tendon). The tendon appears larger but shorter than the common extensor tendon.

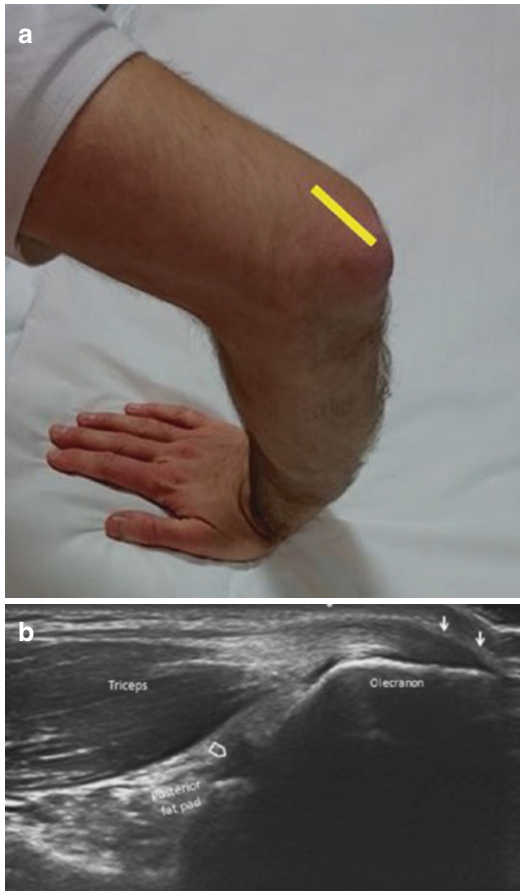


Fig. 3.11 Triceps tendon. Transducer placement (a). The distal triceps tendon (b) appears as a fibrillary echoic structure. Pre-insertional fibers appear hypoechoic owing to the anisotropy artifact (arrows). Ultrasound examination of the triceps tendon can be performed on transverse and longitudinal planes moving the transducer from myotendinous junction to the olecranon. Deep in the triceps, the olecranon fossa, the posterior recess (void arrow), and the posterior elbow fat pad may be evaluated

The ulnar collateral ligament complex (Fig. 3.14) is composed of the anterior band, a posterior band, and a transverse band. The anterior and posterior bands arise from the inferior aspect of the medial epicondyle. The anterior band inserts distally at the sublime tubercle of the ulna [19]. The posterior band inserts at the postero-medial margin of the trochlear notch of

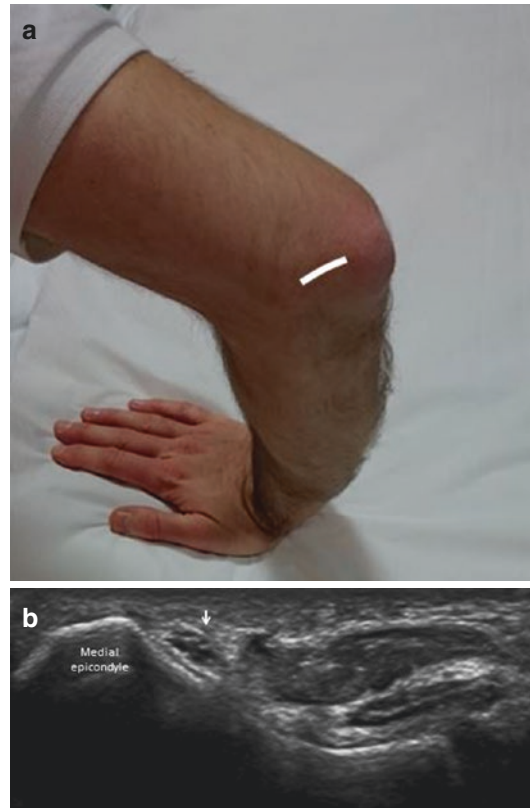


Fig. 3.12 Ulnar nerve. Transducer placement (a). Ulnar nerve (b) (arrow) in the elbow courses through the cubital tunnel, a retroepicondylar osseous groove at the postero-medial aspect of the elbow. It is evaluated using ultrasound on short-axis planes

the ulna. The anterior band of the medial collateral ligament is depicted as an elongated structure crossing the trochlea-ulna joint deep to the flexor muscles. The ligament has a uniform thickness and echotexture. The posterior band is depicted during evaluation of the ulnar nerve.

The pronator teres is composed of a humeral head and an ulnar head. The larger humeral head is located superficially [38]. At the elbow, in more than 80% of individuals, the median nerve runs between the two bellies of the pronator teres. Sonographic evaluation of the pronator teres is performed with patient seated

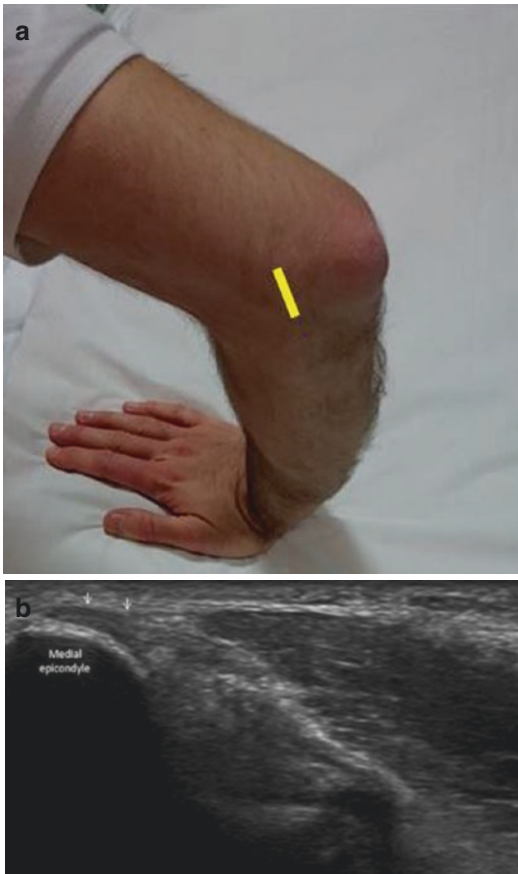


Fig. 3.13 Common flexor tendon. Transducer placement (a). The tendon (b) appears larger but shorter than the common extensor tendon (arrows). It is evaluated with probe place longitudinally (long axis of the tendon)

with the elbow extended and in supination on the examination bed. The examination may start with transverse sonograms, obtained at the level of the medial epicondyle and then moving the transducer caudally to the distal tendon.

References

1. Tagliafico AS, Bignotti B, Martinoli C. Elbow US: anatomy, variants, and scanning technique. *Radiology*. 2015;275(3):636–50.
2. Konin GP, Nazarian LN, Walz DM. US of the elbow: indications, technique, normal anatomy, and pathologic conditions. *Radiographics*. 2013;33(4):E125–47.

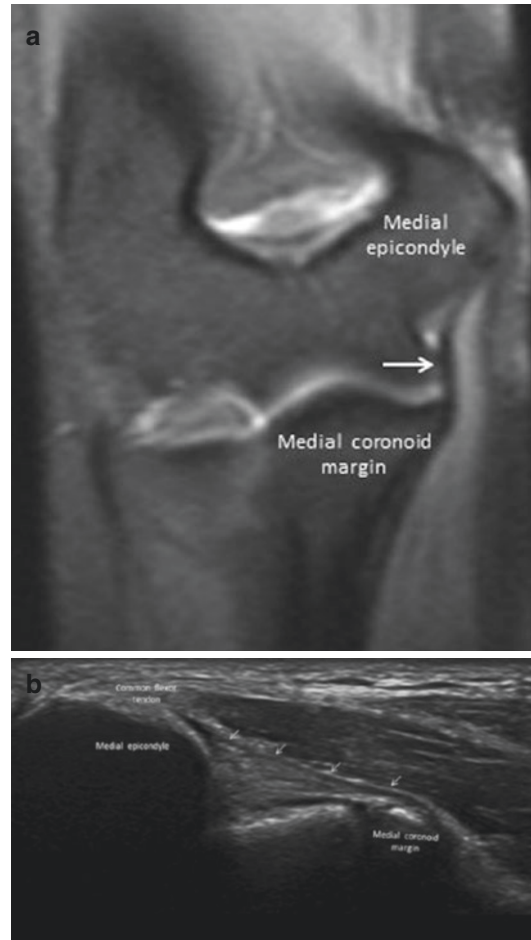


Fig. 3.14 Anterior band of the medial collateral ligament. The anterior band (arrow) arises from the inferior aspect of the medial epicondyle and inserts distally at the sublime tubercle of the ulna (a: MRI image). It is generally examined in the same position as the common flexor tendon and appears hypoechoic (arrows) (b)

3. Martinoli C, Bianchi S, Giovagnorio F, Pugliese F. Ultrasound of the elbow. *Skelet Radiol*. 2001;30(11):605–14.
4. Draghi F, Danesino GM, de Gautard R, Bianchi S. Ultrasound of the elbow: examination techniques and US appearance of the normal and pathologic joint. *J Ultrasound*. 2007;10(2):76–84.
5. Schmidt CC, Savoie FH, Steinmann SP, Hausman M, Voloshin I, Morrey BF, Sotereanos DG, Bero EH, Brown BT. Distal biceps tendon history, updates, and controversies: from the closed American Shoulder and Elbow Surgeons meeting-2015.
6. Blasi M, de la Fuente J, Martinoli C, Blasi J, Pérez-Bellmunt A, Domingo T, Miguel-Pérez M. Multidisciplinary approach to the persistent dou-

- ble distal tendon of the biceps brachii. *Surg Radiol Anat.* 2014;36(1):17–24.
7. Tagliafico A, Michaud J, Capaccio E, Derchi LE, Martinoli C. Ultrasound demonstration of distal biceps tendon bifurcation: normal and abnormal findings. *Eur Radiol.* 2010;20(1):202–8.
 8. Brasseur JL. The biceps tendons: from the top and from the bottom. *J Ultrasound.* 2012;15(1):29–38.
 9. Sanal HT, Chen L, Negro P, Haghighi P, Trudell DJ, Resnick DL. Distal attachment of the brachialis muscle: anatomic and MRI study in cadavers. *Am J Roentgenol.* 2009;192(2):468–72.
 10. Tagliafico A, Michaud J, Perez MM, Martinoli C. Ultrasound of distal brachialis tendon attachment: normal and abnormal findings. *Br J Radiol.* 2013;86(1025):20130004.
 11. De Maeseneer M, Jacobson JA, Jaovisidha S, et al. Elbow effusions: distribution of joint fluid with flexion and extension and imaging implications. *Investig Radiol.* 1998;33(2):117–25.
 12. Husarik DB, Saupé N, Pfirrmann CW, Jost B, Hodler J, Zanetti M. Elbow nerves: MR findings in 60 asymptomatic subjects--normal anatomy, variants, and pitfalls. *Radiology.* 2009;252(1):148–56. <https://doi.org/10.1148/radiol.2521081614>.
 13. Bianchi S, Draghi F, Beggs I. Ultrasound of the peripheral nerves. In: *Clinical ultrasound*, vol. 2. Philadelphia: Elsevier; 2011. p. 1158–67.
 14. Gregoli B, Bortolotto C, Draghi F. Elbow nerves: normal sonographic anatomy and identification of the structures potentially associated with nerve compression. A short pictorial-video article. *J Ultrasound.* 2013;16(3):119–21.
 15. Korschake M, Stofferin H, Moriggl B. Ultrasound visualization of an underestimated structure: the bicipital aponeurosis. *Surg Radiol Anat.* 2017;39(12):1317–22. <https://doi.org/10.1007/s00276-017-1885-0>.
 16. Connell D, Burke F, Coombes P, McNealy S, Freeman D, Pryde D, Hoy G. Sonographic examination of lateral epicondylitis. *Am J Roentgenol.* 2001;176(3):777–82.
 17. Klauser AS, Pamminger M, Halpern EJ, Abd Ellah MMH, Moriggl B, Taljanovic MS, Deml C, Sztankay J, Klima G, Jäschke WR. Extensor tendinopathy of the elbow assessed with sonoelastography: histologic correlation. *Eur Radiol.* 2017;27(8):3460–6.
 18. Daniels DL, Mallisee TA, Erickson SJ, Boynton MD, Carrera GF. The elbow joint: osseous and ligamentous structures. *Radiographics.* 1998;18(1):229–36.
 19. Cohen MS, Bruno RJ. The collateral ligaments of the elbow: anatomy and clinical correlation. *Clin Orthop Relat Res.* 2001;383:123–30.
 20. Stroyan M, Wilk KE. The functional anatomy of the elbow complex. *J Orthop Sports Phys Ther.* 1993;17(6):279–88.
 21. Ozturk A, Kutlu C, Taskara N, Kale AC, Bayraktar B, Cecen A. Anatomic and morphometric study of the arcade of Frohse in cadavers. *Surg Radiol Anat.* 2005;27(3):171–5.
 22. Spinner M. The arcade of Frohse and its relationship to posterior interosseous nerve paralysis. *J Bone Joint Surg Br.* 1968;50(4):809–12.
 23. Tatar I, Kocabiyik N, Gayretli O, Ozan H. The course and branching pattern of the deep branch of the radial nerve in relation to the supinator muscle in fetus elbow. *Surg Radiol Anat.* 2008;31(8):591–6.
 24. Belentani C, Pastore D, Wangwinyuvirat M, Dirim B, Trudell DJ, Haghighi P, Resnick D. Triceps brachii tendon: anatomic-MR imaging study in cadavers with histologic correlation. *Skelet Radiol.* 2009;38(2):171–5.
 25. Dunn JC, Kusnezov N, Fares A, Rubin S, Orr J, Friedman D, Kilcoyne K. Triceps tendon ruptures: a systematic review. *Hand.* 2017;12(5):431–8.
 26. Shuttlewood K, Beazley J, Smith CD. Distal triceps injuries (including snapping triceps): a systematic review of the literature. *World J Orthop.* 2017;8(6):507–13.
 27. Babusiaux D, Laulan J, Bouilleau L, Martin A, Adrien C, Aubertin A, Rabarin F. Contribution of static and dynamic ultrasound in cubital tunnel syndrome. *Orthop Traumatol Surg Res.* 2014;100(4 Suppl):S209–12.
 28. Draghi F, Bortolotto C. Importance of the ultrasound in cubital tunnel syndrome. *Surg Radiol Anat.* 2016;38(2):265–8.
 29. Reilly D, Kaminen S. Olecranon bursitis. *J Shoulder Elb Surg.* 2016;25(1):158–67.
 30. Floemer F, Morrison WB, Bongartz G, Ledermann HP. MRI characteristics of olecranon bursitis. *Am J Roentgenol.* 2004;183(1):29–34.
 31. Del Buono A, Franceschi F, Palumbo A, Denaro V, Maffulli N. Diagnosis and management of olecranon bursitis. *Surgeon.* 2012;10(5):297–300.
 32. Assmus H, Antoniadis G, Bischoff C, Hoffmann R, Martini AK, Preissler P, Scheglmann K, Schwerdtfeger K, Wessels KD, Wüstner-Hofmann M. Cubital tunnel syndrome - a review and management guidelines. *Cen Eur Neurosurg.* 2011;72(2):90–8.
 33. Martinoli C, Bianchi S, Pugliese F, Bacigalupo L, Gauglio C, Valle M, Derchi LE. Sonography of entrapment neuropathies in the upper limb (wrist excluded). *J Clin Ultrasound.* 2004;32(9):438–50.
 34. Blackwell JR, Hay BA, Bolt AM, Hay SM. Olecranon bursitis: a systematic overview. *Should Elb.* 2014;6(3):182–90.
 35. do Nascimento AT, Claudio GK. Arthroscopic surgical treatment of medial epicondylitis. *J Shoulder Elb Surg.* 2017;26(12):2232–5.
 36. Morris HJ. Rider's sprain. *Lancet.* 1882;2:557.
 37. Ciccotti MG, Ramani MN. Medial epicondylitis. *Tech Hand Up Extrem Surg.* 2003;7:190–6.
 38. Créteur V, Madani A, Sattari A, Bianchi S. Sonography of the pronator teres: normal and pathologic appearances. *J Ultrasound Med.* 2017;36(12):2585–97. <https://doi.org/10.1002/jum.14306>.

Content Overview

Tendon-overuse syndromes

- Lateral epicondylitis
- Medial epicondylitis
- Triceps enthesopathy
- Distal biceps tendon enthesopathy

Tendon tears

Repaired tendons

Joint effusion

Intra-articular bodies

Bursitis

- Olecranon bursitis
- Bicipitoradial bursitis

Nerve compression

- Radial nerve compression
- Median nerve compression
- Ulnar nerve compression

Neuromas

Ulnar nerve instability

Traumatic elbow injuries

Soft-tissue masses

Skin and subcutaneous tissue lesions

Tendon-overuse syndromes, lateral epicondylitis (Fig. 4.1), medial epicondylitis (Fig. 4.2), triceps enthesopathy, distal biceps tendon enthesopathy (Table 4.1) (Fig. 4.3), can be caused by micro-trauma (Table 4.2), vascular compromise, and aging [1]. The most common cause is considered to be repetitive microtrauma, which results in the rupture of individual collagen fibers with a repar-

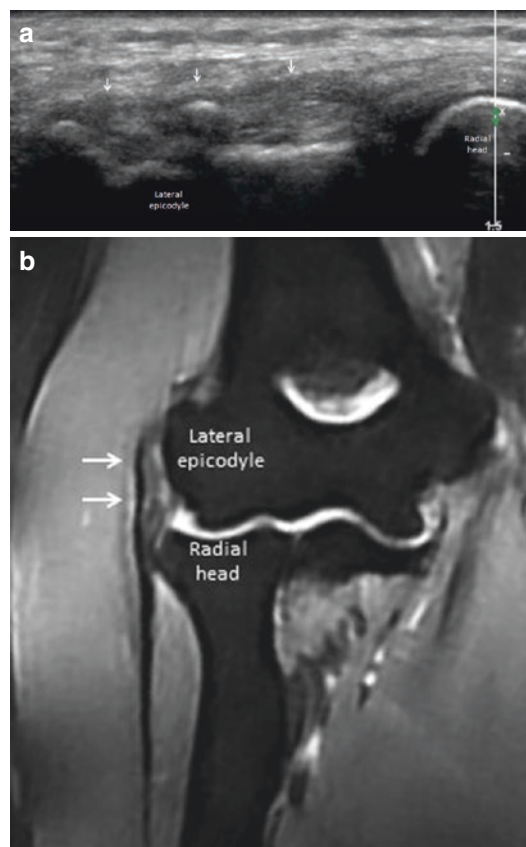


Fig. 4.1 Lateral epicondylitis. B-mode ultrasound image (a) of common extensor tendon (arrows) shows loss of echogenicity, hypoechoic areas (myxoid degeneration), hyperechoic areas (fibrosis, calcifications) of the tendon and bone irregularity of the lateral epicondyle. MRI image (b) same case as in (a). Arrows: common extensor tendon

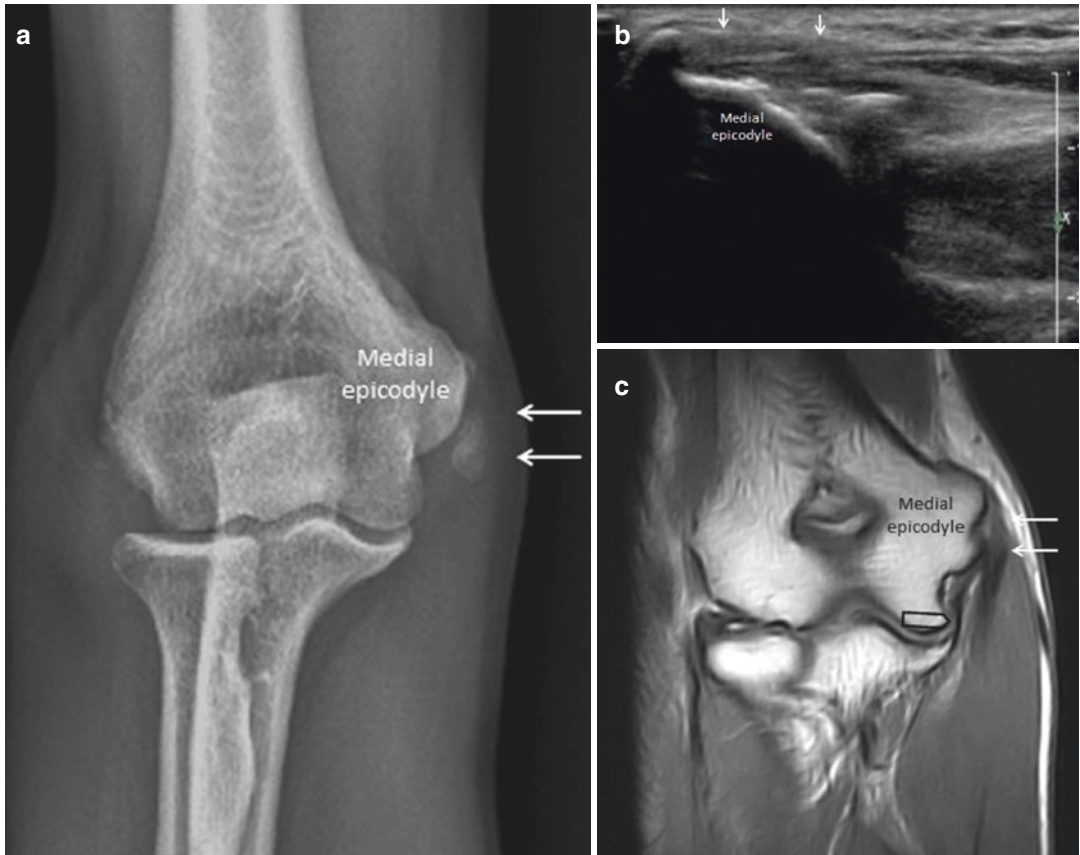


Fig. 4.2 Medial epicondylitis. Standard radiograph (a) shows extensive calcifications of common flexor tendon (arrows). B-mode ultrasound image (b) of common flexor tendon (arrows) shows loss of echogenicity and hyper-

echoic areas (fibrosis, calcifications) of the tendon. MRI image (c): same case as in (a, b). Arrows: common flexor tendon, void arrow: ulnar collateral ligament (anterior bundle)

Table 4.1 Most common pathologic conditions of the elbow by compartment

Compartment	Most common pathologic conditions
Lateral	Lateral epicondylitis
	Posterior interosseous nerve entrapment
Anterior	Distal biceps tendon tear
	Bicipitoradial bursitis
	Median nerve entrapment and/or tear
	Joint effusion
Medial	Medial epicondylitis
Posterior	Distal triceps tendon tear
	Olecranon bursitis
	Joint effusion
	Ulnar nerve compression and/or dislocation

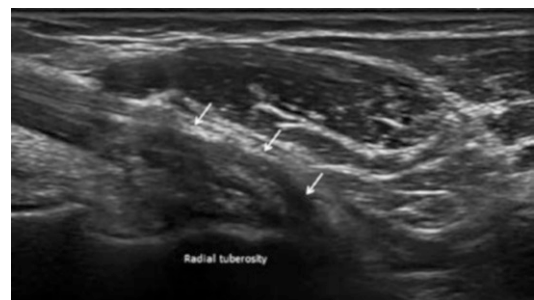


Fig. 4.3 Distal biceps tendon enthesopathy. B-mode ultrasound image shows loss of echogenicity, hypoechoic areas (myxoid degeneration), hyperechoic areas (fibrosis, calcifications) of the tendon (arrows)

Table 4.2 Elbow sports-related injuries

Sport activity	Injuries
Tennis	Lateral epicondylitis
Golf	Medial epicondylitis, ulnar nerve entrapment, pronator teres syndrome
Javelin	Medial collateral ligament sprain
Weightlifting	Distal biceps tendinopathy, ulnar nerve entrapment, radial tunnel syndrome
Boxing	Triceps tendinopathy
Skiing	Ulnar nerve entrapment
Swimming	Radial tunnel syndrome

ative response and tendon degeneration. In chronic disease, tendon microrupture and repair results in weakening of the tendon and leads to the risk of rupture [2].

Histological examination shows non-inflammatory, degenerative, angio-fibroblastic changes, with focal areas of myxoid and hyaline degeneration, fibrosis, and calcifications [1, 2]. There is no evidence of inflammatory cells in either the acute or chronic stage [3].

The most common symptoms are localized pain (Table 4.3) and reduced function [4].

The ultrasound findings are the same in all overuse syndromes: the tendon is frequently thickened, with loss or not of the normal internal fibrillar pattern; hypoechoic foci (myxoid degeneration) and/or hyperechoic areas (fibrosis or calcifications) within the affected tendon; bone irregularity can also be seen [5, 6]. Color Doppler signals correlate with neoangiogenesis and capillary proliferation. Sonoelastography may provide improvement in correlation with histologic results [7].

Elbow tendon tears include complete or partial tears and avulsions that involve the tendons' distal insertion.

Partial tears of the common extensor tendon are the most frequent tendon ruptures in the elbow, generally seen after intra-tendinous steroid injections for the local treatment of overuse syndromes (Fig. 4.4) [1, 5, 6, 8]. Partial tears of common flexor tendons are rarer. The most frequent tendon complete ruptures are those of the distal biceps brachii tendon (Fig. 4.5). They gen-

Table 4.3 Pain and differential diagnosis

Lateral pain	Lateral epicondylitis, lateral epicondyle—radial head fractures, varus-posterolateral instability
Anterior pain	Biceps tendonitis-tears-avulsion, bicipitoradial bursitis, anterior impingement
Medial pain	Medial epicondylitis, cubital tunnel syndrome, medial epicondyle fractures, valgus instability
Posterior pain	Olecranon bursitis, triceps tendon injury, olecranon fractures, posterior impingement



Fig. 4.4 Partial tear of the common extensor tendon. B-mode ultrasound image shows epicondylitis with a partial tear (arrows) in a patient after intra-tendinous steroid injections for the local treatment of overuse syndromes

erally occur in middle-aged subjects as a result of violent traction on the tendon, while the elbow is flexed. Triceps ruptures are relatively rare, while tendon avulsions from the olecranon are more frequent [9].

Sonographically, complete ruptures present with complete interruption of tendon fiber continuity. Widening of the gap between the proximal and distal tendon stumps can be proved by using dynamic maneuvers. Partial tears present with incomplete disruption of tendon fiber continuity. Hemorrhage is present in cases of acute or sub-acute tears. Generally, there is no evidence of hematoma in the case of chronic injuries (Fig. 4.6).

After surgery, tendon appearance differs from that of a healthy non-operated tendon in several characteristics [10, 11]. Repaired tendons are larger and wider than non-operated ones and show an inhomogeneous echo texture with a loss of the fibrillar pattern (Fig. 4.7). The surgical material can be found in the context of the tendon. Tendon gliding is physiologically reduced

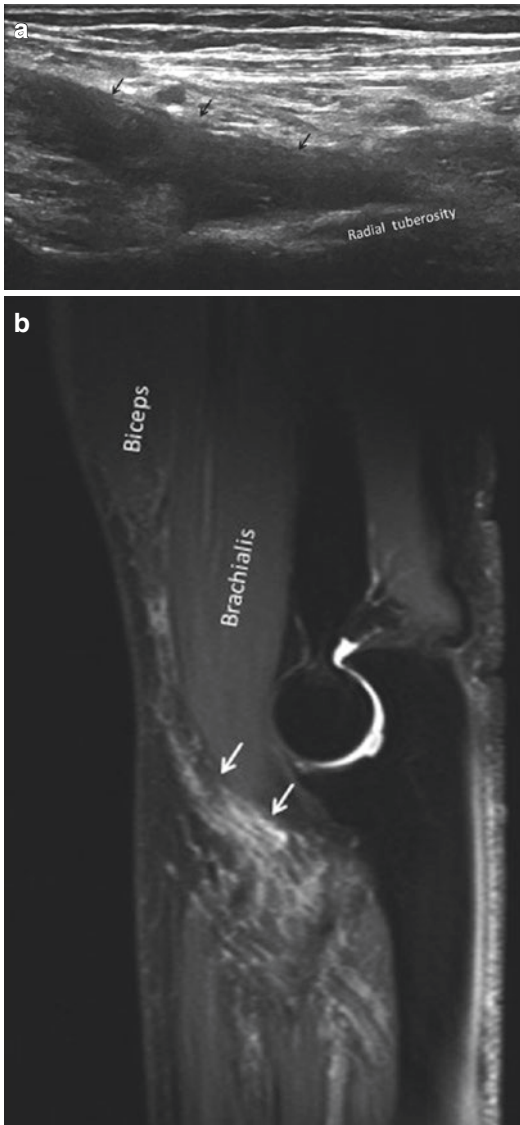


Fig. 4.5 Complete, recent, distal biceps tear. Long-axis ultrasound scan (a) shows complete interruption of tendon fiber and a large hematoma (arrows). MRI image (b): same case as in figure a. Arrows: hematoma

under a dynamic examination. Large fluid collections as well as extensive calcifications should instead be considered pathologic findings. Doppler imaging shows no vascularization in the immediate postoperative period. Intra-tendinous vascularization physiologically increases in the first 3 months after surgery and then stabilizes and finally regresses within 6 months. Beyond the first 6 months, persistent hypervasculariza-

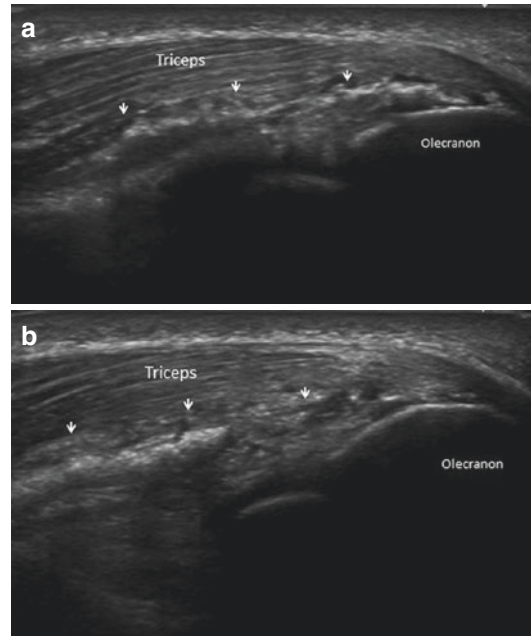


Fig. 4.6 Chronic triceps partial tear. B-mode ultrasound image (a, b) shows partial loss of echogenicity, extensive calcifications (arrows)



Fig. 4.7 Common extensor tendon after surgery. The tendon is larger and wider than non-operated ones and shows an inhomogeneous echo texture with a loss of the fibrillar pattern

tion is pathologic. Sonography has been proven to be effective in evaluating tendon integrity and detecting complications after surgical repair. Knowledge of the normal and pathologic sonographic features after surgery is required.

Joint effusion may be the result of overuse syndromes, chronic osteoarthritis, inflammatory arthropathy (rheumatoid arthritis, gout, pseudogout), or infection. A synovial thickening of variable echogenicity within the synovial fluid may be

seen in patients with rheumatoid arthritis, synovial proliferative disorder as pigmented villonodular synovitis or synovial osteochondromatosis [5, 12].

Joint effusions may be simple and anechoic or complex containing internal echogenicity. Internal echogenicity may indicate inflammation, infection, hemorrhage, or intra-articular bodies [13].

Ultrasound detection of an elbow effusion is readily amenable as fluid distention of the anterior or posterior joint recesses. Sonography with joint in flexion is the most sensitive means to demonstrate effusion in the posterior recess [14]. With the transducer in the sagittal plane, displacement of the posterior fat pad superiorly will be appreciated.

The elbow is the second most common site of intra-articular bodies after the knee [15]. The recesses are common sites for intra-articular bodies (Fig. 4.8). The fluid helps in the identification of intra-articular ossified and non-ossified bodies that will appear hyperechoic [16]. Additional findings, including the mobility of loose bodies, and synovial proliferation, can also be assessed with ultrasound.

Synovial bursae consist of a synovial membrane enveloping a film of liquid. They are located at interfaces between moving structures, where friction must be reduced [17, 18].

Inflammation of a bursa is often caused by repetitive microtrauma, other causes of bursitis include infection (tuberculosis, etc.), arthropathy (rheumatoid arthritis, psoriatic arthritis, etc.),

villonodular synovitis, osteochondromatosis, and amyloidosis.

The most common forms of bursitis of the elbow are olecranon (Fig. 4.9) and Bicipitoradial

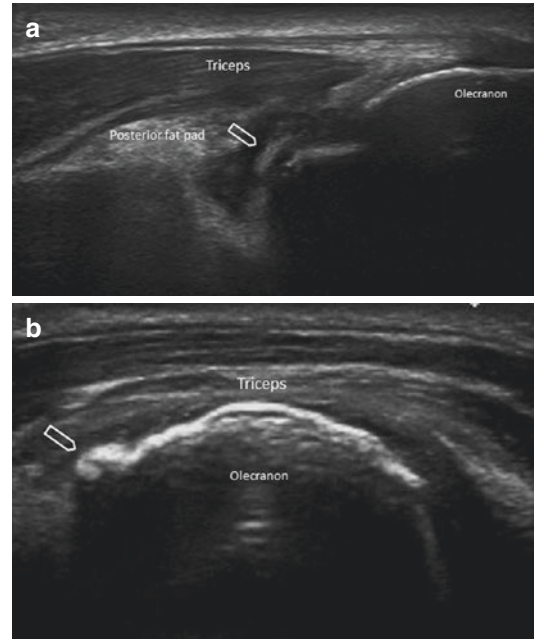


Fig. 4.8 Elbow effusion. Sonography, with joint in flexion, demonstrates effusion in the posterior recess. With the transducer in the sagittal plane, displacement of the posterior fat pad superiorly is appreciated (a). Intra-articular bodies (void arrow) are evident in both the sagittal (a) and axial (b) planes

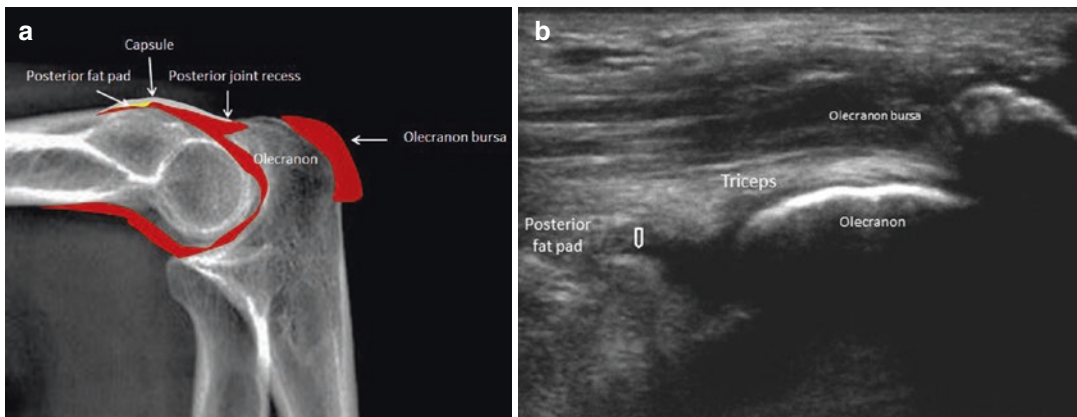


Fig. 4.9 Patient with rheumatoid arthritis and chronic olecranon bursitis. Longitudinal posterior elbow: schematic diagram (a), sonogram (b). With joint in flexion, effusion and intra-articular bodies (void arrow) in the pos-

terior recess are evident; displacement of the posterior fat pad superiorly is also appreciated. Mixed echogenicity, fluid, debris, and rice bodies are evident in the olecranon bursa

bursitis (Fig. 4.10). Because of its superficial location, the olecranon bursa is a common site for injury, inflammation, and infection [19]. Patients present with a tender palpable swelling over the posterior elbow. The bicipitoradial bursa is located between the distal biceps tendon and the radial tuberosity to reduce friction during pronation of the forearm. Bursitis, which is usually the result of distal biceps tendon tears, microtrauma, or rheumatoid arthritis, results in swelling, pain, and in some cases neurological symptoms related to radial nerve compression [20].

Ultrasound examination can easily confirm the diagnosis of bursitis, demonstrating also small amounts of fluid collection and/or synovial wall hypertrophy. Fluid collection and/or synovial wall hypertrophy may result in a complex appearance in hemorrhagic and septic bursitis.

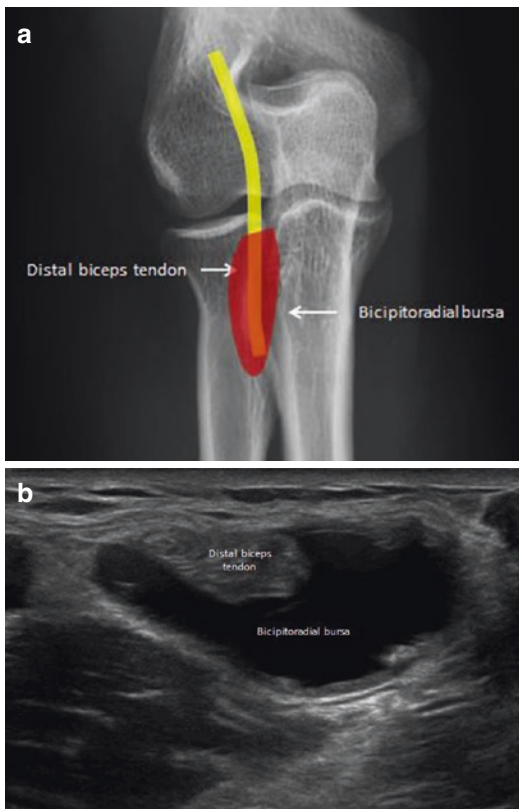


Fig. 4.10 Bicipitoradial bursitis: schematic diagram (a), sonogram (b). Sonography (b) shows an anechoic formation (bicipitoradial bursa) surrounding the distal biceps tendon

Hyperemia of the soft-tissue around the bursa is often recognized with Doppler imaging as an accompanying finding.

In the elbow many structures are potentially associated with nerve compression [21, 22].

The radial nerve is situated in a fat plane between the brachial muscle and the long radial extensor muscle of the wrist, subsequently dividing below the elbow joint into the superficial and the posterior interosseous branches. The superficial radial nerve may be most often subject to chronic compression by bicipitoradial bursa. The posterior interosseous nerve may be compressed between the superficial and deep portions of the supinator muscle during pronation-supination of the elbow.

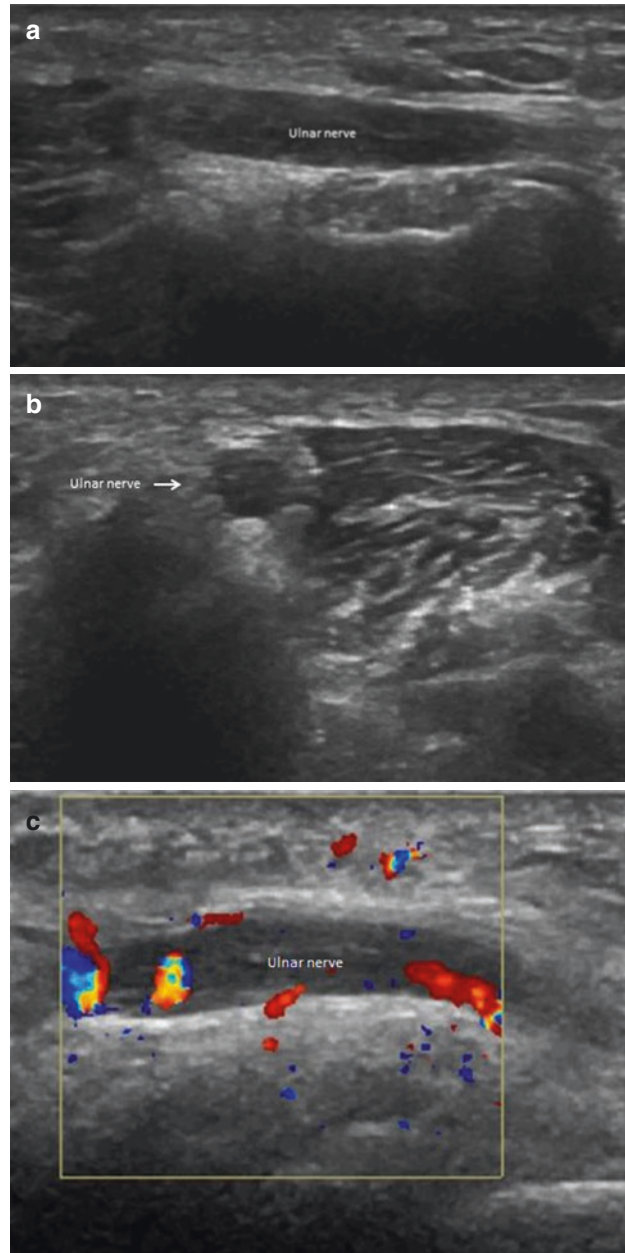
The median nerve travels between the brachial and pronator teres muscles, coursing between the ulnar and radial heads of the latter. The median nerve may be compressed, for example, by thickened lacertus fibrosus, the bicipital aponeurosis which descends medially, across the brachial artery and median nerve, to fuse with fascia of flexor muscles of the forearm.

The ulnar nerve is positioned superficially at the elbow. It runs posterior to the medial humeral epicondyle and medial to the LCL, along with the posterior recurrent ulnar artery and vein. These elements occupy the cubital tunnel, which is covered by a thin arcuate ligament. Physiologic compression of the nerve in the cubital tunnel occurs during elbow flexion, but compression may also occur owing to bursae, effusion, and anconeus epitrochlearis muscles, etc. [23, 24].

The main sonographic signs of nerve compression are swelling proximal to the site of compression, thinning at the site of compression, the hypoechoic appearance of the nerve with loss of the fascicular pattern (Fig. 4.11a, b) and hyperemia with Doppler imaging (Fig. 4.11c). Sonography may be required to locate nerve lesions, but primarily to evaluate the causes of compression and help with the therapy.

Because of its superficial location, the elbow's nerves often present post-traumatic lesions [25]. Partial and complete tears of a nerve may result in neuromas. Neuromas are a hyperplastic disorder

Fig. 4.11 Entrapment neuropathy of the ulnar nerve. Sonography shows hypoechoic swelling of the ulnar nerve with loss of the fascicular pattern (**a, b**) and hyperemia with Doppler imaging (**c**)



ganized proliferation of cells (neural cells, axons, myelin, Schwann cells, and fibroblasts), which represent an attempt at nerve regeneration. The proliferation passes beyond the perineurium and infiltrates the perineural connective tissue [26]. Neuromas can be classified into terminal neuroma and neuroma in-continuity. The terminal neuroma is most frequently localized at the proximal stump; the neuroma-in-continuity is similar

to the terminal neuroma, but connects the two nerve stumps with a variable saving of nervous tissue.

They are often clinically palpable as painful small, firm, tender masses. The ultrasound appearance is that of a hypoechoic mass (Fig. 4.12) and placing and pressing the transducer on the neuroma may cause local pain and paresthesia.

Intermittent instability typically affects the ulnar nerve at the elbow. An absence of the superficial retinaculum at the proximal cubital tunnel predisposes to anterior instability of the nerve during elbow flexion [27]. The instability usually does not lead to any pathological nerve changes but chronic friction can lead to nerve and impaired function in some patients (Fig. 4.13).

Traumatic elbow injuries are commonly encountered, but their complexity and clinical significance often go unrecognized at the initial evaluation [28]. Among the various elbow injuries that initially have normal radiographs, a cer-

tain number of occult fractures are only diagnosed correctly after the fact, during a follow-up visit, particularly in children [29].

Ultrasonography is highly sensitive for elbow fracture [30, 31], showing fractures as an interruption of the hyperechogenic line representing the cortical bone (Figs. 4.14 and 4.15). In traumatic elbow injuries, sonography may detect bone abnormalities but also soft-tissue injuries (Fig. 4.14), that could place the patient at risk of chronic joint instability.

Collateral ligaments are thickenings of the joint capsule that limit valgus and varus displacement. Parts of the radial and ulnar collateral ligaments are shown by sonography. No evidence and consensus exist to evaluate the ligamentous complex by ultrasound. It is, however, possible to evaluate ligament injury or loss of ligaments in some cases (Fig. 4.16).

Soft-tissue masses (Figs. 4.17, 4.18, 4.19, and 4.20) are common entities encountered in musculoskeletal patients. Ultrasound has high sensitivity in detection of lesions but low specificity with the exception of structures such as ganglia.

Proper management requires a specific process of evaluation: a detailed history and physical examination must be performed. Appropriate imaging studies must be obtained: MRI is the imaging modality of choice for the diagnosis of soft-tissue masses, with ultrasonography used as a secondary option [32].

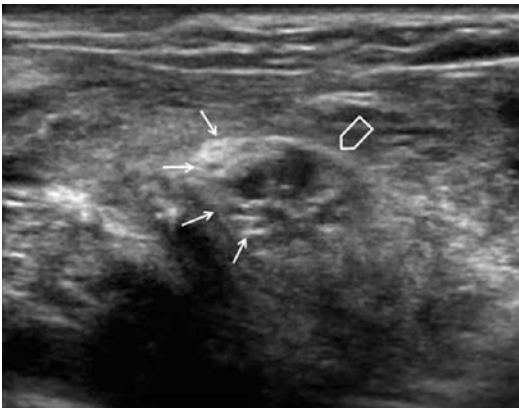


Fig. 4.12 Post-traumatic in-continuity neuroma of median nerve at the elbow. The axial sonogram, obtained over the injured portion of the nerve shows a hypoechoic post-traumatic neuroma (white arrow) affecting the anterior part of the nerve. The nerve presents a normal fascicular pattern in the posterolateral part (arrows)

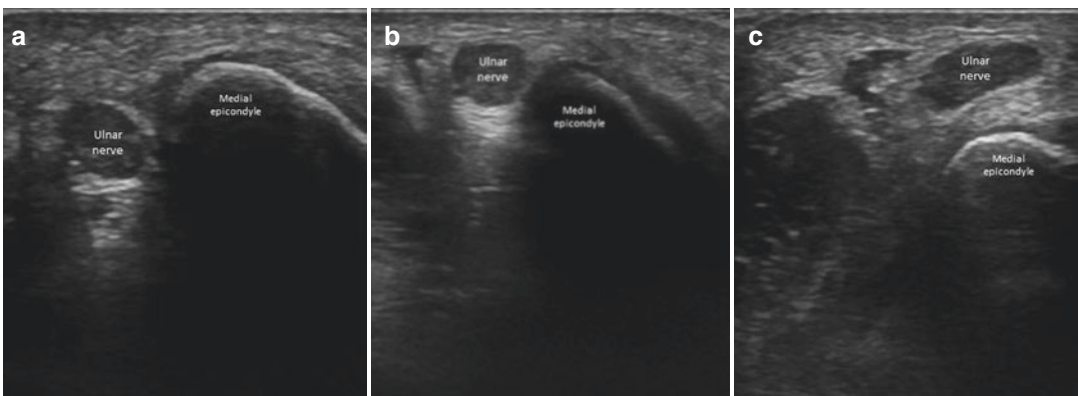


Fig. 4.13 Ulnar nerve instability. Axial sonograms of the cubital tunnel during elbow flexion (a–c) show that the nerve is suddenly displaced anterior to the medial epicondyle (c). The nerve is hypoechoic and swelling

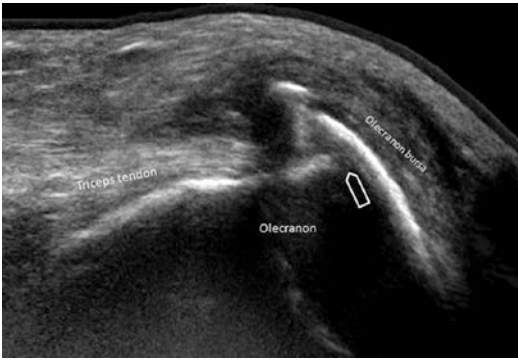


Fig. 4.14 Olecranon fracture. The ultrasound shows the olecranon fracture (void arrow) as interruption of the hyperechogenic line representing the cortical bone, the bursitis of the olecranon bursa, and a normal triceps tendon



Fig. 4.17 Ganglion cyst. Ultrasonography shows a firm, poorly compressible anechoic masse with well-defined margins. The etiology is unknown; ganglia are probably the result of mucinous degeneration of periarticular and peritendinous connective tissues. Usually do not communicate with the joints

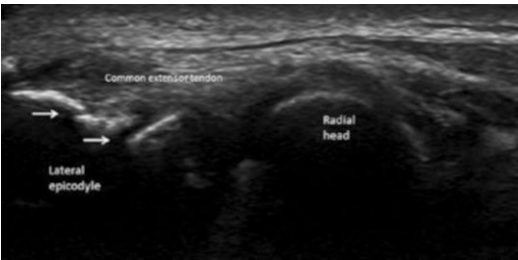


Fig. 4.15 Epicondyle fracture. The ultrasound shows the epicondyle fractures (arrows) as an interruption of the hyperechogenic line representing the cortical bone and the normal extensor tendon

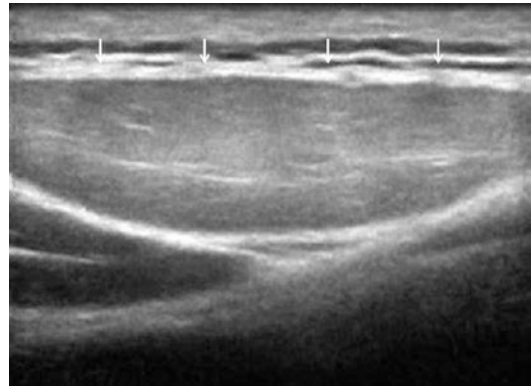


Fig. 4.18 Subcutaneous lipoma. Long-axis image shows an elongated well-defined mass with its greatest diameter parallel to the skin. The mass appears slightly hyperechoic relative to adjacent fat

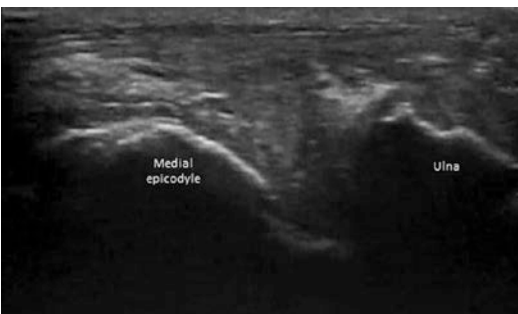


Fig. 4.16 Chronic humero-ulnar joint dislocation. Ultrasonography shows widening of the joint space

A sonographic diagnostic procedure is often useful to obtain a biological sample (fluid or cellular) in order to determine the etiology of the lesion [33]. These modalities aid the clinician in

developing an appropriate differential diagnosis and treatment plan.

To evaluate lesions of the skin and subcutaneous tissue, sonography is useful in many settings: measurement of the thickness of skin and subcutaneous tissue in abnormalities such as edema (Fig. 4.21) cellulitis, abscess and necrotizing fasciitis, and in chronic inflammatory processes in the evaluation of tumors prior to and during therapy. As for other lesions, a sonographic diagnostic procedure is often useful to obtain a biological sample (fluid or cellular) in order to determine the etiology of the lesion [33].

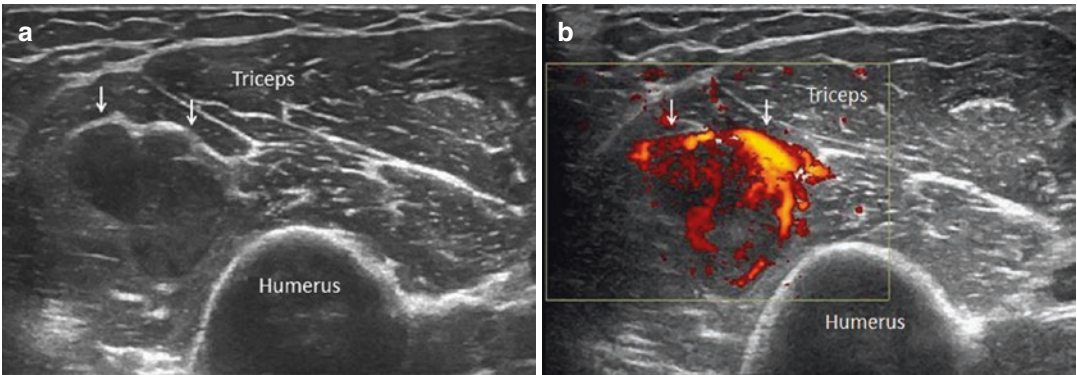
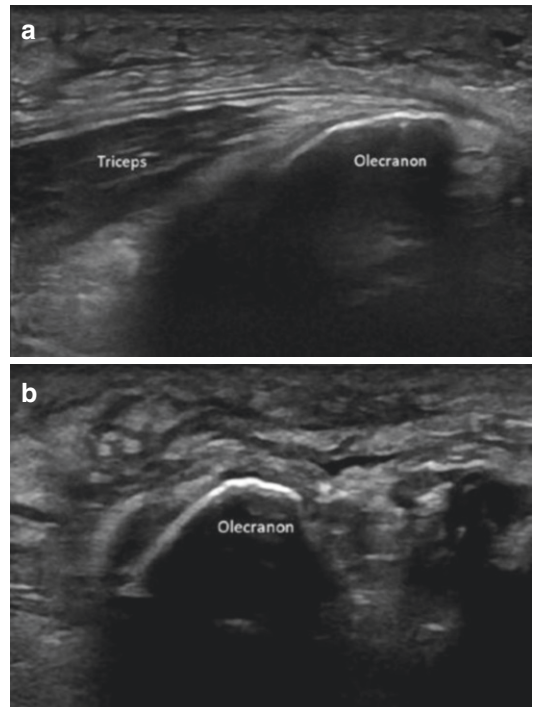


Fig. 4.19 Triceps myeloma. Gray-scale sonogram shows a circumscribed, oval, complex mass within the triceps muscle (a) (arrows). Power Doppler sonogram demonstrates a rich vascularization within the mass (b)



Fig. 4.20 Triceps rhabdomyosarcoma. Gray-scale sonograms shows a complex mass within the triceps muscle (a, b) (arrows). Color Doppler sonogram demonstrates a rich vascularization within the mass (c)

Fig. 4.21 Subcutaneous tissue edema. Longitudinal (a) and transverse (b) ultrasound images over the triceps region shows fluid distention of the lymphatics and increased echogenicity of fat lobules



References

1. Draghi F, Danesino GM, de Gautard R, Bianchi S. Ultrasound of the elbow: examination techniques and US appearance of the normal and pathologic joint. *J Ultrasound*. 2007;10(2):76–84.
2. De Zordo T, Lill SR, Fink C, Feuchtner GM, Jaschke W, Bellmann-Weiler R, Klauser AS. Real-time sonoelastography of lateral epicondylitis: comparison of findings between patients and healthy volunteers. *Am J Roentgenol*. 2009;193(1):180–5.
3. Ashe MC, McCauley T, Khan KM. Tendinopathies in the upper extremity: a paradigm shift. *J Hand Ther*. 2004;17:329–34.
4. Connell D, Burke F, Coombes P, et al. Sonographic examination of lateral epicondylitis. *Am J Roentgenol*. 2001;176:777–82.
5. Konin GP, Nazarian LN, Walz DM. US of the elbow: indications, technique, normal anatomy, and pathologic conditions. *Radiographics*. 2013;33(4):E125–47.
6. Radunovic G, Vlad V, Micu MC, Nestorova R, Petranova T, Porta F, Iagnocco A. Ultrasound assessment of the elbow. *Med Ultrason*. 2012;14(2):141–6.
7. Klauser AS, Pamminger MJ, Halpern EJ, Abd Ellah MMH, Moriggl B, Taljanovic MS, Deml C, Sztankay J, Klima G, Gruber L, Jaschke WR. Sonoelastography of the common flexor tendon of the elbow with histologic agreement: a cadaveric study. *Radiology*. 2017;283(2):486–91.
8. Nichols AW. Complications associated with the use of corticosteroids in the treatment of athletic injuries. *Clin J Sport Med*. 2005;15(5):370–5.
9. Stevens MA, El-Khoury GY, Khatol MH, Brandser EA, Chow S. Imaging features of avulsion injuries. *Radiographics*. 1999;19:655–72.
10. Cohen M. US imaging in operated tendons. *J Ultrasound*. 2012;15:69–75.
11. Gitto S, Draghi AG, Bortolotto C, Draghi F. Sonography of the Achilles tendon after complete rupture repair: what the radiologist should know. *J Ultrasound Med*. 2016;35:2529–36.
12. Draghi F, Urciuoli L, Alessandrino F, Corti R, Scudeller L, Grassi R. Joint effusion of the knee: potentialities and limitations of ultrasonography. *J Ultrasound*. 2015;18(4):361–71.
13. Finlay K, Ferri M, Friedman L. Ultrasound of the elbow. *Skelet Radiol*. 2004;33(2):63–79.
14. De Maeseneer M, Jacobson JA, Jaovisidha S, et al. Elbow effusions: distribution of joint fluid with flexion and extension and imaging implications. *Investig Radiol*. 1998;33(2):117–25.
15. Martinoli C, Bianchi S, Giovagnorio F, Pugliese F. Ultrasound of the elbow. *Skelet Radiol*. 2001;30(11):605–14.
16. Bianchi S, Martinoli C. Detection of loose bodies in joints. *Radiol Clin N Am*. 1999;37(4):679–90.
17. Bianchi S, Martinoli C. Ultrasound of the musculoskeletal system. Berlin: Springer; 2007. p. 349–407.
18. Draghi F, Corti R, Urciuoli L, Alessandrino F, Rotondo A. Knee bursitis: a sonographic evaluation. *J Ultrasound*. 2015;18(3):251–7.
19. Shell D, Perkins R, Cosgarea A. Septic olecranon bursitis: recognition and treatment. *J Am Board Fam Pract*. 1995;8:217–20.
20. Draghi F, Gregoli B, Sileo C. Sonography of the bicipitoradial bursa: a short pictorial essay. *J Ultrasound*. 2012;15(1):39–41.
21. Bianchi S, Draghi F, Beggs I. Ultrasound of the peripheral nerves. In: *Clinical ultrasound*, vol. 2. Philadelphia: Elsevier; 2011. p. 1158–67.
22. Gregoli B, Bortolotto C, Draghi F. Elbow nerves: normal sonographic anatomy and identification of the structures potentially associated with nerve compression. A short pictorial-video article. *J Ultrasound*. 2013;16(3):119–21.
23. Draghi F, Bortolotto C. Importance of the ultrasound in cubital tunnel syndrome. *Surg Radiol Anat*. 2016;38(2):265–8.
24. Padua L, Di Pasquale A, Liotta G, Granata G, Pazzaglia C, Erra C, Briani C, Coraci D, De Franco P, Antonini G, Martinoli C. Ultrasound as a useful tool in the diagnosis and management of traumatic nerve lesions. *Clin Neurophysiol*. 2013;124(6):1237–43.
25. Alessandrino F, Pagani C, Draghi F. In-continuity neuroma of the median nerve at the elbow. *J Ultrasound*. 2014;17(3):229–31.
26. Martinoli C, Bianchi S, Dahmane M, Pugliese F, Bianchi S, Zamorani MP, Valle M. Ultrasound of tendons and nerves. *Eur Radiol*. 2002;12(1):44–55.
27. Martinoli C, Bianchi S, Gandolfo N, et al. Ultrasound of nerve entrapments in osteofibrous tunnels. *Radiographics*. 2000;20:S199–213.
28. Sheehan SE, Dyer GS, Sodickson AD, Patel KI, Khurana B. Traumatic elbow injuries: what the orthopedic surgeon wants to know. *Radiographics*. 2013;33(3):869–88. <https://doi.org/10.1148/rg.333125176>.
29. Burnier M, Buisson G, Ricard A, Cunin V, Pracros JP, Chotel F. Diagnostic value of ultrasonography in elbow trauma in children: prospective study of 34 cases. *Orthop Traumatol Surg Res*. 2016;102(7):839–43.
30. Rabiner JE, Khine H, Avner JR, Friedman LM, Tsung JW. Accuracy of point-of-care ultrasonography for diagnosis of elbow fractures in children. *Ann Emerg Med*. 2013;61(1):9–17.
31. Gitto S, Draghi AG, Draghi F. Sonography of non-neoplastic disorders of the hand and wrist tendons. *J Ultrasound Med*. 2018;37:51–68.
32. Mayerson JL, Scharschmidt T, Lewis VO, Morris CD. Diagnosis and management of soft-tissue masses. *Instr Course Lect*. 2015;64:95–103.
33. Draghi F, Robotti G, Jacob D, Bianchi S. Interventional musculoskeletal ultrasonography: precautions and contraindications. *J Ultrasound*. 2010;13(3):126–33.

Content Overview

Biceps muscle and tendon

- Complete tendon rupture
- Partial tendon rupture
- Avulsion fractures
- Tendinopathy

Lacertus fibrosus

- Complete tear
- Partial tear
- Median nerve compression

Brachialis muscle and tendon

- Complete tear
- Partial tear

Bicipitoradial bursa

- Bursitis
- Compression of the radial nerve

Median nerve

- Median nerve compression
- Median nerve neuroma

Anterior recess

- Elbow effusion
- Loose bodies

The biceps muscle is located superficial to the brachialis muscle, lateral to the brachial artery and median nerve. Its tendon is a long tendon, approximately 7 cm long, that has an oblique course and 90° rotation, and attaches to the radial tuberosity [1, 2].

From the morphological point of view, two main sonographic patterns have been described, a

single tendon and a tendon with two separate components [3, 4]. Recent studies show that the tendon is always formed by two components of strictly parallel fascicles, joined by a common paratenon and a lax endotenon septum. The two fascicles correspond to the long head of the muscle (lateral), that has a deep insertion, and to the short head (medial), that has a superficial insertion [5].

Complete rupture of the tendon generally occurs as a single traumatic injury, with forced extension against resistance and the elbow positioned in mid-flexion [6]. Typically, patients present with sudden anterior elbow pain and describe a popping sensation [7, 8]. Clinically, there is often a palpable defect in the antecubital fossa, proximal soft tissue mass, and difficulty with flexion and supination.

Complete rupture appears on ultrasound as an anechoic or hypoechoic discontinuity of tendon fibers, with or without retraction, and surrounding hypoechoic fluid (Fig. 5.1).

Retracted tears do not always require imaging, since they are clinically evident. However, sonography plays an important role in evaluating partial (Fig. 5.2) or nonretracted tears due to an intact lacertus fibrosus (Fig. 5.3).

Also, partial tears of the distal biceps tendon occur as a single traumatic event, sustained by a sudden eccentric contraction of the muscle against resistance. There is an important difference between the patients with a tear involving the short head and those with a tear involving the

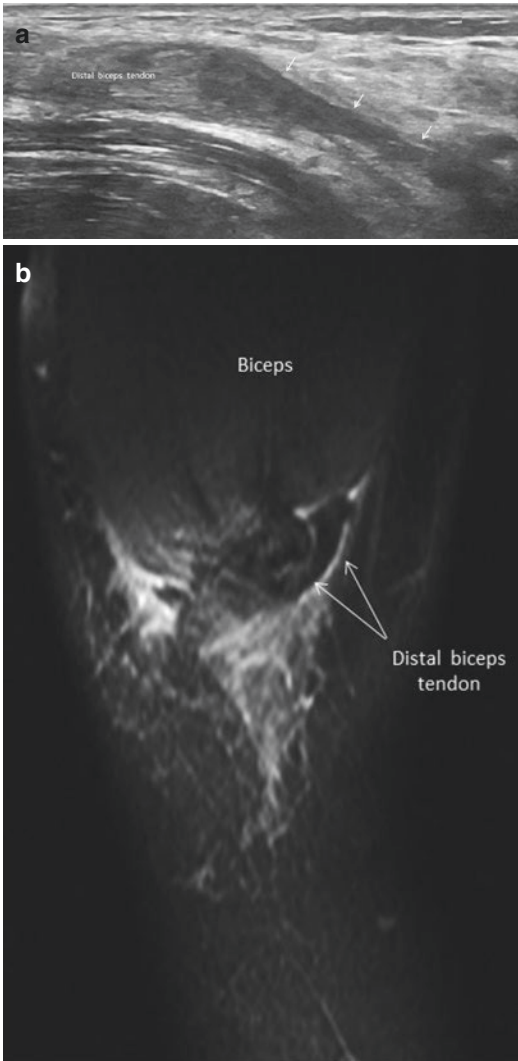


Fig. 5.1 Distal biceps tendon complete tear. Long-axis ultrasound scan (a) shows complete interruption of the tendon, which is retracted and twisted with a large hematoma (arrows). MRI image (b): same case as in (a)

long head. The first generally do not present retraction of the muscle, while the patients with a tear of the long head have the typical Popeye sign, mimicking a complete tear.

Partial rupture appears on ultrasound as an anechoic or hypochoic partial discontinuity of tendon fibers and surrounding hypochoic fluid (Fig. 5.2); in the chronic phase, no fluid is present and the tendon presents with heterogeneity and thickening (Fig. 5.4).

Common lesions, such as avulsion fractures and detached bony fragments, are more often

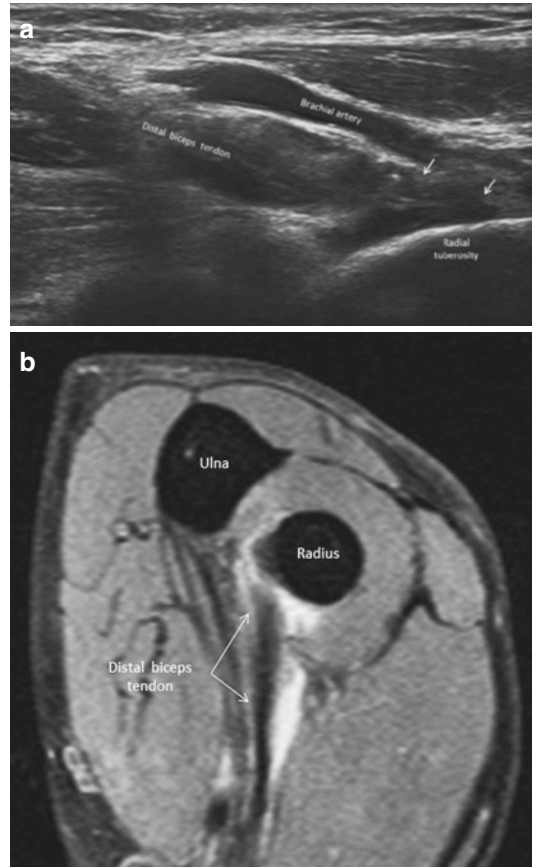


Fig. 5.2 Distal biceps partial tear. Longitudinal ultrasound image shows a partial tear of the deep portion of the tendon, while anterior fibers (arrows) remain attached to the radial tuberosity; fluid is present around the tendon. MRI image (b): same case as in (a)

related to the deep head. Also small bony avulsions are easily visible with ultrasound for the presence of edema and effusion.

Tendinopathy is unusual and generally associated with chronic pain, that has a progressive course. It causes disorganized, diffuse, heterogeneous thickening of the tendon, with loss of the fibrillar aspect [9] (Fig. 5.5). These tendinopathies may be worsened by fissuration. There is need for studies of these lesions with the tendon relaxed (elbow slightly flexed), to avoid collapse of the fissures during extension/supination [10]. Enthesopathies are far more common than tendinopathies. They are associated with hypochoic swelling that involves one or both of the tendons corresponding to the short head or long head. A posterior approach is useful to evaluate these lesions with ultrasound.

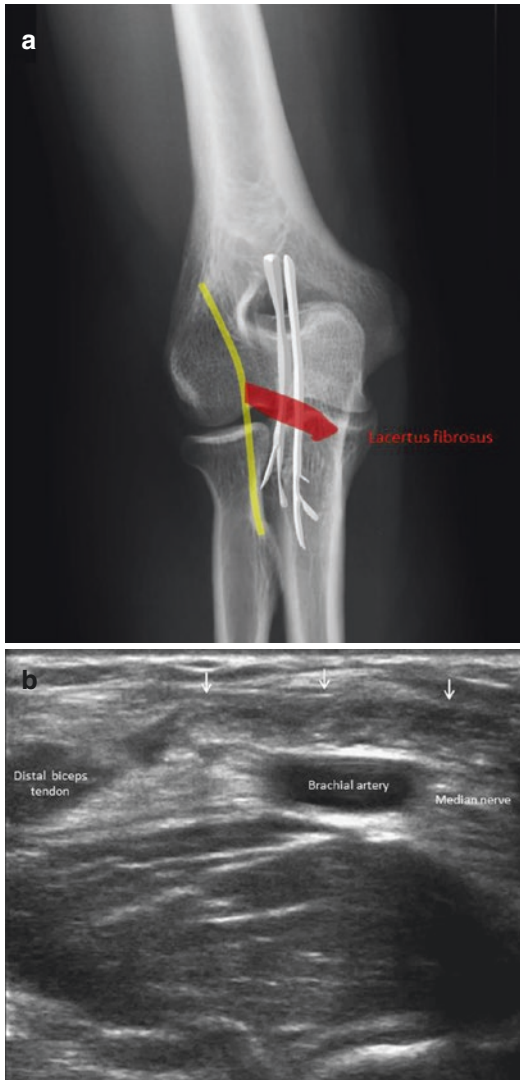


Fig. 5.3 Distal biceps and lacertus fibrosus partial tear. (a) Schematic diagram. (b) Ultrasound image showing thickening of the lacertus fibrosus (arrows) with brachial artery and median nerve compression

The biceps muscle is attached distally to the radial tuberosity, via the biceps tendon, and to the antebrachial fascia, via the bicipital aponeurosis or lacertus fibrosus [11].

The function of the lacertus fibrosus is transmission of the force from muscle to non-muscular tissue. In doing so, it supports flexion of the elbow and stabilizes the distal biceps tendon, reducing its stress at the enthesis.

The lacertus fibrosus is seen as a double contour emerging from the myotendinous junction of

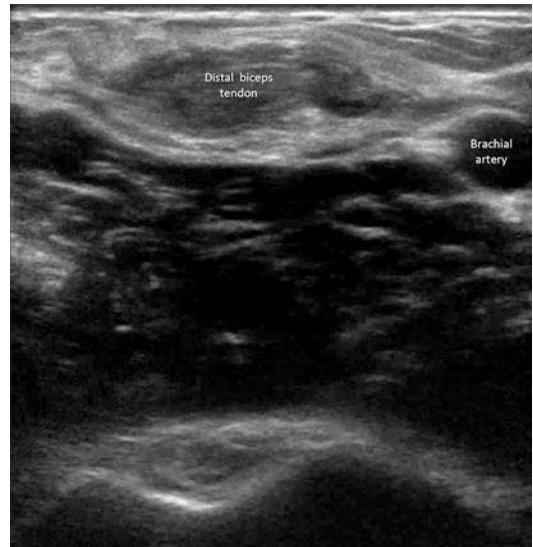


Fig. 5.4 Distal biceps tendon after partial tear. Short-axis ultrasound image shows heterogeneity and marked thickening of the tendon; no fluid is present



Fig. 5.5 Distal biceps tendinosis. Long-axis ultrasound image shows heterogeneity and marked thickening of the tendon (arrows)

the biceps brachii muscle, bridging the brachial artery and the median nerve and connecting to the antebrachial fascia that covers the pronator teres muscle.

Sonographic imaging of the lacertus fibrosus could provide a fast and cost-effective tool in several different pathologies, particularly in partial tears of the distal biceps' attachments, where a contiguity of the short biceps head and an intact lacertus fibrosus prevents typical retraction of the muscle belly, complicating a fast diagnosis.

Another distinct entity is median nerve compression by the lacertus fibrosus as a result of partial rupture of the aponeurosis (Fig. 5.3) or partial rupture of the lateral, distal myotendinous junction of the biceps.

The brachialis muscle is located deep to the biceps brachii muscle and inserts onto the anterior surface of the coronoid process of the ulna.

The distal insertion of the brachialis on the ulnar tuberosity may be purely muscular, tendinous, or mixed. The brachialis muscle has been described as having two separate heads, superficial and deep. The attachment of the superficial head is farther distal than that of the deep head. However, the two heads attach to the ulnar tuberosity as a single contiguous structure in a blended manner. Isolated tears of the brachialis tendon and muscle are rare injuries that have been infrequently reported in the literature [12–19].

The bicipitoradial bursa lies between the distal biceps tendon (anterior) and the radial tuberosity (posterior) [20] and envelopes the biceps tendon [21]. Particularly during supination of the forearm, the bursa surrounds the distal biceps tendon, while during pronation it is compressed between the radial tuberosity, which becomes posterior, and the distal tendon of the biceps.

It is a fairly large bursa ranging from 2.4 to 3.9 cm. Sometimes septated, it does not communicate with the joint cavity, but may communicate with the interosseous bursa.

The role of this bursa is to reduce friction between the biceps tendon and the tuberosity of the radius [22]. The most common causes of bicipitoradial bursitis are microtrauma, partial or complete tears of the distal biceps tendon and rheumatoid arthritis. It is an unusual site for chronic bursitis.

Clinically manifestations of the bicipitoradial bursitis are: a mass in the cubital fossa, sensorial and/or motorial symptoms related to compression of the radial nerve or a combination of the two.

The bursa can be evaluated with ultrasound only when distended by fluid. The examination is generally carried out during forced supination of the forearm, the distal biceps tendon can be used as landmark. Sonography is sensitive in identifying bursitis (Fig. 5.6), but also in assessing macroscopic radial nerve lesions (Fig. 5.7);



Fig. 5.6 Bicipitoradial bursitis. Sonography shows an anechoic formation (bicipitoradial bursa) (arrows) surrounding the distal biceps tendon

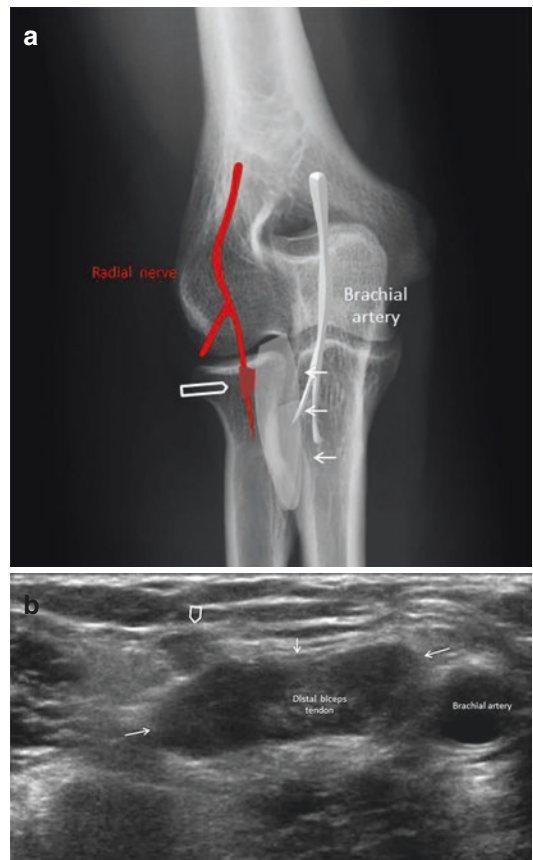


Fig. 5.7 Bicipitoradial bursitis with radial nerve compression. Schematic diagram (a) and sonography (b) show the bicipitoradial bursa (arrows) compressing the superficial branch of the radial nerve (void arrow) enlarged and hypoechoic

furthermore, it provides guidance for intrabursal injections of therapeutic agents. Bicipitoradial bursitis can be treated conservatively, with aspiration and steroid injection; surgical excision of the bursa is indicated only in cases of infection or failed conservative treatment [23].

The median nerve is one of the five terminal divisions of the brachial plexus.

It travels along the median bicipital groove in a neurovascular bundle with the brachial artery. In the elbow, it travels under the bicipital aponeurosis (lacertus fibrosus), then through the convergence point of the humeral and ulnar heads of the pronator teres. In the elbow, the median nerve is particularly exposed to trauma because it lies on a rather superficial level [24–27] (Fig. 5.8).

By ultrasound, an elbow effusion is readily detectable in the anterior or posterior recesses. Joint effusion may be the result of overuse syndromes, chronic osteoarthritis, inflammatory arthropathy (Fig. 5.9) (rheumatoid arthritis, gout, pseudogout), or infection [28–31]. The elbow is probably the second most common site for detection of loose bodies in a joint space after the knee, and the loose bodies are most often found in the anterior recess. The surrounding effusion enhances their visualization [32].

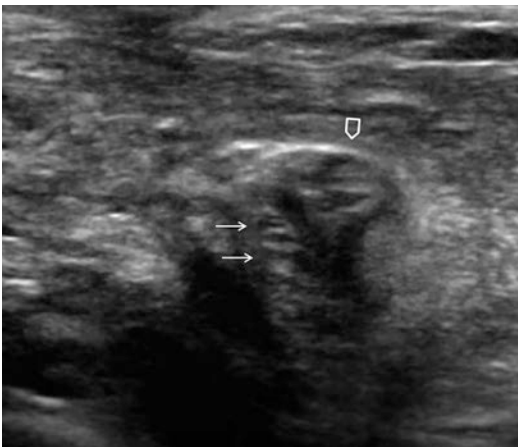


Fig. 5.8 Post-traumatic neuroma of median nerve. The axial sonogram, obtained over the injured portion of the nerve, shows a hypoechoic neuroma (void arrow). The nerve presents a normal fascicular pattern in the posterolateral part (arrows)

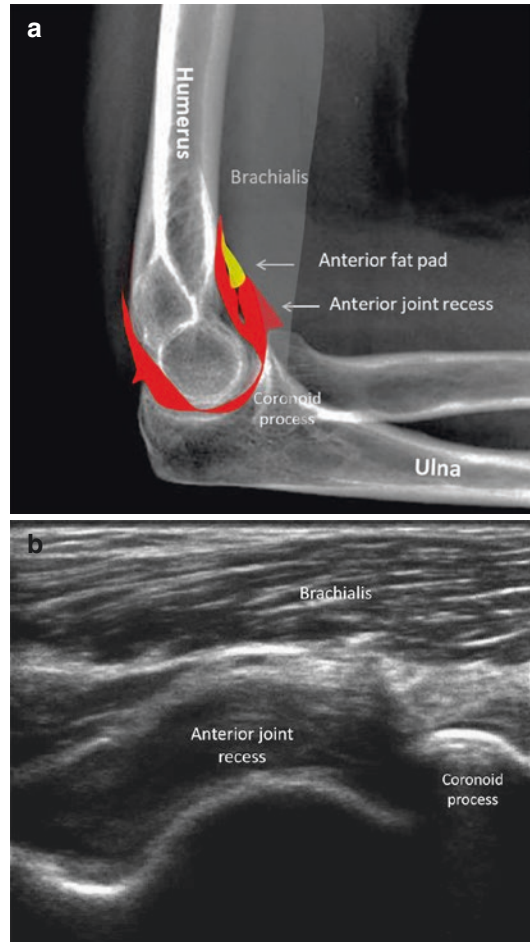


Fig. 5.9 Joint effusion in patient with rheumatoid arthritis: schematic diagram (a), sonogram (b). Effusion with mixed echogenicity in the anterior recess, deep to the brachialis muscle, is evident

Key points

- The most frequent lesion of the distal biceps tendon is the complete rupture; generally occurs as a single traumatic injury, with forced extension against resistance and the elbow positioned in mid-flexion
- Sonographic imaging of the lacertus fibrosus could provide a fast and cost-effective tool in several different pathologies, particularly in partial tears of the distal biceps' attachments
- Isolated tears of the brachialis tendon and/or muscle are rare injuries
- The bicipitoradial bursa envelops the biceps tendon. The role of this bursa is to reduce friction between the biceps tendon and the tuberosity of the radius
- In the elbow, the median nerve is particularly exposed to trauma because it lies on a rather superficial level
- By ultrasound, an elbow effusion is readily detectable in the anterior or posterior recesses

References

- Schmidt CC, Savoie FH, Steinmann SP, Hausman M, Voloshin I, Morrey BF, Sotereanos DG, Bero EH, Brown BT. Distal biceps tendon history, updates, and controversies: from the closed American Shoulder and Elbow Surgeons meeting-2015.
- Geaney LE, Mazzocca AD. Biceps brachii tendon ruptures: a review of diagnosis and treatment of proximal and distal biceps tendon ruptures. *Phys Sportsmed*. 2010;38(2):117–25.
- Blasi M, de la Fuente J, Martinoli C, Blasi J, Pérez-Bellmunt A, Domingo T, Miguel-Pérez M. Multidisciplinary approach to the persistent double distal tendon of the biceps brachii. *Surg Radiol Anat*. 2014;36(1):17–24.
- Tagliafico A, Michaud J, Capaccio E, Derchi LE, Martinoli C. Ultrasound demonstration of distal biceps tendon bifurcation: normal and abnormal findings. *Eur Radiol*. 2010;20(1):202–8.
- Tagliafico AS, Bignotti B, Martinoli C. Elbow US: anatomy, variants, and scanning technique. *Radiology*. 2015;275(3):636–50.
- Draghi F, Danesino GM, de Gautard R, Bianchi S. Ultrasound of the elbow: examination techniques and US appearance of the normal and pathologic joint. *J Ultrasound*. 2007;10(2):76–84.
- Konin GP, Nazarian LN, Walz DM. US of the elbow: indications, technique, normal anatomy, and pathologic conditions. *Radiographics*. 2013;33(4):E125–47.
- Radunovic G, Vlad V, Micu MC, Nestorova R, Petranova T, Porta F, Iagnocco A. Ultrasound assessment of the elbow. *Med Ultrason*. 2012;14(2):141–6.
- Chew ML, Giuffrè BM. Disorders of the distal biceps brachii tendon. *Radiographics*. 2005;25(5):1227–37.
- Brasseur JL. The biceps tendons: from the top and from the bottom. *J Ultrasound*. 2012;15(1):29–38.
- Konschake M, Stofferin H, Moriggl B. Ultrasound visualization of an underestimated structure: the bicipital aponeurosis. *Surg Radiol Anat*. 2017;39(12):1317–22. <https://doi.org/10.1007/s00276-017-1885-0>.
- Sanal HT, Chen L, Negro P, Haghghi P, Trudell DJ, Resnick DL. Distal attachment of the brachialis muscle: anatomic and MRI study in cadavers. *Am J Roentgenol*. 2009;192(2):468–72.
- Krych AJ, Kohan RB, Rodeo SA, Barnes RP, Warren RF, Hotchkiss RN. Acute brachialis muscle rupture caused by closed elbow dislocation in a professional American football player. *J Shoulder Elb Surg*. 2012;21:e1–5.
- Murugappan KS, Mohammed K. Acute traumatic brachialis rupture in a young rugby player: a case report. *J Shoulder Elb Surg*. 2012;21:e12–4.
- Nishida Y, Tsukushi S. Brachialis muscle tear mimicking an intramuscular tumor: a report of two cases. *J Hand Surg [Am]*. 2007;32:1237.
- Scheonberger TJ, Ernst MF. A brachialis muscle rupture diagnosed by ultrasound; case report. *Int J Emerg Med*. 2011;4:46.
- Van den Bergh GR, Queenan JF. Isolated rupture of the brachialis: a case report. *J Bone Joint Surg Am*. 2001;83:1074–5.
- Wasserstein D, White L. Traumatic brachialis muscle injury by elbow hyperextension in a professional hockey player. *Clin J Sport Med*. 2010;20:211–2.
- Winblad JB, Escobedo E, Hunter JC. Brachialis muscle rupture and hematoma. *Radiol Case Rep*. 2008;3:251.
- Draghi F, Gregoli B, Sileo C. Sonography of the bicipitoradial bursa: a short pictorial essay. *J Ultrasound*. 2012;15(1):39–41.
- Skaf AY, Boutin RD, Dantas RW, Hooper AW, Muhle C, Chou DS, Lektrakul N, Trudell DJ, Haghghi P, Resnick DL. Bicipitoradial bursitis: MR imaging findings in eight patients and anatomic data from contrast material opacification of bursae followed by routine radiography and MR imaging in cadavers. *Radiology*. 1999;212(1):111–6.
- Bak B. Bicipitoradial bursitis. *Ugeskr Laeger*. 2008;170(40):3123–4.
- Lui TH, Sit YK, Pan XH. Endoscopic resection of the bicipitoradial bursa. *Sports Med Arthrosc*. 2016;24(1):7–10.
- Husarik DB, Saupé N, Pfirrmann CW, Jost B, Hodler J, Zanetti M. Elbow nerves: MR findings in 60 asymptomatic subjects—normal anatomy, variants, and pitfalls. *Radiology*. 2009;252(1):148–56.
- Gregoli B, Bortolotto C, Draghi F. Elbow nerves: normal sonographic anatomy and identification of the structures potentially associated with nerve compression. A short pictorial-video article. *J Ultrasound*. 2013;16(3):119–21.
- Alessandrino F, Pagani C, Draghi F. In-continuity neuroma of the median nerve at the elbow. *J Ultrasound*. 2014;17(3):229–31.
- Bianchi S, Draghi F, Beggs I. Ultrasound of the peripheral nerves. In: *Clinical ultrasound*, vol. 2. Philadelphia: Elsevier; 2011. p. 1158–67.
- Finlay K, Ferri M, Friedman L. Ultrasound of the elbow. *Skelet Radiol*. 2004;33(2):63–79.
- De Maeseneer M, Jacobson JA, Jaovisidha S, et al. Elbow effusions: distribution of joint fluid with flexion and extension and imaging implications. *Investig Radiol*. 1998;33(2):117–25.
- Martinoli C, Bianchi S, Giovagnorio F, Pugliese F. Ultrasound of the elbow. *Skelet Radiol*. 2001;30(11):605–14.
- Gitto S, Draghi AG, Draghi F. Sonography of non-neoplastic disorders of the hand and wrist tendons. *J Ultrasound Med*. 2018;37:51–68.
- Bianchi S, Martinoli C. Detection of loose bodies in joints. *Radiol Clin N Am*. 1999;37(4):679–90.

Content Overview

Common extensor tendon

- Epicondylitis
- Partial tear
- Full-thickness tear
- Treatment of epicondylitis

Lateral collateral ligament

Supinator muscle

Posterior interosseous nerve

Soft-tissue masses

The common extensor tendon origin is composed of longitudinal fibrils of the extensor carpi radialis brevis, extensor digitorum communis, extensor digiti minimi, and extensor carpi ulnaris [1–3]. The extensor carpi radialis brevis fibers constitute most of the deep tendon and the extensor digitorum communis the superficial part.

Extensor tendinopathy or lateral epicondylitis, or tennis elbow, is the most common disorder of the elbow, characterized by lateral elbow pain and functional impairment.

The most frequent cause of epicondylitis is considered to be repetitive microtrauma. Overuse with supination of the forearm and dorsiflexion of the wrist results in tendon degeneration, with rupture of individual collagen fibers that stimulate a reparative response [4].

Histology of the normal common extensor tendon shows parallel collagen fibrils, no fatty infiltration, and no capillary proliferation. Histology in extensor tendinopathy shows alteration of the fibrillar structure with a wavy outline, loss of parallel collagen structure, multiple fatty infiltrates, areas of fat necrosis, and neovascularization.

Epicondylitis commonly presents with lateral elbow pain, aggravated by repetitive use of the extensor muscles during sport, job, or daily activities.

The diagnosis is generally based on clinical findings. The role of imaging is to confirm the clinical diagnosis, to determine disease severity and to exclude other possible pathologies [5].

The epicondylitis B-mode ultrasound images show hypoechoic areas and calcifications of the tendon, with or without tendon thickening (Fig. 6.1a). Hypoechoic areas in the posterior portion of the tendon are generally the first manifestation of the disease. These focal areas corresponded histologically to collagen degeneration with fibroblastic proliferation [6].

Color Doppler signals correlate with neoangiogenesis and capillary proliferation (Fig. 6.1b). Combination of B-mode ultrasound and sonoelastography (Fig. 6.2) proved efficient in diagnosing lateral epicondylitis, which better correlates to histology and provides improved sensitivity without loss of specificity [7].

Fig. 6.1 Epicondylitis. B-mode ultrasound images (a) show loss of echogenicity and calcifications of the tendon (arrows), with bone irregularity of the medial epicondyle. The power Doppler (b) shows hyperemia of the common extensor tendon due to the angiofibroblastic response

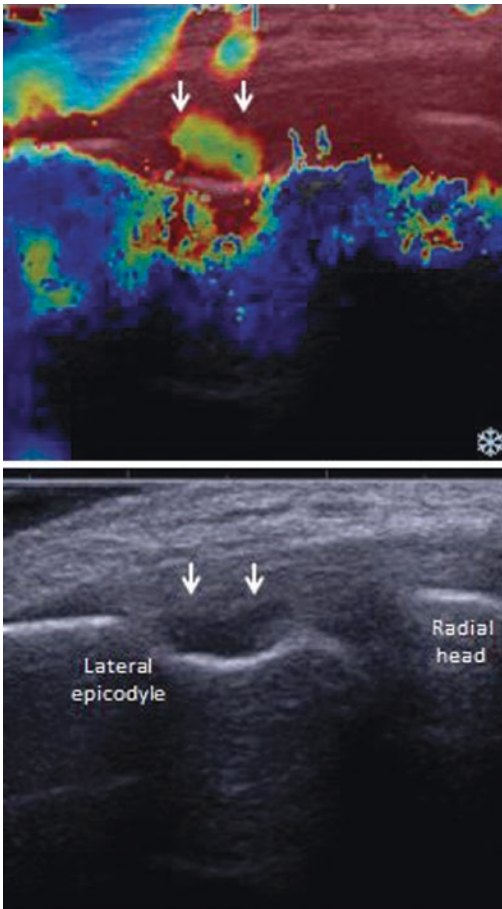
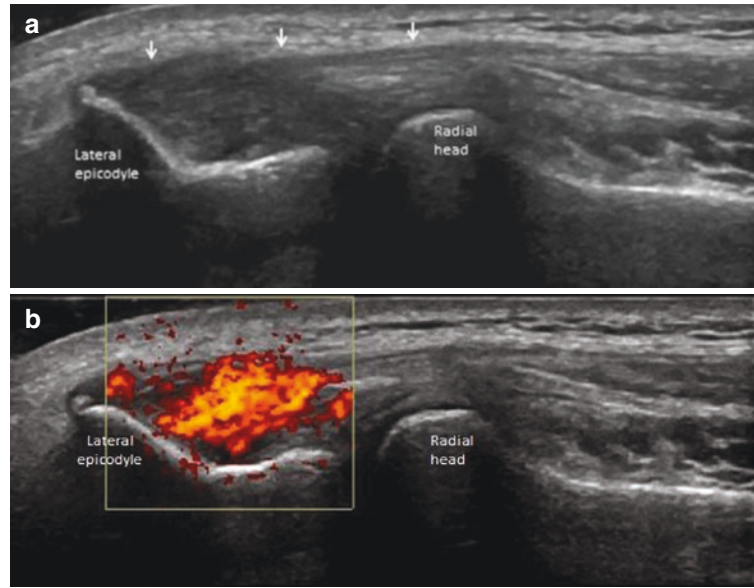


Fig. 6.2 Epicondylitis longitudinal scans. B-mode image shows an area of intratendinous tendinopathy (arrows), softening on real-time sonoelastographic images (arrows)

In tendons with epicondylitis, partial or full-thickness tears can occur, particularly after corticosteroid injection (Fig. 6.3) [8–10]. Tears may be also unrelated to chronic tendinosis but secondary to an acute traumatic episode.

A variety of non-operative methods have been proposed for treatment of epicondylitis, including physical therapy, activity modification, nonsteroidal anti-inflammatory medications, steroid injections, and orthotic devices [8, 11–13]. Surgical intervention for lateral epicondylitis is typically reserved for patients with persistent pain after 6–12 months of non-operative treatment, and generally exhibits good outcomes [14, 15].

After surgery, tendon appearance differs from that of a healthy, non-operated tendon in several characteristics (Fig. 6.4) [16, 17]. Repaired tendons are larger and wider, and show an inhomogeneous echo texture with a loss of the fibrillar pattern. Doppler imaging shows no vascularization in the immediate postoperative period. Intratendinous vascularization physiologically increases in the first 3 months after surgery, and then stabilizes and finally regresses within 6 months. Beyond the first 6 months, persistent hypervascularization is pathologic. Sonography has proven to be effective in evaluating common flexor tendon integrity and detecting complications after surgical repair [18].

Fig. 6.3 Common extensor tendon partial tear, different cases (a, b). Ultrasound images show a partial tear (arrows) occurred in patients with chronic tendinosis, after intratendinous steroid injections for local treatment of the overuse syndrome

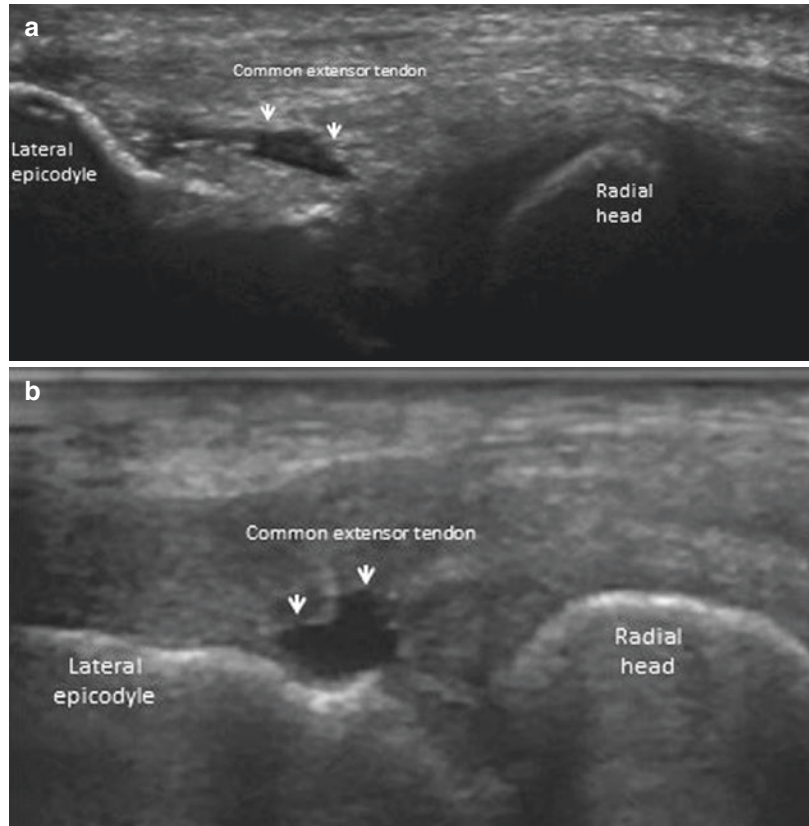
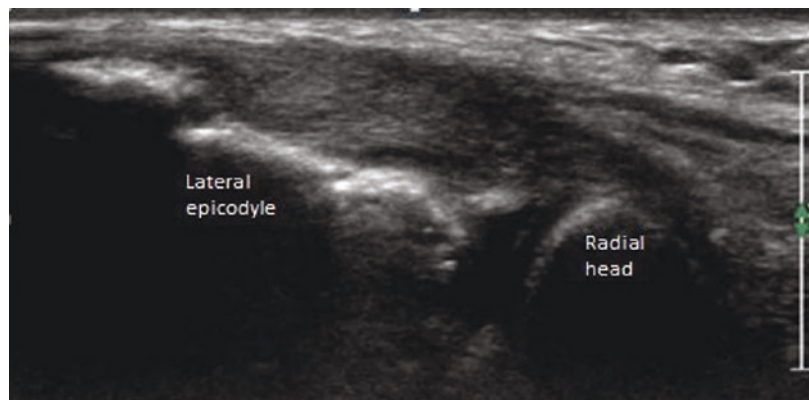


Fig. 6.4 Common extensor tendon after surgery. The tendon is larger and wider than non-operated ones and shows an inhomogeneous echo texture with a loss of the fibrillar pattern



Evaluation of the lateral collateral ligament is often difficult with sonography and MRI may be indicated as it is a more sensitive modality. However, with a complete tear there is no sonographic evidence of the ligament, and hematoma is present in the acute phase (Fig. 6.5); a partial tear appears as heterogeneous focal hypoechoic

thickening. The lateral collateral ligament is also intimately associated with the common extensor tendon and should be carefully assessed in cases of lateral epicondylitis [1].

The supinator muscle arises from the humerus, lateral collateral ligament and ulna, to insert onto the radius by superficial and deep layers [19, 20].

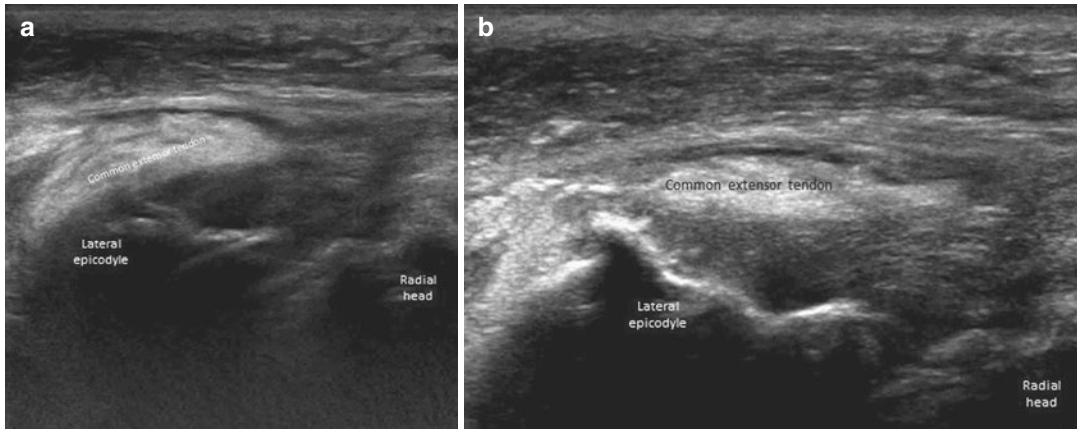


Fig. 6.5 Full-thickness tear of lateral collateral ligament. Ultrasound scan (a, b) shows complete interruption of ligament fibers and a large hematoma; the overlying extensor tendon is also injured

These two layers are separated by an interstice, which runs the deep branch of the radial nerve.

Various anatomical elements have been described as potentially associated with deep branch of the radial nerve compression syndromes [21], the most known is the proximal edge of the superficial layer of the supinator muscle, called the arcade of Frohse [22, 23]. The supinator muscle is always muscular in newborn full-term fetuses [23], but chronic repetition of pronation-supination movements can cause modifications of the muscular structure. It was suggested that the most superior part of the superficial layer can become a fibrous arch, to the point of creating a real pathology.

The main sonographic signs of nerve compression are swelling with loss of the fascicular pattern (Fig. 6.6) and hyperemia with Doppler imaging [21, 24–26]. To better evaluate the posterior interosseous nerve, dynamic transverse images are used [27].

Soft-tissue masses are common entities encountered in the musculoskeleton of patients. Ultrasound has high sensitivity in detection of these lesions, but low specificity, with the exception of some of these such as ganglia (Fig. 6.7) [28–31].



Fig. 6.6 Entrapment neuropathy of the deep branch of the radial nerve. Sonography shows hypoechoic swelling of the deep branch of the radial nerve with loss of the fascicular pattern

Implication for patient care

In tendons with epicondylitis, partial or full-thickness tears can occur, particularly after corticosteroid injection.

Key points

Extensor tendinopathy or lateral epicondylitis, or tennis elbow, is the most common disorder of the elbow. Color Doppler signals correlate with neoangiogenesis and capillary proliferation.

Evaluation of the lateral collateral ligament is often difficult with sonography and MRI may be indicated as it is a more sensitive modality.

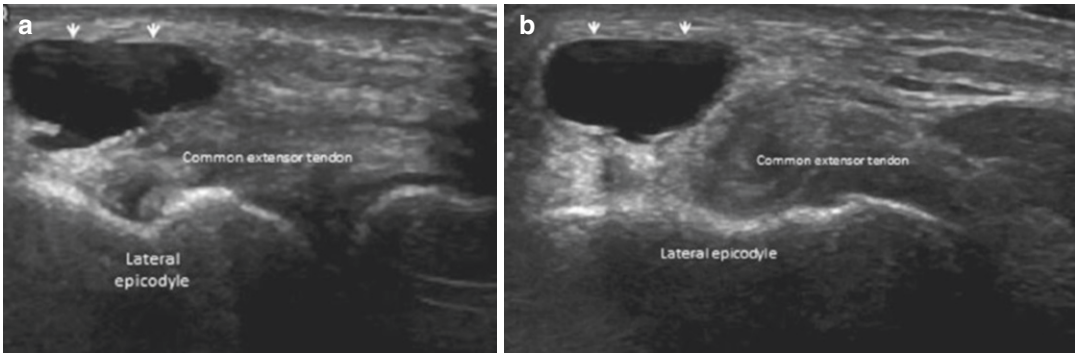


Fig. 6.7 Ganglion cyst. Ultrasonography shows an anechoic, with well-defined margins, lesion (arrows) superficial to the common extensor tendon ((a) sagittal scan, (b) axial scan)

The supinator muscle consists of two layers separated by an interstice, which runs the deep branch of the radial nerve or posterior interosseous nerve.

Various anatomical elements have been described as potentially associated with deep branch of the radial nerve compression syndromes, the most known is the proximal edge of the superficial layer of the supinator muscle, called the arcade of Frohse.

References

- Konin GP, Nazarian LN, Walz DM. US of the elbow: indications, technique, normal anatomy, and pathologic conditions. *Radiographics*. 2013;33(4):E125–47.
- Draghi F, Danesino GM, de Gautard R, Bianchi S. Ultrasound of the elbow: examination techniques and US appearance of the normal and pathologic joint. *J Ultrasound*. 2007;10(2):76–84.
- Radunovic G, Vlad V, Micu MC, Nestorova R, Petranova T, Porta F, Iagnocco A. Ultrasound assessment of the elbow. *Med Ultrason*. 2012;14(2):141–6.
- De Zordo T, Lill SR, Fink C, Feuchtner GM, Jaschke W, Bellmann-Weiler R, Klauser AS. Real-time sonoelastography of lateral epicondylitis: comparison of findings between patients and healthy volunteers. *AJR Am J Roentgenol*. 2009;193(1):180–5.
- Levin D, Nazarian LN, Miller TT, O’Kane PL, Feld RI, Parker L, McShane JM. Lateral epicondylitis of the elbow: US findings. *Radiology*. 2005;237(1):230–4.
- Connell D, Burke F, Coombes P, McNealy S, Freeman D, Pryde D, Hoy G. Sonographic examination of lateral epicondylitis. *AJR Am J Roentgenol*. 2001;176(3):777–82.
- Klauser AS, Pamminger M, Halpern EJ, Abd Ellah MMH, Moriggl B, Taljanovic MS, Deml C, Sztankay J, Klima G, Jaschke WR. Extensor tendinopathy of the elbow assessed with sonoelastography: histologic correlation. *Eur Radiol*. 2017;27(8):3460–6.
- Hart L. Corticosteroid and other injections in the management of tendinopathies: a review. *Clin J Sport Med*. 2011;21(6):540–1.
- Draghi F, Robotti G, Jacob D, Bianchi S. Interventional musculoskeletal ultrasonography: precautions and contraindications. *J Ultrasound*. 2010;13(3):126–33.
- Robotti G, Canepa MG, Bortolotto C, Draghi F. Interventional musculoskeletal US: an update on materials and methods. *J Ultrasound*. 2013;16(2):45–55.
- Faro F, Wolf JM. Lateral epicondylitis: review and current concepts. *J Hand Surg Am*. 2007;32(8):1271–9.
- Smidt N, Van der Windt DA, Assendelft WJ, Devillé WL, Korthals-de Bos IB, Bouter LM. Corticosteroid injections, physiotherapy, or a wait-and-see policy for lateral epicondylitis: a randomized controlled trial. *Lancet*. 2002;359(9307):657–62.
- Calfee RP, Patel A, DaSilva MF, Akelman E. Management of lateral epicondylitis: current concepts. *J Am Acad Orthop Surg*. 2008;16(1):19–29.
- Knutsen EJ, Calfee RP, Chen RE, Goldfarb CA, Park KW, Osei DA. Factors associated with failure of nonoperative treatment in lateral epicondylitis. *Am J Sports Med*. 2015;43(9):2133–7.
- Sotereanos DG, Varitimidis SE, Giannakopoulos PN, Westkaemper JG. Results of surgical treatment for radial tunnel syndrome. *J Hand Surg Am*. 1999;24(3):566–70.
- Gitto S, Draghi AG, Bortolotto C, Draghi F. Sonography of the achilles tendon after complete rupture repair: what the radiologist should know. *J Ultrasound Med*. 2016;35(12):2529–36.

17. Cohen M. US imaging in operated tendons. *J Ultrasound*. 2012;15:69–75.
18. Gitto S, Draghi AG, Draghi F. Sonography of non-neoplastic disorders of the hand and wrist tendons. *J Ultrasound Med*. 2018;37:51–68.
19. Berton C, Wavreille G, Lecomte F, Miletic B, Kim HJ, Fontaine C. The supinator muscle: anatomical bases for deep branch of the radial nerve entrapment. *Surg Radiol Anat*. 2013;35(3):217–24.
20. Riffaud L, Morandi X, Godey B, Brassier G, Guegan Y, Darnault P, Scarabin JM. Anatomic bases for the compression and neurolysis of the deep branch of the radial nerve in the radial tunnel. *Surg Radiol Anat*. 1999;21(4):229–33.
21. Gregoli B, Bortolotto C, Draghi F. Elbow nerves: normal sonographic anatomy and identification of the structures potentially associated with nerve compression. A short pictorial-video article. *J Ultrasound*. 2013;16(3):119–21.
22. Frohse F, Frankel M, editors. *Die Muskeln des menschlichen Armes*. K Von Bardeleben. Jena: Fischer Verlag; 1908. p. 164–9.
23. Ozturk A, Kutlu C, Taskara N, Kale AC, Bayraktar B, Cecen A. Anatomic and morphometric study of the arcade of Frohse in cadavers. *Surg Radiol Anat*. 2005;27(3):171–5.
24. Bianchi S, Draghi F, Beggs I. Ultrasound of the peripheral nerves. In: *Clinical ultrasound*, vol. 2. London: Elsevier Ltd; 2011. p. 1158–67.
25. Draghi F, Bortolotto C. Importance of the ultrasound in cubital tunnel syndrome. *Surg Radiol Anat*. 2016;38(2):265–8.
26. Padua L, Di Pasquale A, Liotta G, Granata G, Pazzaglia C, Erra C, Briani C, Coraci D, De Franco P, Antonini G, Martinoli C. Ultrasound as a useful tool in the diagnosis and management of traumatic nerve lesions. *Clin Neurophysiol*. 2013;124(6):1237–43.
27. Tagliafico AS, Bignotti B, Martinoli C. Elbow US: anatomy, variants, and scanning technique. *Radiology*. 2015;275(3):636–50.
28. Chang WK, Li YP, Zhang DF, Liang BS. The cubital tunnel syndrome caused by the intraneural or extraneural ganglion cysts: case report and review of the literature. *J Plast Reconstr Aesthet Surg*. 2017;70(10):1404–8.
29. Mobbs RJ, Phan K, Maharaj MM, Chaganti J, Simon N. Intraneural ganglion cyst of the ulnar nerve at the elbow masquerading as a malignant peripheral nerve sheath tumor. *World Neurosurg*. 2016;96:613.
30. Rodriguez Miralles J, Natera Cisneros L, Escolà A, Fallone JC, Cots M, Espiga X. Type A ganglion cysts of the radiocapitellar joint may involve compression of the superficial radial nerve. *Orthop Traumatol Surg Res*. 2016;102(6):791–4.
31. Vaishya R, Kapoor C, Agarwal AK, Vijay V. A rare presentation of ganglion cyst of the elbow. *Cureus*. 2016;8(7):e665.

Content overview

Common flexor-pronator tendon

- Medial epicondylitis
- Partial tear
- Full-thickness tear
- Ulnar neuropathy

Pronator teres muscle

- Median nerve compression

Ulnar collateral ligament

Fractures

Orthopedic hardware impingement

Soft-tissue masses

The common flexor-pronator tendon is thicker and shorter than the common extensor tendon and has a less broad-based attachment [1–3]. The common flexor tendon includes the flexor carpi radialis, the palmaris longus, the flexor carpi ulnaris, and the flexor digitorum superficialis. It originates at the medial epicondyle of the humerus [4–7]. The pronator teres has two origins, one at the humeral and the other at the medial coronoid process [8, 9].

The most common lesion of the medial elbow is the medial epicondylitis. Also referred to as golfer's elbow [10], medial epicondylitis was first described by Henry J. Morris in 1882 [11].

Overuse of the elbow in patients practicing sports activities that produce valgus stress and repetitive flexion and pronation (such as golf,

baseball, tennis, fencing, and swimming) results in tendon degeneration, with rupture of individual collagen fibers that stimulates a reparative response [12–15]. The condition is also observed as a result of labor-intensive activities that require movements of the hand, wrist, and forearm.

Medial epicondylitis is characterized by pain at the base of the common flexor tendon.

Histology of common flexor tendinopathy, as in extensor tendinopathy, shows alteration of the fibrillar structure with wavy outline, loss of parallel collagen structure, multiple fatty infiltrates, areas of fat necrosis, and neovascularization. In the chronic phase, calcifications can be present. The sonographic appearance (Fig. 7.1a, b) is similar to that of the more common lateral epicondylitis: ultrasound images show hypoechoic areas and calcifications of the tendon, with or without tendon thickening. These focal areas corresponded histologically to collagen degeneration with fibroblastic proliferation [16, 17].

Color Doppler signals correlate with neoangiogenesis and capillary proliferation (Fig. 7.1c, d).

Combination of B-mode ultrasound and sonoelastography proved efficient in diagnosing medial epicondylitis, with better correlation to histology, which provides improved sensitivity without loss of specificity.

In tendons with chronic tendinosis, partial or full-thickness tears can occur, particularly after corticosteroid injection (Fig. 7.2) [18–20]. Partial

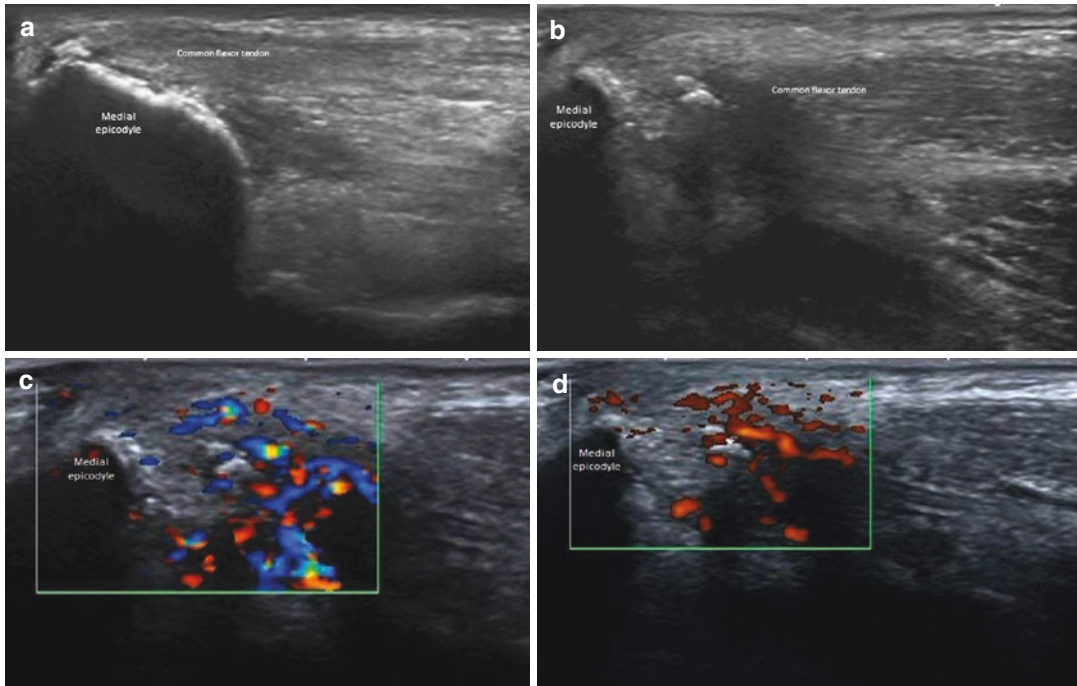
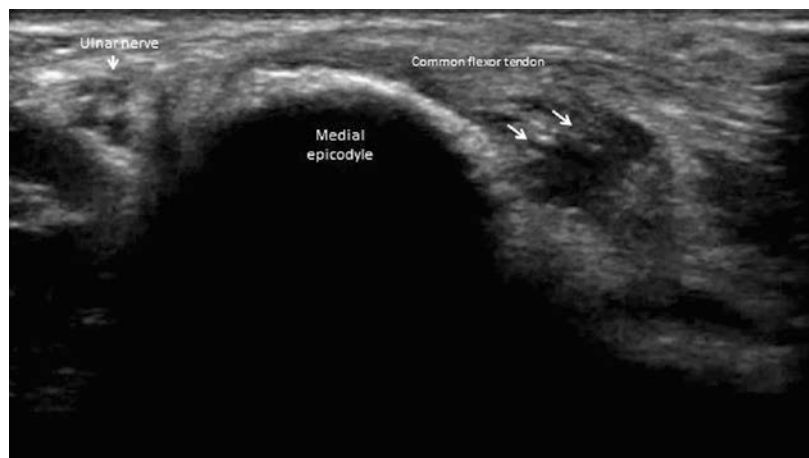


Fig. 7.1 Medial epicondylitis. B-mode ultrasound images of common flexor tendon (**a**, **b**) show loss of echogenicity, calcifications of the tendon and bone irregularity

of the medial epicondyle. Color (**c**) and power Doppler (**d**) show hyperemia within the common flexor tendon due to the angiofibroblastic response

Fig. 7.2 Common flexor tendon partial tear. B-mode ultrasound image shows partial tear (arrows) occurred in patient with chronic tendinosis, after intratendinous steroid injections for local treatment of the overuse syndrome



or full-thickness tears may be also unrelated to chronic tendinosis, but secondary to an acute traumatic episode.

Ulnar neuropathy may be associated with medial epicondylitis in approximately 50% of cases [21–23]. Surgical treatment for medial epicondylitis sometimes may be necessary, and

exhibits good outcomes [10]. After surgery, tendon appearance differs from that of a healthy non-operated tendon in several characteristics [24, 25]. Repaired tendons are larger and wider than non-operated ones and show an inhomogeneous echo texture with a loss of the fibrillar pattern.

Doppler imaging shows no vascularization in the immediate postoperative period. Intratendinous vascularization physiologically increases in the first 3 months after surgery, then stabilizes, and finally regresses within 6 months. Beyond the first 6 months, persistent hypervascularization is pathologic. Sonography has proven to be effective in evaluating common flexor tendon integrity and detecting complications after surgical repair.

The pronator teres muscle can be affected by a variety of pathological conditions, including trauma (Fig. 7.3), forearm fractures, dislocations, and tumors, and can be implicated in compression of the median nerve [8] in the so-called pronator teres syndrome (Fig. 7.4).

Compression of the median nerve by the pronator teres may be evaluated with transverse sonograms obtained from proximal to distal: at the distal part of the arm in full supination, at the level of the radial head, at the anterior crease of the elbow, in complete extension and supination (dynamic sonographic examination performed at this level is necessary to assess potential compression of the median nerve by the pronator teres) and at the forearm, in complete supination.

The principal function of the ulnar collateral ligament complex is to maintain medial joint stability to valgus stress, and the anterior bundle is the most important component of the ligamentous complex.

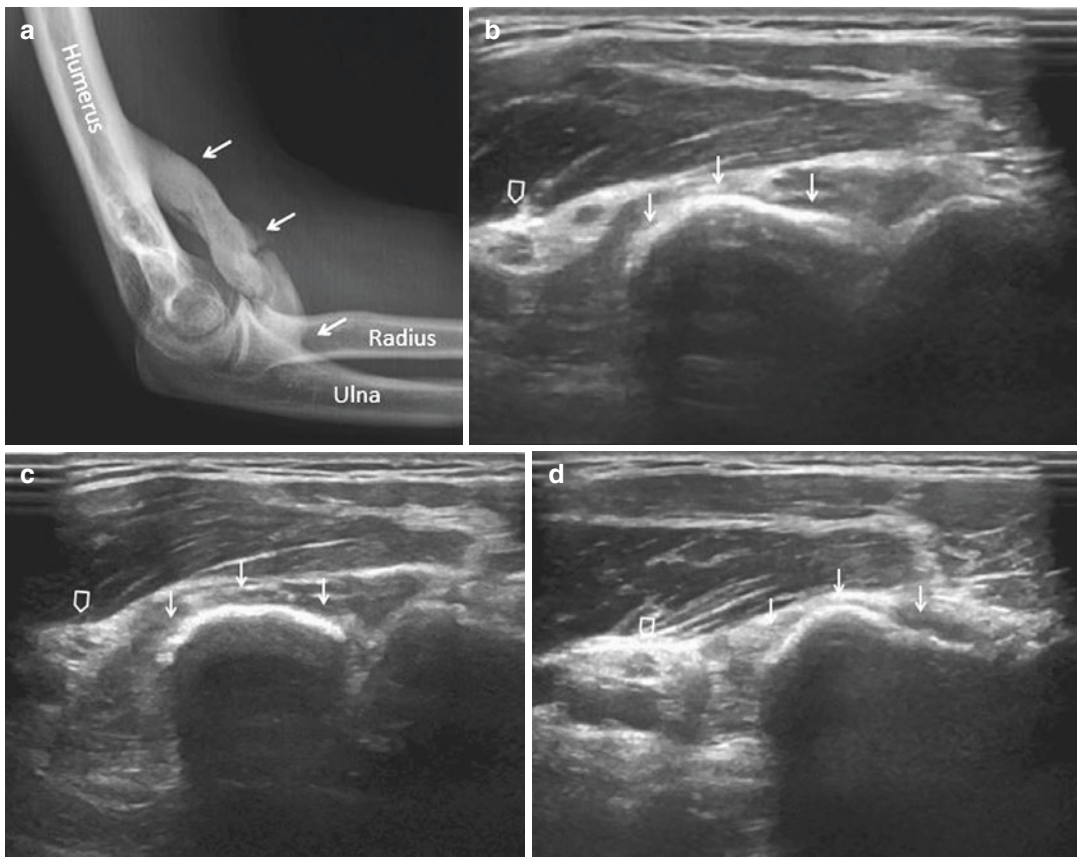


Fig. 7.3 Pronator teres intramuscular extensive calcification. Standard radiograph of hemophilic patient at a distance of time from a modest trauma shows extensive

calcifications at the anterior side of the arm (a) (arrows), sonography shows that the calcifications are intramuscular (pronator teres) (b–d) (Void arrow: median nerve)

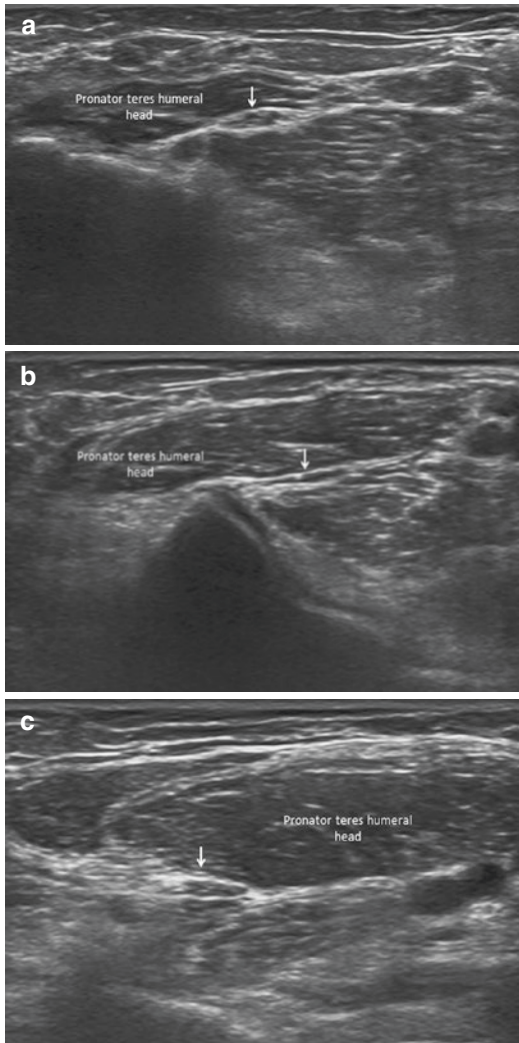


Fig. 7.4 Pronator teres syndrome. Transverse sonograms obtained from proximal to distal (**a**, **b**, **c**) show flattening of the median nerve (**b**) (arrow) between the two heads of the pronator teres

The ulnar collateral ligament may be injured acutely or, more commonly, from chronic repetitive microtrauma [26–31], often concomitant with the overlying common flexor-pronator mass.

Chronic overuse repetitive insults to the ligament cause microscopic tears that progress to significant attenuation or frank tearing within its substance; the development of heterotopic ossification along the course of the ligament has been described (Fig. 7.5).



Fig. 7.5 Chronic tear of ulnar collateral ligament. Ultrasonography shows heterogeneous thickening and calcifications of the ligament

The ulnar collateral ligament and its lesions are well seen with magnetic resonance imaging, while differentiation between complete and incomplete tears with sonography is often difficult. Dynamic imaging, however, with valgus stress allows assessment of ligamentous complete tear in acute phase and laxity in chronic phase [29]. In chronic cases, ultrasonography shows heterogeneous thickening and calcifications of the ligament (Fig. 7.5).

Deep to the anterior bundle of the medial collateral ligament there is an articulate space that, like all elbow spaces, can be seen with ultrasound only when effusion is present (Fig. 7.6). The pathologies [32] are the same as in the other joint spaces and recesses of the elbow.

Among the various elbow medial injuries are the fractures, whose diagnosis is made with standard radiograph. However, sometimes the fractures initially have normal radiograph, and a certain number of occult fractures are only diagnosed correctly after the fact during a follow-up visit, particularly in children [33]. Ultrasonography is highly sensitive for elbow fracture, showing fractures as interruption of the

Fig. 7.6 Joint effusion. Deep to the ulnar collateral ligament (arrows) anechoic joint effusion is evident

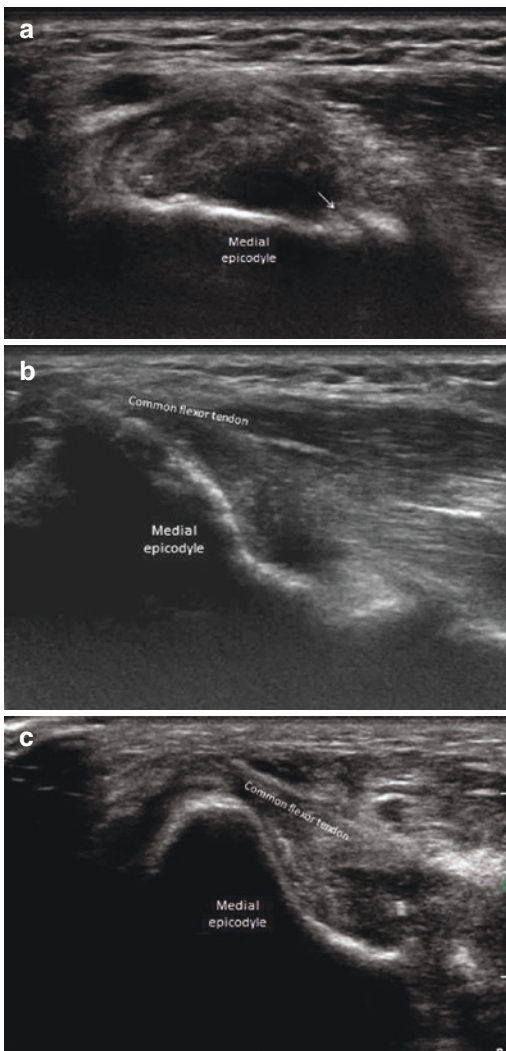
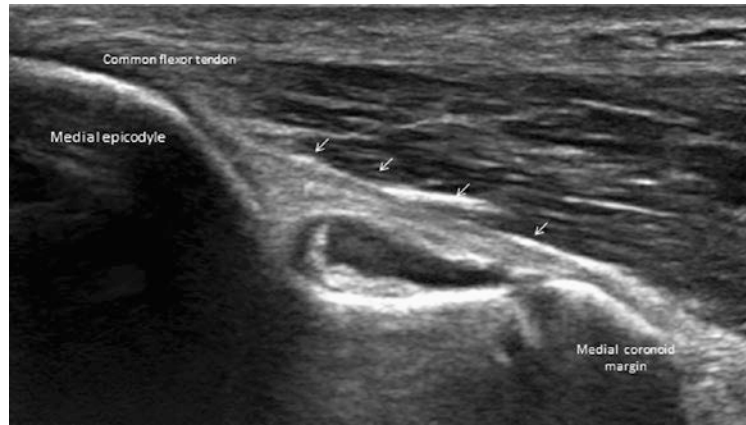


Fig. 7.7 Medial epicondyle fracture. The ultrasound shows medial epicondyle fracture (arrow) (a), with hematoma between medial epicondyle and flexor muscles' tendons (b, c)

hyperechogenic line representing the bone cortex (Fig. 7.7), and may be helpful in the diagnosis of occult fractures.

As the tendons of the elbow are in close contact with the bone plane, during muscle contraction, they may conflict with orthopedic hardware positioned in several surgical interventions and sonography may be helpful in the diagnosis of orthopedic hardware impingement [34].

Soft-tissue masses are common entities encountered in the musculoskeleton of patients (Fig. 7.8). Ultrasound has high sensitivity in detection of lesions, but low specificity. A sonographic diagnostic procedure is often useful to obtain a biological sample (fluid or cellular) in order to determine the etiology of the lesion [18, 20]. These modalities aid the clinician in developing an appropriate differential diagnosis and treatment plan.

Key points

Medial epicondylitis is the most common lesion of the medial elbow and is similar to the more common lateral epicondylitis.

Ulnar neuropathy may be associated with medial epicondylitis in approximately 50% of cases.

The pronator teres muscle can be implicated in compression of the median nerve, in the so-called pronator teres syndrome.

The ulnar collateral ligament may be injured acutely or, more commonly, from chronic repetitive microtrauma, often concomitant with the overlying common flexor-pronator mass.

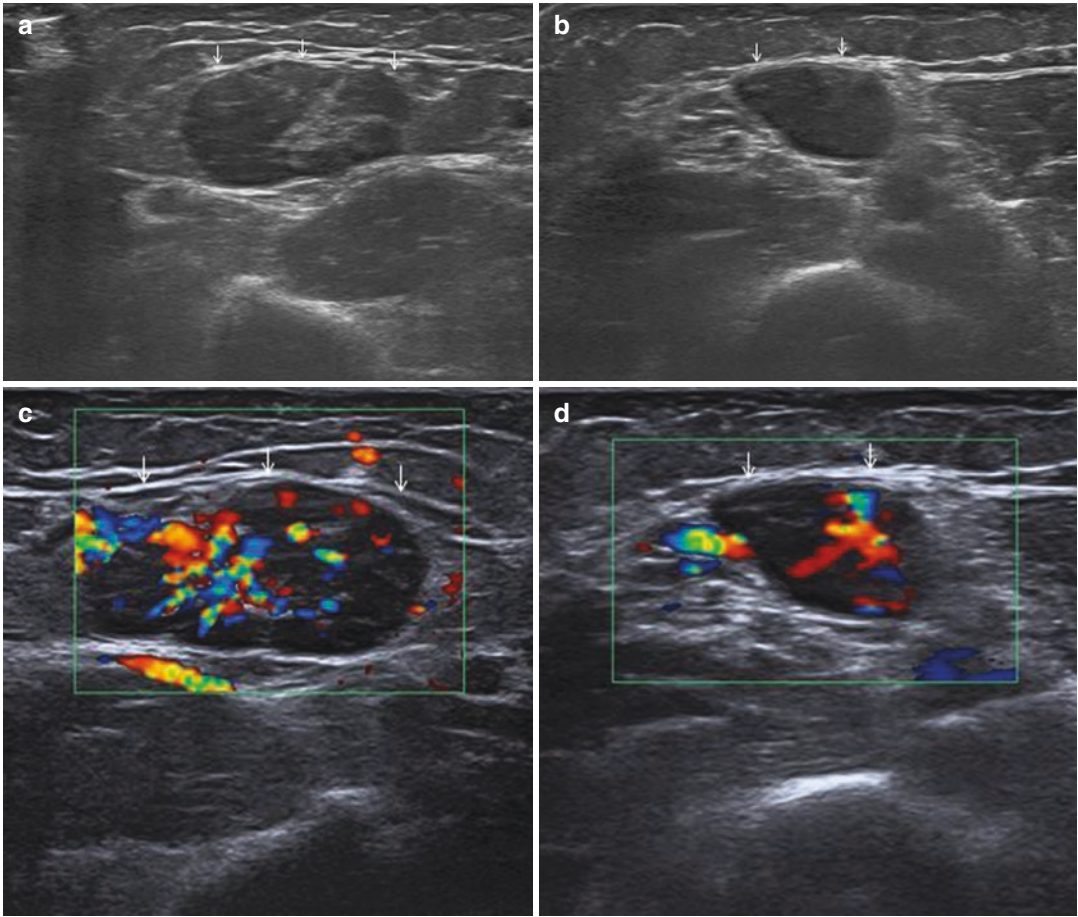


Fig. 7.8 Patient with non-Hodgkin lymphoma. Gray-scale sonograms show round-oval lymph nodes masses in the subcutaneous tissue (**a, b**) (arrows). Color Doppler

sonograms demonstrate a rich vascularization within the masses (**c, d**) (arrows)

References

1. Bianchi S, Martinoli C. Elbow. In: Bianchi S, Martinoli C, editors. *Ultrasound of the musculoskeletal system*. New York: Springer; 2007. p. 349–408.
2. Martinoli C, Bianchi S, Giovagnorio F, Pugliese F. Ultrasound of the elbow. *Skelet Radiol*. 2001;30(11):605–14.
3. Finlay K, Ferri M, Friedman L. Ultrasound of the elbow. *Skelet Radiol*. 2004;33(2):63–79.
4. Blease S, Stoller DW, Safran MR, Li AE, Fritz RC. The elbow. In: Stoller DW, editor. *Magnetic resonance imaging in orthopaedics and sports medicine*. 3rd ed. Philadelphia: Lippincott, Williams & Wilkins; 2007. p. 1463–626.
5. Konin GP, Nazarian LN, Walz DM. US of the elbow: indications, technique, normal anatomy, and pathologic conditions. *Radiographics*. 2013;33(4):E125–47.
6. Draghi F, Danesino GM, de Gautard R, Bianchi S. Ultrasound of the elbow: examination techniques and US appearance of the normal and pathologic joint. *J Ultrasound*. 2007;10(2):76–84.
7. Radunovic G, Vlad V, Micu MC, Nestorova R, Petranova T, Porta F, Iagnocco A. Ultrasound assessment of the elbow. *Med Ultrason*. 2012;14(2):141–6.
8. Créteur V, Madani A, Sattari A, Bianchi S. Sonography of the pronator teres: normal and pathologic appearances. *J Ultrasound Med*. 2017;36(12):2585–97. <https://doi.org/10.1002/jum.14306>.
9. Tagliafico AS, Bignotti B, Martinoli C. Elbow US: anatomy, variants, and scanning technique. *Radiology*. 2015;275(3):636–50.
10. do Nascimento AT, Claudio GK. Arthroscopic surgical treatment of medial epicondylitis. *J Shoulder Elb Surg*. 2017;26(12):2232–5.
11. Morris HJ. Rider's sprain. *Lancet*. 1882;2:557.
12. Nordander C, Ohlsson K, Åkesson I, Arvidsson I, Balogh I, Hansson GA, et al. Risk of musculoskeletal

- disorders among females and males in repetitive/constrained work. *Ergonomics*. 2009;52:1226–39.
13. Barco R, Antuña SA. Medial elbow pain. *EFORT Open Rev*. 2017;2(8):362–71.
 14. Donaldson O, Vannet N, Gosens T, Kulkarni R. Tendinopathies around the elbow part 2: medial elbow, distal biceps and triceps tendinopathies. *Shoulder Elbow*. 2014;6(1):47–56.
 15. van Holsbeeck MT, Introcaso JH. *Musculoskeletal ultrasound*. 2nd ed. St Louis: Mosby-Year Book; 2001.
 16. Connell D, Burke F, Coombes P, McNealy S, Freeman D, Pryde D, Hoy G. Sonographic examination of lateral epicondylitis. *AJR Am J Roentgenol*. 2001;176(3):777–82.
 17. Klauser AS, Pamminer M, Halpern EJ, Abd Ellah MMH, Moriggl B, Taljanovic MS, Deml C, Sztankay J, Klima G, Jaschke WR. Extensor tendinopathy of the elbow assessed with sonoelastography: histologic correlation. *Eur Radiol*. 2017;27(8):3460–6.
 18. Hart L. Corticosteroid and other injections in the management of tendinopathies: a review. *Clin J Sport Med*. 2011;21(6):540–1.
 19. Draghi F, Robotti G, Jacob D, Bianchi S. Interventional musculoskeletal ultrasonography: precautions and contraindications. *J Ultrasound*. 2010;13(3):126–33.
 20. Robotti G, Canepa MG, Bortolotto C, Draghi F. Interventional musculoskeletal US: an update on materials and methods. *J Ultrasound*. 2013;16(2):45–55.
 21. Ciccotti MG, Ramani MN. Medial epicondylitis. *Tech Hand Up Extrem Surg*. 2003;7:190–6.
 22. Draghi F, Bortolotto C. Importance of the ultrasound in cubital tunnel syndrome. *Surg Radiol Anat*. 2016;38(2):265–8.
 23. Gregoli B, Bortolotto C, Draghi F. Elbow nerves: normal sonographic anatomy and identification of the structures potentially associated with nerve compression. A short pictorial-video article. *J Ultrasound*. 2013;16(3):119–21.
 24. Cohen M. US imaging in operated tendons. *J Ultrasound*. 2012;15:69–75.
 25. Gitto S, Draghi AG, Bortolotto C, Draghi F. Sonography of the Achilles tendon after complete rupture repair: what the radiologist should know. *J Ultrasound Med*. 2016;35:2529–36.
 26. Schwab GH, Bennett JB, Woods GW, Tullos HS. Biomechanics of elbow instability: the role of the medial collateral ligament. *Clin Orthop Relat Res*. 1980;146(146):42–52.
 27. Jacobson JA, Propeck T, Jamadar DA, Jebson PJ, Hayes CW. US of the anterior bundle of the ulnar collateral ligament: findings in five cadaver elbows with MR arthrographic and anatomic comparison -nital observations. *Radiology*. 2003;227(2):561–6.
 28. Ward SI, Teefey SA, Paletta GA Jr, et al. Sonography of the medial collateral ligament of the elbow: a study of cadavers and healthy adult male volunteers. *AJR Am J Roentgenol*. 2003;180(2):389–94.
 29. Nazarian LN, McShane JM, Ciccotti MG, O’Kane PL, Harwood MI. Dynamic US of the anterior band of the ulnar collateral ligament of the elbow in asymptomatic major league baseball pitchers. *Radiology*. 2003;227(1):149–54.
 30. Morrey BF, An KN. Articular and ligamentous contributions to the stability of the elbow joint. *Am J Sports Med*. 1983;11(5):315–9.
 31. Mulligan SA, Schwartz ML, Broussard MF, Andrews JR. Heterotopic calcification and tears of the ulnar collateral ligament: radiographic and MR imaging findings. *AJR Am J Roentgenol*. 2000;175:1099–102.
 32. Draghi F, Urciuoli L, Alessandrino F, Corti R, Scudeller L, Grassi R. Joint effusion of the knee: potentialities and limitations of ultrasonography. *J Ultrasound*. 2015;18(4):361–71.
 33. Rabiner JE, Khine H, Avner JR, Friedman LM, Tsung JW. Accuracy of point-of-care ultrasonography for diagnosis of elbow fractures in children. *Ann Emerg Med*. 2013;61(1):9–17.
 34. Gitto S, Draghi AG, Draghi F. Sonography of non-neoplastic disorders of the hand and wrist tendons. *J Ultrasound Med*. 2018;37:51–68.

Content Overview

Triceps muscle and tendon

- Complete tear
- Partial tear
- Avulsive tears
- Tendinopathy

Olecranon bursa

- Bursitis

Effusion

Loose bodies

Posterior fat pad

Ulnar nerve

- Entrapment neuropathies
- Ulnar nerve instability
- Cubital tunnel syndrome
- Therapy of neuropathy
- Ulnar nerve transposition

The triceps muscle is made up of three heads, medial, lateral, and long; it inserts onto the olecranon with a single, thick tendon consisting of a superficial portion composed of the lateral and long heads, and a deep portion composed of the medial head [1–3].

Muscle [4] and tendon injuries are uncommon. Local or systemic steroid use, renal disease, hyperparathyroidism, Marfan's syndrome, osteogenesis imperfecta and chronic olecranon bursitis are some of the factors predisposing to triceps brachii lesions [5].

Triceps tendon tears usually occur from a direct blow or a deceleration force applied to the arm while the triceps muscle is contracted, usually during a fall on an out-stretched hand. Tears can be differentiated between complete (Fig. 8.1), partial, and avulsive. The complete tear needs surgical intervention, versus possible conservative treatment in partial tears.

Ultrasound can differentiate complete from partial tears: disruption of the distal triceps tendon fibers with a fluid gap, retraction and surrounding fluid indicates an acute full-thickness, whereas partial-thickness tears demonstrate incomplete disruption of the tendon fibers.

Distal triceps tendon tears are frequently avulsive at the tendon–bone interface [6]. An avulsion fracture will appear as a shadowing hyperechoic focus within the distal triceps tendon with discontinuity of this fragment with the olecranon [6].

Distal triceps tendinopathy is the rarest of the tendinopathies around the elbow.

Symptoms for distal triceps tendinopathy are consistent with other tendinopathies in that an activity-related pain is the predominant feature. Ultrasound shows reduced echogenicity and occasional calcification (Fig. 8.2) [7].

The olecranon bursa is a subcutaneous synovial space to provide smooth and almost frictionless motion between the skin, the subcutaneous tissues, and the olecranon.

Fig. 8.1 Distal triceps tendon complete tear. Long-axis ultrasound scan (panoramic imaging) shows complete interruption of tendon fiber and muscle retraction

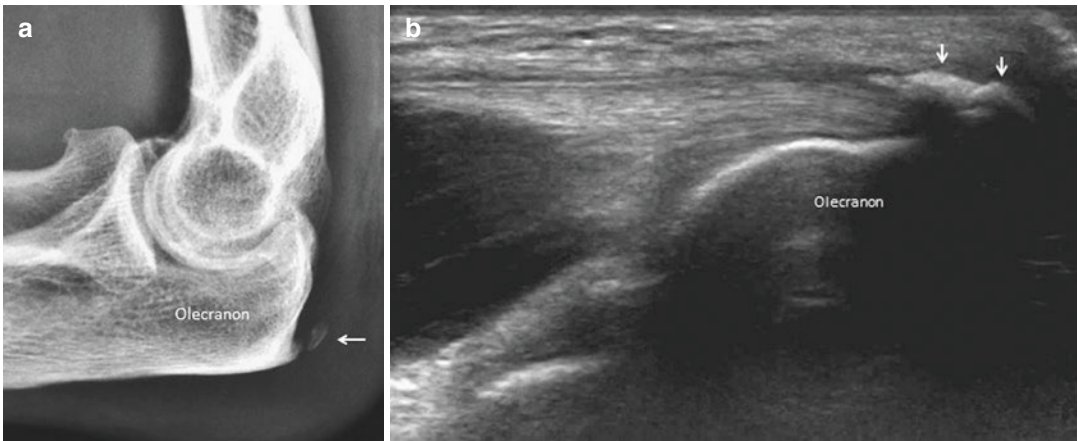


Fig. 8.2 Distal triceps tendon enthesopathy. Lateral radiograph (a) shows tendon calcifications (arrow), B-mode ultrasound (b) shows loss of echogenicity and calcifications of the tendon (arrows)

Because of its superficial location, it is a common site for injury, inflammation, and infection [8–12]. So olecranon bursitis is a common condition, and can result from infection (Figs. 8.3, and 8.4), inflammatory arthropathy, trauma, synovial proliferative disease (Fig. 8.5), crystalline disease (Fig. 8.6) [13] or, more commonly, repetitive mechanical trauma.

It may be classified as acute chronic, septic, or nonseptic.

The post-traumatic form is the most frequent, consequent to intrabursal bleeding and release of inflammatory mediators, often as response to a minor trauma.

Crystal-induced bursitis is usually associated with gout.

Rheumatoid arthritis seems also to predispose to development of nonseptic olecranon bursitis, but the true cause–effect relationship is still unknown.

Septic bursitis is traditionally thought of as a condition of young to middle-aged men involved in manual labor, related specifically to direct traumatic inoculation.

Common comorbid conditions that have a direct association with olecranon bursitis are diabetes, alcoholism, immunosuppression, and chronic steroid therapy [14].

Normal bursae are not visualized sonographically but are easily seen when distended with fluid, which may be septated and demonstrate variable echogenicity. Effusions may be simple and anechoic or complex containing internal echogenicity, the latter of which may indicate infection, hemorrhage, or inflammation.

Deep to the triceps there is a joint space, the posterior recess, also known as the olecranon recess [15, 16].

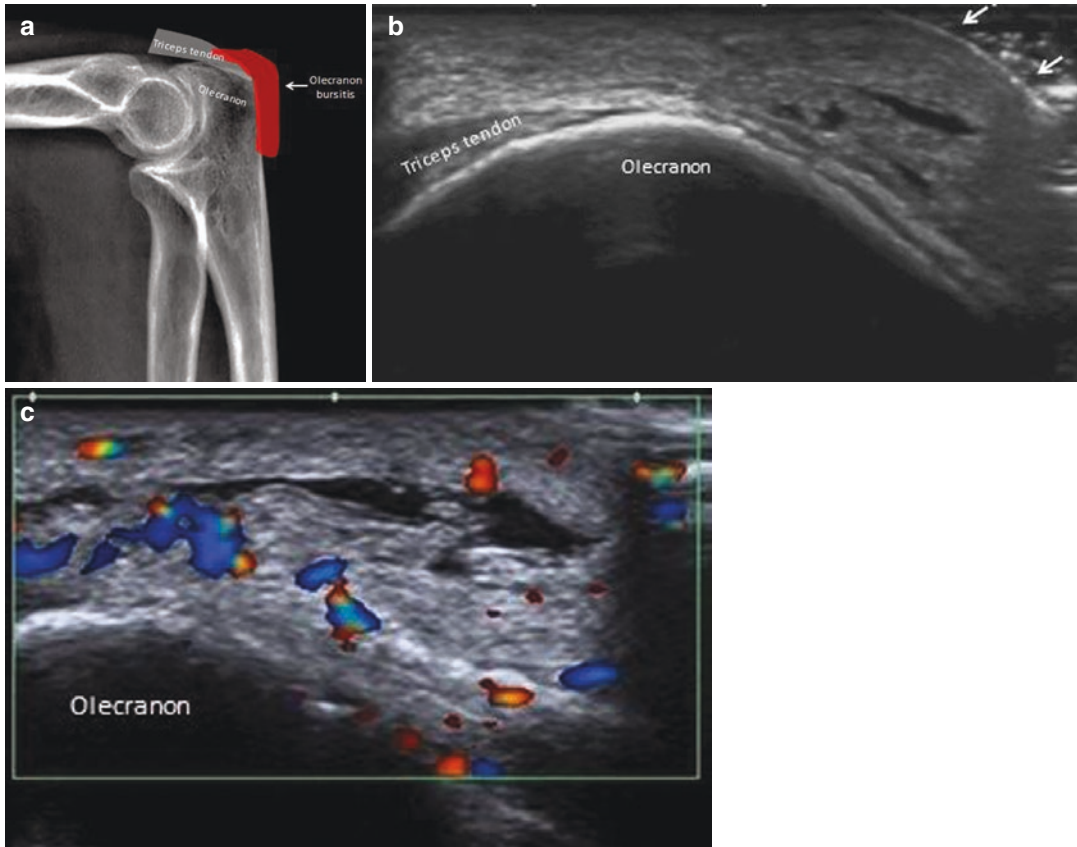


Fig. 8.3 Olecranon infectious bursitis. Schematic diagram (a). Sonogram of the posterior aspect of the elbow reveals complex-solid appearance of the bursa (arrows)

(b). Color Doppler demonstrates increased flow within the bursal lining (c)

In flexion, fluid collects posteriorly and, only when in larger quantities, anteriorly, so it is possible for identification also of only 1–3 ml of fluid with sonography posteriorly with the elbow flexed.

The elbow is probably the second most common site for detection of loose bodies in the joint space after the knee, and loose bodies are most often found in the anterior recess but may be found also in the posterior recess. The surrounding effusion enhances their visualization (Fig. 8.7) [17].

The posterior fat pad during extension is highly mobile, while during flexion rests in the olecranon fossa, applied closely to bone by the overlying triceps tendon. Distension of the synovium elevates the fat pad, providing the basis for the fat pad sign [18].

The ulnar nerve in the elbow courses through the cubital tunnel [19–21], a retroepicondylar osseous groove at the postero-medial aspect of the elbow.

The cubital tunnel is bordered by the posterior surface of the medial epicondyle and by the olecranon. The posterior bundle of the medial collateral ligament and the retinaculum (Osborne's ligament), respectively, form floor and ceiling of the cubital tunnel.

The retinaculum is anatomically highly variable, is present in 77–91% of patients, and sometimes, when present, it is lax. Authors have also stated that when the anconeus epitrochlearis muscle is present it replaces Osborne's ligament.

The loss of the normal aspect of the ulnar nerve, with a focal, homogeneous hypoechogenicity, can be observed in asymptomatic subjects at

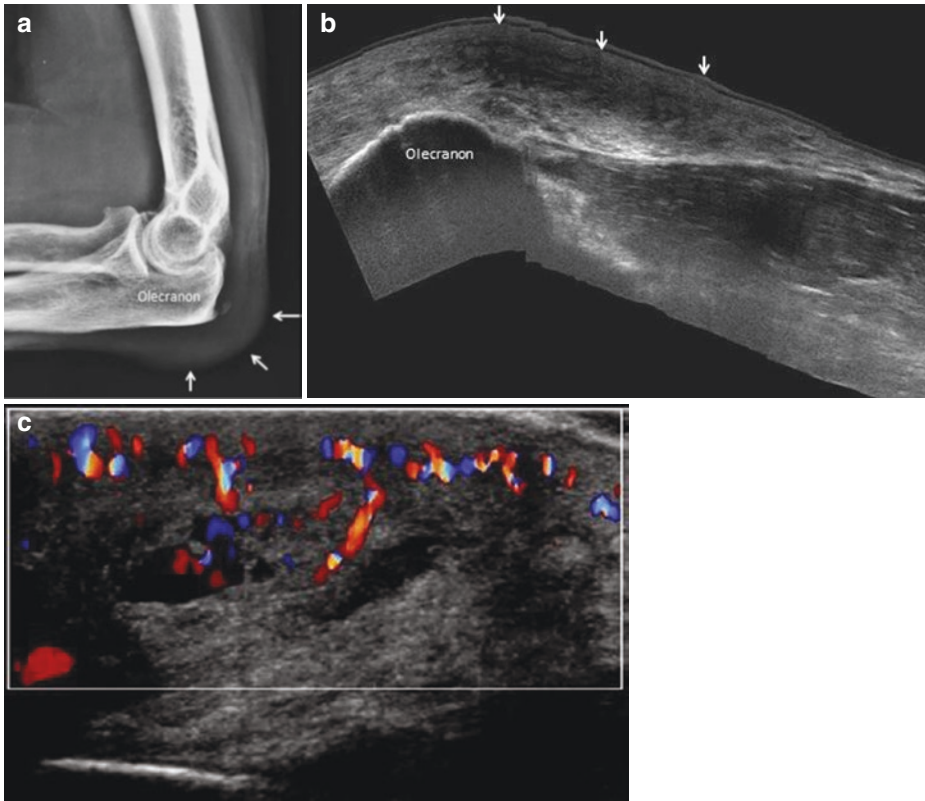


Fig. 8.4 Olecranon infectious bursitis. Lateral radiograph (a) of a patient with bursitis (arrows). Panoramic imaging of the posterior aspect of the elbow reveals

complex-solid appearance of the bursa (arrows) (b). Color Doppler demonstrates increased flow within the bursal lining (c)

Fig. 8.5 Olecranon bursitis in a patient with rheumatoid arthritis. Sonography shows fluid distension of the bursa (arrows), with synovial thickening and proliferation. (a) Long-axis ultrasound image, (b) short-axis ultrasound image

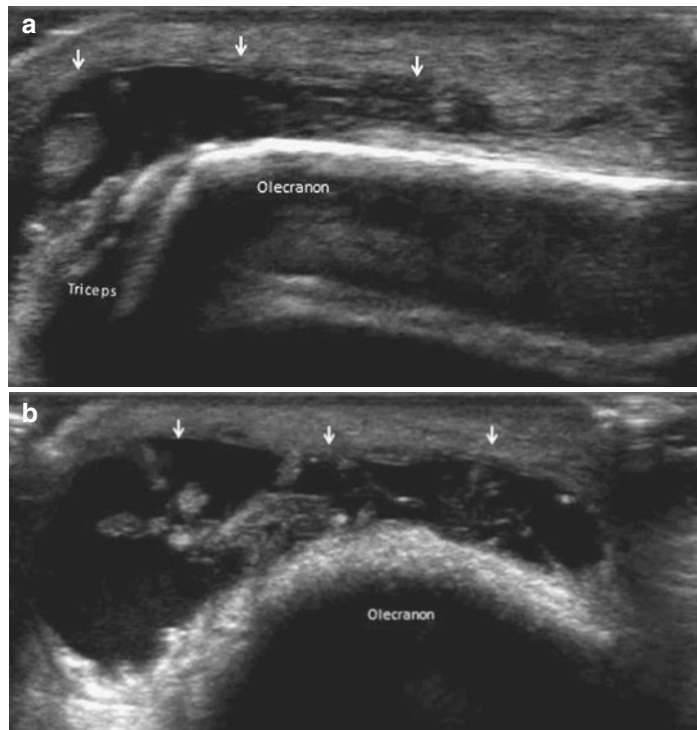


Fig. 8.6 Crystal deposition diseases bursitis. Panoramic imaging of the posterior aspect of the elbow reveals complex-solid appearance of the bursa (arrows)

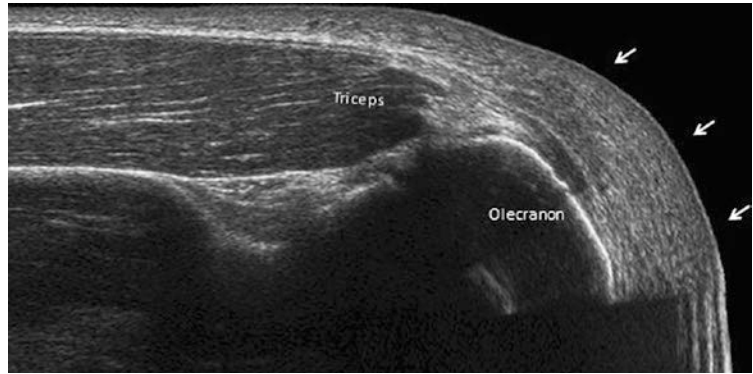
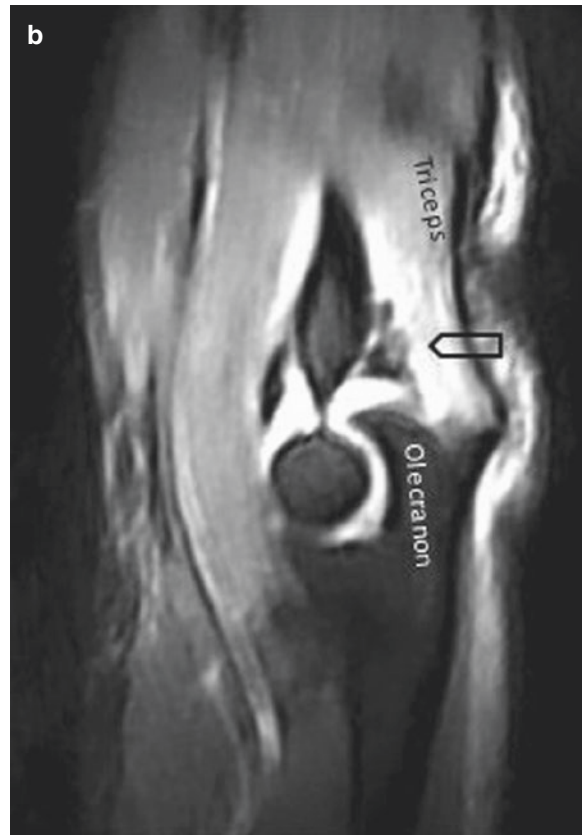
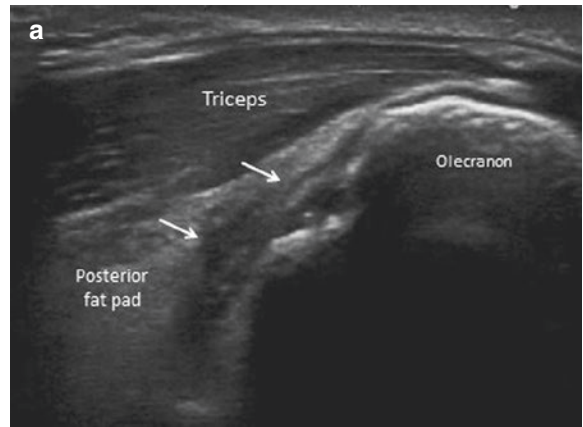


Fig. 8.7 Elbow effusion. Sonography, with joint in flexion, demonstrates effusion in the posterior recess, superior displacement of the posterior fat pad and intraarticular bodies (void arrow) (a) MRI image (b) same case as in (a)



the cubic tunnel, where the nerve undergoes a physiological compression and stretching (Fig. 8.8).

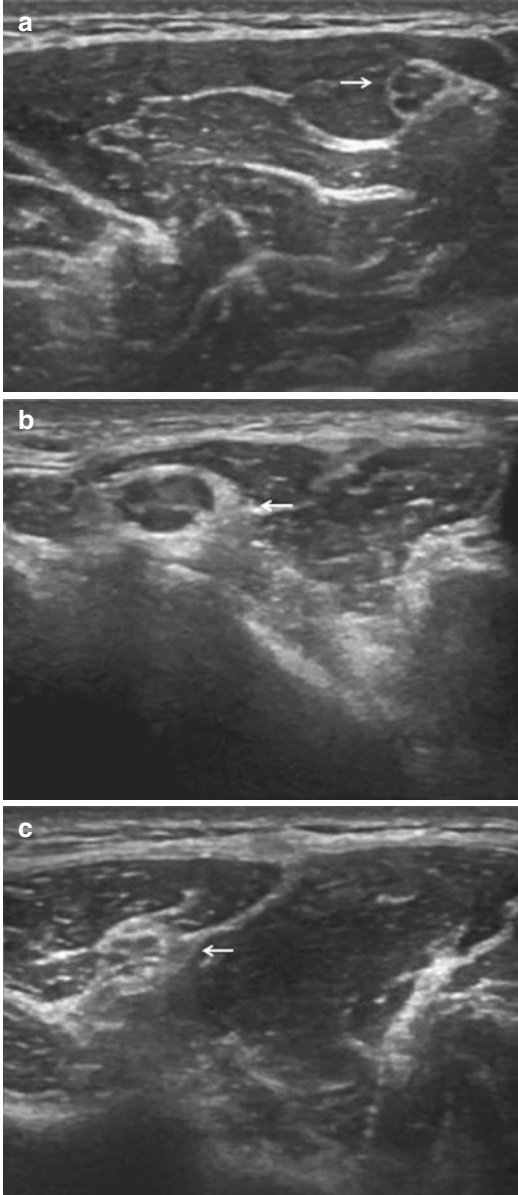


Fig. 8.8 Hypoconogenicity of the ulnar nerve in the cubic tunnel. From proximal to distal, in asymptomatic woman, sonography shows: normal appearance of ulnar nerve proximally (arrow) (a) hypoconogenicity at the level of the cubital tunnel (arrow) (b) and normal appearance distally (arrow) (c) There is a fibrous septum that divides the nerve

The ulnar nerve is the most commonly injured nerve at the elbow, owing to its location, unprotected by soft tissue. Most common conditions that affect the ulnar nerve include entrapment neuropathy (Figs. 8.9, 8.10, and 8.11), dislocation (Fig. 8.12), and dislocation of the medial head of the triceps muscle with ulnar nerve dislocation [21–23].

Entrapment neuropathies are a heterogeneous group of conditions, in which the ulnar nerve is chronically entrapped in the cubital tunnel. Ulnar neuropathy can manifest alone or with nerve or muscle dislocation (Fig. 8.13). Symptoms of neuropathy include sensory problems in the 40 or 50 digit and motor problems in muscles innervated by the ulnar nerve.

Ulnar nerve instability consists of subluxation or dislocation of the ulnar nerve during elbow flexion.

Surgical treatment of neuropathy may be required and has two main approaches: decompression of the nerve in its usual position or transposition. Secondary neuropathy after surgical decompression may occur and can be assessed by sonography (Fig. 8.14).

Cubital tunnel syndrome, the second most common peripheral compression neuropathy after carpal tunnel syndrome, is a symptom complex with sensory and motor deficiencies or dysesthesia (medial elbow pain, sensory symptoms in the fourth and fifth fingers, weakness of the intrinsic hand muscles) [22–24].

The syndrome can be primary or idiopathic and secondary or symptomatic. The primary form includes abnormalities such as luxation of the ulnar nerve (Fig. 8.12), hypertrophy/dislocation of the medial head of the triceps muscle (Fig. 8.13), and the presence of anconeus epitrochlearis muscle (Fig. 8.11). The secondary forms follow a previous injury of the elbow, such as distal humerus fractures, osteoarthritic changes with exostoses, unstable elbow joint, joint effusion (Fig. 8.9), rheumatoid arthritis with proliferative synovium (Fig. 8.10), or heterotopic ossifications. Other less common causes are osteochondromatosis, veins or venous plexus and primary soft tissue lesions, such as lipomas and ganglia.

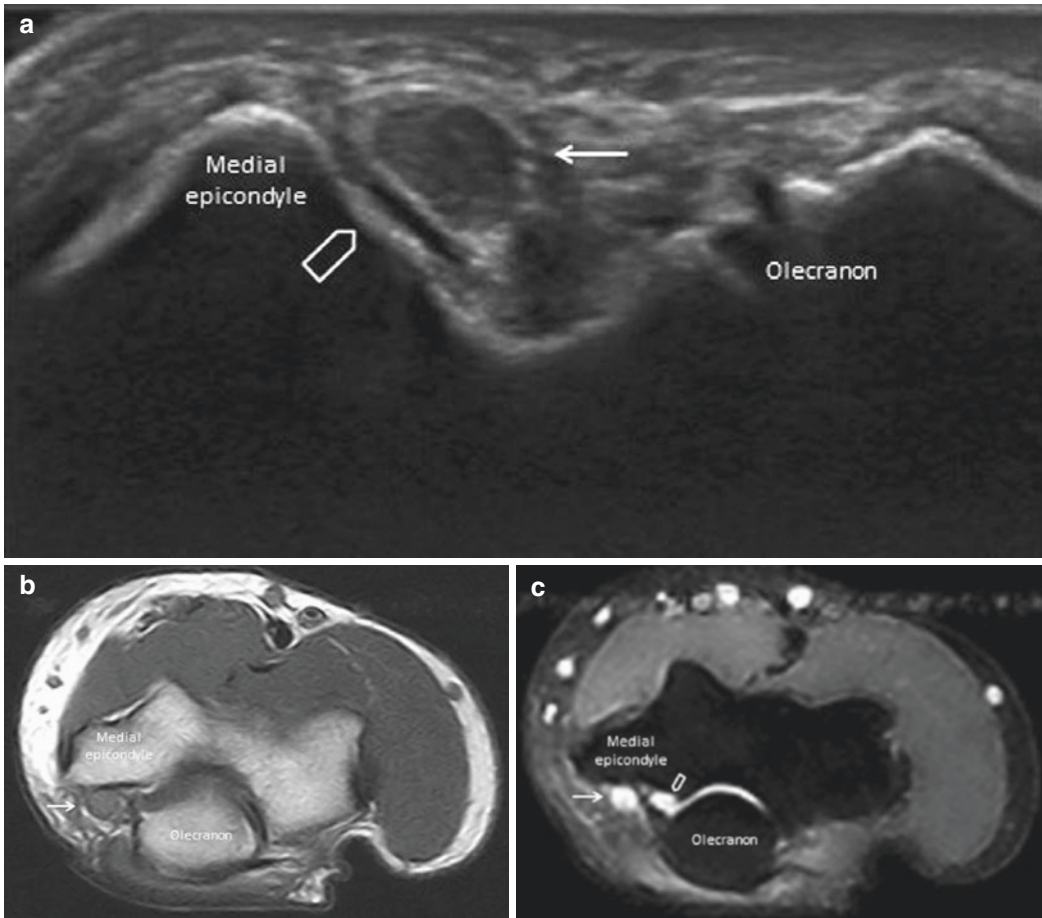


Fig. 8.9 Entrapment neuropathy of the ulnar nerve. Sonography shows hypochoic swelling of the ulnar nerve with loss of the fascicular pattern (arrow) and joint affu-

sion (void arrows) (a) Same case as Fig. 8.1a: MRI shows increased signal intensity of the ulnar nerve (arrows) on transverse T1 (b) and DP fat-saturate MRI images (c) and joint effusion (void arrows) (c)

Fig. 8.10 Entrapment neuropathy of the ulnar nerve in patients with rheumatoid arthritis. Sonography (panoramic imaging) shows hypochoic swelling of the ulnar nerve with loss of the fascicular pattern (arrow), joint effusion and superior displacement of the posterior fat pad

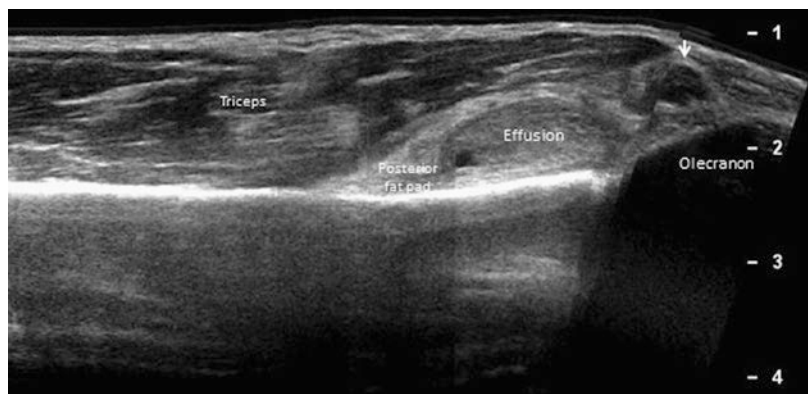


Fig. 8.11 Entrapment neuropathy of the ulnar nerve. Sonography shows hypoechoic swelling of the ulnar nerve with loss of the fascicular pattern (arrow), and an anconeus epitrochlearis muscle

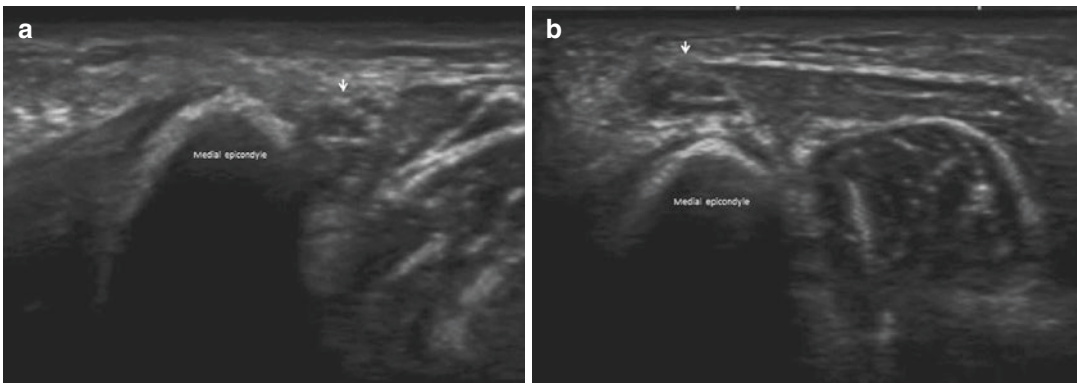
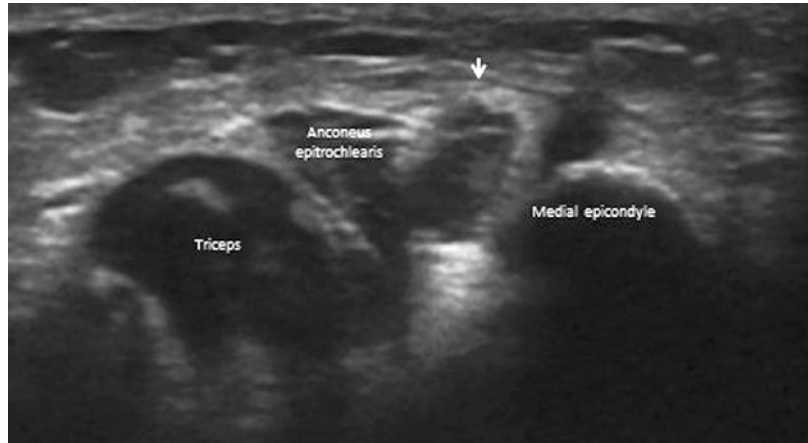


Fig. 8.12 Ulnar nerve instability. Axial sonograms of the cubital tunnel during elbow flexion (**a**, **b**) show that the nerve (arrows) is suddenly displaced anterior to the medial epicondyle (**b**). The nerve has a normal appearance

The main sonographic sign of cubital tunnel syndrome is a hypoechoic swelling of the ulnar nerve with loss of the fascicular pattern [22].

Sonography and MRI may be required primarily to evaluate the causes of compression, but also to locate nerve lesions.

Ulnar nerve instability at the cubital tunnel is frequent (16–47% of asymptomatic healthy people), bilateral in almost three quarters of cases and often asymptomatic.

Dislocation or subluxation of the ulnar nerve occurs, over the apex of the medial epicondyle, near the origin of the common flexor tendon, in the congenital partial or complete absence of the cubital tunnel retinaculum or when it is lax, during flexion of the elbow, to return inside the tunnel when the joint is extended (Figs. 8.12, and 8.13) [2, 3].

The retinaculum seems to be of critical importance in terms of the stability of the ulnar nerve in the cubital tunnel. It originates from the medial epicondyle and inserts into the olecranon, superficially bridges the medial side of the elbow, posteromedially closing the tunnel just superficial to the ulnar nerve. When a retinaculum is present, the stability of the ulnar nerve is maintained in contrast, no retinaculum is visible when the nerve is unstable.

Patients may have only mild discomfort with tingling and paresthesias or microtrauma of the nerve over the medial epicondyle due to repetitive dislocation, which can cause friction neuritis with symptoms and signs of ulnar nerve impairment. When the nerve is dislocated, patients may have a transient snapping sensation.

The ultrasound technique to evaluate these conditions can vary; however, it consists initially of an evaluation of the ulnar nerve to look for signs of neuropathy, subsequently the ulnar nerve is examined during active flexion and extension (Fig. 8.12) with transducer positioned transversely, with ends over the olecranon and the medial epicondyle.

With elbow flexion, anterior dislocation of the medial head of the triceps muscle relative to the medial epicondyle, referred to as snapping triceps syndrome, leads to concurrent dislocation of the adjacent ulnar nerve [25] (Fig. 8.13).

Predisposing factors include accessory musculotendinous slip of the medial head of the triceps, muscle bulk in body builders and prior fracture with alteration of bone alignment.

Clinical presentation is variable with medial elbow pain, snapping sensation, and ulnar neuropathy; snapping triceps syndrome may, however, remain asymptomatic in most cases.

The ultrasound technique to evaluate these conditions is the same as dislocating nerve [24], but in nerve instability the nerve and medial triceps often appear separate, whereas in the snapping triceps syndrome often the ulnar nerve and triceps appear to travel as one unit.

The identification of a dislocating medial head of the triceps in conjunction with a dislocating ulnar nerve allows selection of the correct surgical treatment.

Therapy of neuropathy may be conservative or surgical [26]. There are two main approaches for the surgical treatment of this condition: decompression of the nerve in its usual position or transposition to the ulnar flexor side (subcutaneous, intramuscular, and submuscular) [27].

Anterior transposition of the ulnar nerve is a common surgical procedure for entrapment neuropathy, which provides direct decompression of the ulnar nerve as well as elimination of traction during elbow flexion. Anterior transposition, however, may create new sites of constriction and sometimes patients have persisting symptoms for recurrent or persistent neuropathy. The most common new sites of constriction are the internal brachial ligament, or “arcade of Struthers,” the medial intermuscular septum, the

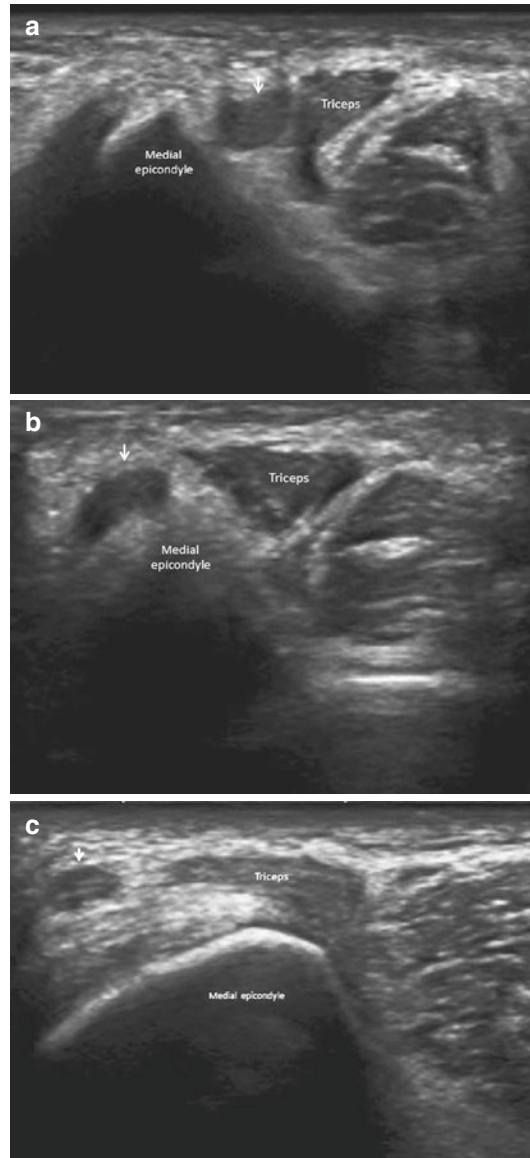


Fig. 8.13 Snapping triceps syndrome. Axial sonograms during elbow flexion (a, b, c) show anterior dislocation of the medial head of the triceps muscle relative to the medial epicondyle, and concurrent dislocation of the adjacent ulnar nerve (arrows). Hypoechoic swelling of the ulnar nerve is present

humeral and ulnar heads of the flexor carpi ulnaris, and the common aponeurosis of the humeral head of the flexor carpi ulnaris and flexor digitorum superficialis. The common aponeurosis encountered between the flexor digitorum superficialis and flexor carpi ulnaris muscles represents

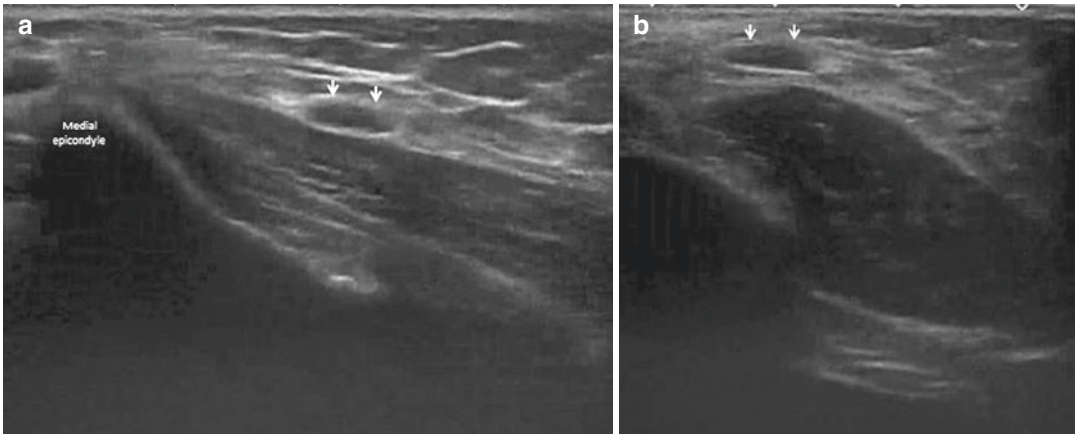


Fig. 8.14 Recurrent neuropathy after anterior transposition of ulnar nerve. Sonography shows hypoechoic swelling of the ulnar nerve entrapped at the level of the common aponeurosis of the humeral head of the flexor carpi ulnaris

the most common site of post-transposition entrapment, which may account for a subset of failed anterior transpositions.

Nerve constriction can cause blood flow restriction and secondary neuropathy [28].

Secondary neuropathy after ulnar nerve transposition can be assessed by sonography (Fig. 8.14). Sonographic signs of nerve compression are the same as all nerve compression, a hypoechoic swelling of the nerve with loss of the fascicular pattern and hyperemia with Doppler imaging. Sonographic exploration, with release of compressing structures, is recommended to provide an unconstrained distal course for a transposed ulnar nerve [29, 30].

Implication for patient care

The loss of the normal aspect of the ulnar nerve, with a focal, homogeneous hypoecogenicity, can be observed in asymptomatic subjects at the cubic tunnel, where the nerve undergoes a physiological compression and stretching

Key points

Triceps muscle and tendon injuries are uncommon. Distal triceps tendinopathy is the rarest of the tendinopathies around the elbow.

Because of its superficial location, olecranon bursa is a common site for injury, inflammation, and infection

The ulnar nerve is the most commonly injured nerve at the elbow, owing to its location, unprotected by soft tissue.

Ulnar nerve instability at the cubital tunnel is frequent (16–47% of asymptomatic healthy people), bilateral in almost three quarters of cases and often asymptomatic.

and flexor digitorum superficialis muscles, following anterior transposition of the nerve. (a) Long-axis ultrasound image, (b) short-axis ultrasound image

References

1. Belentani C, Pastore D, Wangwinyuvirat M, Dirim B, Trudell DJ, Haghighi P, Resnick D. Triceps brachii tendon: anatomic-MR imaging study in cadavers with histologic correlation. *Skelet Radiol*. 2009;38(2):171–5.
2. Tagliafico AS, Bignotti B, Martinoli C. Elbow US: anatomy, variants, and scanning technique. *Radiology*. 2015;275(3):636–50.
3. Draghi F, Danesino GM, de Gautard R, Bianchi S. Ultrasound of the elbow: examination techniques and US appearance of the normal and pathologic joint. *J Ultrasound*. 2007;10(2):76–84.
4. Draghi F, Zacchino M, Canepari M, Nucci P, Alessandrino F. Muscle injuries: ultrasound evaluation in the acute phase. *J Ultrasound*. 2013;16(4):209–14.
5. Tagliafico A, Gandolfo N, Michaud J, Perez MM, Palmieri F, Martinoli C. Ultrasound demonstration of distal triceps tendon tears. *Eur J Radiol*. 2012;81(6):1207–10.
6. Gitto S, Draghi AG, Draghi F. Sonography of non-neoplastic disorders of the hand and wrist tendons. *J Ultrasound Med*. 2018;37:51–68.
7. Konin GP, Nazarian LN, Walz DM. US of the elbow: indications, technique, normal anatomy, and pathologic conditions. *Radiographics*. 2013;33(4):E125–47.
8. Blankstein A, Ganel A, Givon U, Mirovski Y, Chechick A. Ultrasonographic findings in patients with olecranon bursitis. *Ultraschall Med*. 2006;27(6):568–71.
9. Blackwell JR, Hay BA, Bolt AM, Hay SM. Olecranon bursitis: a systematic overview. *Shoulder Elbow*. 2014;6(3):182–90.
10. Reilly D, Kamineni S. Olecranon bursitis. *J Shoulder Elb Surg*. 2016;25(1):158–67.

11. Floemer F, Morrison WB, Bongartz G, Ledermann HP. MRI characteristics of olecranon bursitis. *AJR Am J Roentgenol*. 2004;183(1):29–34.
12. Del Buono A, Franceschi F, Palumbo A, Denaro V, Maffulli N. Diagnosis and management of olecranon bursitis. *Surgeon*. 2012;10(5):297–300.
13. Patel J, Girishkumar, Mruthyunjaya, Rupakumar CS. Bilateral olecranon bursitis—a rare clinical presentation of calcium pyrophosphate crystal deposition disease. *J Orthop Case Rep*. 2014;4(1):3–6. <https://doi.org/10.13107/jocr.2250-0685.137>.
14. Draghi F, Corti R, Urciuoli L, Alessandrino F, Rotondo A. Knee bursitis: a sonographic evaluation. *J Ultrasound*. 2015;18(3):251–7.
15. Tran N, Chow K. Ultrasonography of the elbow. *Semin Musculoskelet Radiol*. 2007;11(2):105–16.
16. Finlay K, Ferri M, Friedman L. Ultrasound of the elbow. *Skelet Radiol*. 2004;33(2):63–79.
17. Bianchi S, Martinoli C. Detection of loose bodies in joints. *Radiol Clin N Am*. 1999;37(4):679–90.
18. Thornton R, Riley GM, Steinbach LS. Magnetic resonance is highly mobile anechoic imaging of sports injuries of the elbow. *Top Magn Reson Imaging*. 2003;14(1):69–86.
19. Michelin P, Leleup G, Ould-Slimane M, Merlet MC, Dubourg B, Duparc F. Ultrasound biomechanical anatomy of the soft structures in relation to the ulnar nerve in the cubital tunnel of the elbow. *Surg Radiol Anat*. 2017;39(11):1215–21. <https://doi.org/10.1007/s00276-017-1879-y>.
20. Granger A, Sardi JP, Iwanaga J, Wilson TJ, Yang L, Loukas M, Oskoui RJ, Tubbs RS. Osborne’s ligament: a review of its history, anatomy, and surgical importance. *Cureus*. 2017;9(3):e1080. <https://doi.org/10.7759/cureus.1080>.
21. Gregoli B, Bortolotto C, Draghi F. Elbow nerves: normal sonographic anatomy and identification of the structures potentially associated with nerve compression. A short pictorial-video article. *J Ultrasound*. 2013;16(3):119–21.
22. Draghi F, Bortolotto C. Importance of the ultrasound in cubital tunnel syndrome. *Surg Radiol Anat*. 2016;38(2):265–8.
23. Bianchi S, Draghi F, Beggs I. Ultrasound of the peripheral nerves. In: *Clinical ultrasound*, vol. 2. London: Elsevier Ltd; 2011. p. 1158–67.
24. Martinoli C, Bianchi S, Pugliese F, Bacigalupo L, Gauglio C, Valle M, Derchi LE. Sonography of entrapment neuropathies in the upper limb (wrist excluded). *J Clin Ultrasound*. 2004;32(9):438–50.
25. Shuttlewood K, Beazley J, Smith CD. Distal triceps injuries (including snapping triceps): a systematic review of the literature. *World J Orthop*. 2017;8(6):507–13.
26. Caliendo P, La Torre G, Padua R, Giannini F, Padua L. Treatment for ulnar neuropathy at the elbow. *Cochrane Database Syst Rev*. 2016;11:CD006839.
27. Liu CH, Wu SQ, Ke XB, Wang HL, Chen CX, Lai ZL, Zhuang ZY, Wu ZQ, Lin Q. Subcutaneous versus submuscular anterior transposition of the ulnar nerve for cubital tunnel syndrome: a systematic review and meta-analysis of randomized controlled trials and observational studies. *Medicine (Baltimore)*. 2015;94(29):e1207. <https://doi.org/10.1097/MD.0000000000001207>.
28. Mahan MA, Gasco J, Mokhtee DB, Brown JM. Anatomical considerations of fascial release in ulnar nerve transposition: a concept revisited. *J Neurosurg*. 2015;123(5):1216–22.
29. Yang M, Wang J, Yang X, Zhong W, Ma Q, Li S, Zhang W. Use of high-resolution ultrasonography in anterior subcutaneous transposition of the ulnar nerve for cubital tunnel syndrome. *Acta Neurochir Suppl*. 2017;124:277–81. https://doi.org/10.1007/978-3-319-39546-3_40.
30. Won HS, Liu HF, Kim JH, Kwak DS, Chung IH, Kim IB. Intermuscular aponeuroses between the flexor muscles of the forearm and their relationships with the ulnar nerve. *Surg Radiol Anat*. 2016;38(10):1183–9.

Index

A

- Anconeus muscle, 5, 12, 13, 24
- Annular ligament, 3, 4, 9, 11
- Anterior elbow
 - avulsion fractures and detached bony fragments, 42
 - biceps muscle, 41, 43
 - bicipitoradial bursitis, 44, 45
 - brachialis muscle, 44
 - distal biceps tendon
 - after partial tear, 42, 43
 - complete tear, 41, 42
 - partial tear, 41, 42
 - tendinosis, 42, 43
 - lacertus fibrosus, 43
 - post-traumatic neuroma of median nerve, 45
 - rheumatoid arthritis, joint effusion in patient, 45
- Anterior fat pads, 1, 2, 17, 20
- Avulsion fractures, 42, 61

B

- Biceps muscle, 11, 17, 41, 43
- Bicipitoradial bursa, 5, 13, 34, 44
- Bicipitoradial bursitis, 34, 44, 45
- Brachialis muscle, 1, 11, 12, 17–19, 21, 41, 44, 45

C

- Chronic humero-ulnar joint dislocation, 36, 37
- Chronic olecranon bursitis, 33, 61
- Chronic triceps partial tear, 31, 32
- Color Doppler signals, 31, 47, 53
- Common extensor tendon, 5, 11, 13, 21, 22, 25, 31, 32
 - after surgery, 32, 48, 49
 - histology of, 47
 - origin, 47
 - partial tear, 31, 49
- Common flexor tendon, 13, 24, 26, 30, 48, 57, 68
 - B-mode ultrasound images, 54
 - partial tear, 31, 54
- Common flexor-pronator tendon, 53
- Coronoid recesses, 1, 2
- Crystal deposition diseases bursitis, 65

- Crystal-induced bursitis, 62
- Cubital tunnel syndrome, 66, 68

D

- Distal biceps brachii tendon, 31, 32
- Distal biceps muscle, 17
- Distal biceps tendon, 17, 44
 - after partial tear, 42, 43
 - complete tear, 41, 42
 - enthesopathy, 29, 30
 - evaluation, 19, 20
 - partial tears of, 41, 42
- Distal biceps tendinosis, 43
- Distal triceps tendinopathy, 61
- Distal triceps tendon, 13, 25, 61, 62
- Distal triceps tendon enthesopathy, 62

E

- Elbow, anatomy of
 - anconeus muscle, 13
 - annular ligament, 10–11
 - anterior bundle origin, 10
 - articular cartilage, 9
 - biceps muscle, 11
 - brachialis muscle, 11
 - bursae, 13
 - extensor tendon, 11
 - fat pads, 10
 - flexor tendon, 13
 - fossae, 9
 - joint synovium, 9, 10
 - lateral collateral ligament complex, 10
 - lateral muscle group, 11
 - lateral ulnar collateral ligament, 10, 11
 - medial collateral ligament complex, 10
 - medial muscle, 13
 - median nerve, 14
 - muscle, 11, 12
 - normal joint capsule, 9
 - posterior band origin, 10
 - pronator teres, 13

- Elbow, anatomy of (*cont.*)
 proximal ulna, 9
 radial collateral ligament, 11
 radial nerve, 14, 15
 supinator muscle, 11
 tendons, 11
 transverse bundle, 10
 triceps musculo-tendinous unit, 13
 trochlea articulates with the ulna, 9
 ulnar nerve, 14
- Elbow effusion, 65
 with fat pad dislocation, 3
 ultrasound detection of, 33, 45
- Elbow muscles, function of, 4
- Elbow synovium, 2
- Entrapment neuropathies, 35, 50, 66–69
- Epicondyle fracture, 36, 37, 57
- Extensor tendinopathy, *see* Lateral epicondylitis
- G**
- Ganglion cyst, 36, 37, 50, 51
- Golfer's elbow, *see* Medial epicondylitis
- H**
- Humero-radial joint, 1
- Humero-ulnar joint, 1, 2
- Hyperemia, 34, 35, 48, 50, 54, 70
- J**
- Joint capsule, 3, 9, 10, 23, 36
- Joint synovium, 9, 10
- L**
- Lacertus fibrosus partial tear, 43, 45
- Lateral collateral ligament complex, 3, 4, 10, 11, 21, 23, 49, 50
- Lateral elbow
 common extensor tendon
 after surgery, 48, 49
 partial tear, 49
 entrapment neuropathy of deep branch, 50
 ganglion cyst, 50, 51
 lateral collateral ligament, 49, 50
 lateral epicondylitis
 B-mode ultrasound images, 47, 48
 cause of, 47
 characterization, 47
 diagnosis, 47
 histology in, 47
 longitudinal scans, 48
 tendons with, 48
 treatment of, 48
- Lateral epicondylitis, 29
 B-mode ultrasound images, 47, 48
- cause of, 47
 characterization, 47
 diagnosis, 47
 histology in, 47
 longitudinal scans, 48
 tendons with, 48
 treatment of, 48
- Lateral ulnar collateral ligament, 4, 10, 11
- M**
- Medial collateral ligament, 3, 10, 24–26, 56, 63
- Medial elbow, 57
 common flexor-pronator tendon, 53
 common flexor tendon partial tear, 54
 joint effusion, 57
 medial collateral ligament, 56
 medial epicondyle fracture, 57
 medial epicondylitis
 B-mode ultrasound, 53, 54
 characterization, 53
 sonoelastography, 53
 ulnar neuropathy, 54
 non-Hodgkin lymphoma, patient with, 58
 pronator teres intramuscular extensive calcification, 55
 pronator teres syndrome, 55, 56
 ulnar collateral ligament, 55, 56
 ultrasonography, 56
- Medial epicondyle fracture, 57
- Medial epicondylitis, 29, 30
 B-mode ultrasound, 53, 54
 characterization, 53
 sonoelastography, 53
 ulnar neuropathy, 54
- Medial muscle, 4, 12, 13
- Median nerve, 6, 14, 19, 21, 34
 compression of, 55
 post-traumatic neuroma, 35, 36, 45
- Microtrauma, 29, 44, 47, 56, 68
- Muscle compartments, 4, 5
- N**
- Native bursae, 5
- Neoangiogenesis, 31, 47, 53
- Neuromas, 34, 35
- Non-Hodgkin lymphoma, 58
- Non-native bursae, 5
- O**
- Olecranon bursa, 5, 13, 23, 34, 61
- Olecranon bursitis, 62, 64
- Olecranon fracture, 36, 37
- Olecranon recesses, 1
- Orthopedic hardware impingement, 57
- Osborne's ligament, 5, 6, 14, 24, 63

P

Pathology, elbow

- bicipitoradial bursitis, 33–34
- compartment, 29, 30
- chronic humero-ulnar joint dislocation, 36, 37
- chronic olecranon bursitis, patient with, 33
- chronic triceps partial tear, 31, 32
- common extensor tendon, 31, 32
- distal biceps brachii tendon, 31, 32
- distal biceps tendon enthesopathy, 29, 30
- elbow effusion, 33
- elbow sports-related injuries, 29, 31
- entrapment neuropathy of ulnar nerve, 34, 35
- epicondyle fracture, 36, 37
- ganglion cyst, 36, 37
- lateral epicondylitis, 29
- medial epicondylitis, 29, 30
- median nerve, post-traumatic in-continuity
 - neuroma of, 35, 36
- olecranon fracture, 36, 37
- pain and differential diagnosis, 31
- rheumatoid arthritis, patient with, 33
- subcutaneous lipoma, 36, 37
- subcutaneous tissue edema, 37, 38
- triceps myeloma, 36, 38
- triceps rhabdomyosarcoma, 36, 38
- ulnar nerve
 - entrapment neuropathy, 34, 35
 - instability, 36

Posterior elbow

- crystal deposition diseases bursitis, 65
- crystal-induced bursitis, 62
- cubital tunnel, 63
- cubital tunnel syndrome, 66, 68
- distal triceps tendinopathy, 61
- distal triceps tendon complete tear and enthesopathy, 62
- elbow effusion, 65
- entrapment neuropathies, 66
- olecranon bursa, 61
- olecranon infectious bursitis, 61, 63, 64
- post-traumatic form, 62
- predisposing factors, 69
- retinaculum, 63, 68
- rheumatoid arthritis, 62
- septic bursitis, 62
- snapping triceps syndrome, 69
- surgical treatment of neuropathy, 66
- triceps tendon, 61
- ulnar nerve, 63, 66, 68
 - anterior transposition of, 69
 - dislocation/subluxation of, 68
 - entrapment neuropathy of, 67, 68
 - hypoconogenicity of, 66
 - instability of, 66, 68
 - luxation of, 66
 - recurrent neuropathy after anterior transposition, 70

secondary neuropathy, 70

ultrasound technique, 69

- Posterior fat pad, 1, 33, 63, 65, 67
- Posterior interosseous nerve, 6, 7, 15, 23, 24, 34, 50
- Pronator teres syndrome, 55, 56
- Proximal radio-ulnar joint, 1, 2

R

- Radial collateral ligament, 4, 10, 11, 23
- Radial nerve, 6, 7, 14, 15, 23, 24, 34, 50
- Rheumatoid arthritis, 33, 45, 62, 64, 67

S

- Septic bursitis, 34, 62
- Snapping triceps syndrome, 69
- Sonoelastography, 31, 47, 53
- Subcutaneous lipoma, 36, 37
- Subcutaneous tissue edema, 37, 38
- Supinator muscle, 6, 11, 13, 15, 23, 34, 49, 50
- Synovial bursae, 33

T

- Tennis elbow, *see* Lateral epicondylitis
- Transverse bundle, 3, 10
- Triceps myeloma, 36, 38
- Triceps rhabdomyosarcoma, 36, 38
- Triceps tendon, transducer placement, 24, 25

U

- Ulnar collateral ligament complex, 25, 55, 56
- Ulnar nerve, 5, 14, 24, 25
 - entrapment neuropathy of, 34, 35
 - instability, 36
 - posterior elbow, 63, 66, 68
 - anterior transposition of, 69
 - dislocation/subluxation of, 68
 - entrapment neuropathy of, 67, 68
 - hypoconogenicity of, 66
 - instability of, 66, 68
 - luxation of, 66
 - recurrent neuropathy after anterior transposition, 70
 - secondary neuropathy, 70
- Ulnar neuropathy, 54, 66, 69
- Ultrasound examination
 - anconeus muscle, 24
 - anterior elbow, 17, 18
 - articular cartilage, 19, 22
 - biceps muscle, 17
 - brachialis muscle, 19, 21
 - distal biceps tendon, 17, 19, 20
 - elbow effusion, 33
 - extensor tendon, 21, 22
 - flexor tendon, 24, 26

Ultrasound examination (*cont.*)

- lacertus fibrosus, 19

- lateral synovial fringe, 23

- medial collateral ligament, 26

- medial elbow, 56

- medial epicondyle, 24

- median nerve, 19, 21

- olecranon fossa, 24

- posterior elbow, 69

- pronator teres, 25

- radial collateral ligament, 23

- radial nerve, 23, 24

- radiocapitellar joint, 20

- triceps tendon, 24, 25

- ulnar collateral ligament complex, 25

- ulnar nerve, 24, 25

Author Index

A

Abd Ellah, M.M.H., 20, 31, 47, 53
Adrien, C., 23, 24
Agarwal, A.K., 50
Ahmad, C.S., 9
Akelman, E., 48
Åkesson, I., 53
Alcid, J.G., 9
Alessandrino, F., 5, 14, 33, 34, 45, 56, 61, 62
Andrews, J.R., 56
An, K.N., 56
Antoniadis, G., 23, 24
Antonini, G., 5, 34, 20
Antuña, S.A., 53
Arvidsson, I., 53
Ashe, M.C., 31
Assendelft, W.J., 48
Assmus H, 23, 24
Aubertin, A., 23, 24
Avner, J.R., 36, 56

B

Babusiaux, D., 23, 24
Bacigalupo, L., 23, 24, 66, 69
Bak, B., 5, 44
Balogh, I., 53
Barco, R., 53
Barnes, R.P., 44
Bayraktar, B., 11, 23, 50
Beazley, J., 23, 24, 69
Beggs, I., 14, 19, 34, 45, 50, 66
Belentani, C., 13, 23, 24, 61
Bellmann-Weiler, R., 31, 47
Bennett, J.B., 56
Bero, E.H., 17, 41
Berton, C., 11, 15, 49
Bianchi, S., 1, 5, 9, 10, 13, 14, 17, 19, 23–25, 29, 31, 33, 34, 35, 36, 37, 41, 45, 47, 48, 50, 53, 55, 61, 63, 66, 68, 69
Bignotti, B., 13, 17, 19, 41, 50, 53, 61, 68
Bischoff, C., 23, 24
Blackwell, J.R., 5, 13, 24, 62
Blankstein, A., 5, 13, 62

Blasi, J., 11, 17, 41
Blasi, M., 11, 17, 41
Blease, S., 53
Bolt, A.M., 5, 13, 24, 62
Bongartz, G., 5, 23, 62
Borges, N.C., 3
Bortolotto, C., 1, 5, 14, 17, 19, 23, 24, 31, 34, 45, 48, 50, 53, 54, 63, 66, 68
Bouilleau, L., 23, 24
Boutin, R.D., 5, 44
Boynton, M.D., 3, 10, 23
Brandser, E.A., 31
Brasseur, J.L., 17, 19, 42
Brassier, G., 49
Briani, C., 5, 34, 50
Broussard, M.F., 56
Brown, B.T., 17, 41
Brown, J.M., 70
Bruno, R.J., 23–25
Buisson, G., 36
Burke, F., 20, 31, 47, 53
Burnier, M., 36

C

Calfee, R.P., 48
Caliandro, P., 69
Canepa, M.G., 48, 53
Canepari, M., 61
Capaccio, E., 11, 17, 41
Carrera, G.F., 3, 10, 23
Cecen, A., 11, 23, 50
Chaganti, J., 50
Chang, W.K., 50
Chechick, A., 5, 13, 62
Chen, C.X., 69
Chen, L., 11, 17, 19, 44
Chen, R.E., 48
Chew, M.L., 5, 42
Chotel, F., 36
Chou, D.S., 5, 44
Chow, K., 1, 62
Chow, S., 31
Chung, I.H., 70

Ciccotti, M.G., 24, 54, 56
 Claudio, G.K., 24, 53, 54
 Cohen, M., 31, 48, 54
 Cohen, M.S., 23–25
 Connell, D., 20, 31, 47, 53
 Coombes, P., 3, 20, 31, 47, 53
 Coraci, D., 5, 34, 50
 Corti, R., 5, 33, 56, 62
 Cosgarea, A., 34
 Cots, M., 50
 Créteur, V., 13, 14, 24, 25, 53, 55
 Cunin, V., 36
 Curry, M.C., 3, 10

D

Dahmane, M., 35
 Dalmau-Pastor, M., 9
 Danesino, G.M., 1, 5, 9, 10, 17, 29, 31, 41, 47,
 53, 61, 68
 Daniels, D.L., 3, 10, 23
 Dantas, R.W., 5, 44
 Darnault, P., 49
 DaSilva, M.F., 48
 De Franco, P., 5, 34, 50
 de Gautard, R., 1, 5, 9, 10, 17, 29, 31, 41, 47, 53, 61, 68
 de la Fuente, J., 11, 17, 41
 Del Buono, A., 5, 23, 62
 De Maeseneer, M., 17, 23, 24, 33, 45
 Deml, C., 20, 31, 47, 53
 Denaro, V., 5, 23, 62
 Derchi, L.E., 11, 17, 23, 24, 41, 66, 69
 Devillé, W.L., 48
 De Zordo, T., 31, 47
 Di Pasquale, A., 5, 34, 50
 Dirim, B., 13, 23, 24, 61
 Domingo, T., 11, 17, 41
 Donaldson, O., 53
 do Nascimento, A.T., 24, 53, 54
 Draghi, A.G., 31, 36, 45, 48, 54, 57, 61
 Draghi, F., 1, 5, 9, 10, 14, 17, 19, 23, 24, 29, 31, 33,
 34, 36, 37, 41, 44, 45, 47, 48, 50, 53, 54,
 56, 57, 61, 62, 63, 66, 68
 Dubourg, B., 63
 Dunn, J.C., 23, 24
 Duparc, F., 63
 Dyer, G.S., 36

E

El-Khoury, G.Y., 31
 Erickson, S.J., 3, 10, 23
 Ernst, M.F., 44
 Erra, C., 5, 34, 50
 Escobedo, E., 44
 Escolà, A., 50
 Espiga, X., 50

F

Fallone, J.C., 50
 Fares, A., 23, 24
 Faro, F., 48
 Feld, R.I., 47
 Ferri, M., 1, 4, 33, 45, 53, 62
 Ferrozzi, G., 1
 Feuchtner, G.M., 31, 47
 Fink, C., 31, 47
 Finlay, K., 1, 4, 33, 45, 53, 62
 Floemer, F., 5, 23, 62
 Fontaine, C., 11, 15, 49
 Franceschi, F., 5, 23, 62
 Francesc Malagelada, D., 9
 Frankel, M., 50
 Freeman, D., 20, 47, 53
 Friedman, D., 23, 24
 Friedman, L., 1, 4, 33, 45, 53, 62
 Friedman, L.M., 36, 56
 Fritz, R.C., 53
 Frohse, F., 50
 Fu, F., 3
 Fukuta, S., 1, 10

G

Gaetke-Udager, K., 5, 13
 Gandolfo, N., 36, 61
 Ganel, A., 5, 13, 62
 Gasco, J., 70
 Gauglio, C., 23, 24, 66, 69
 Gayretli, O., 13, 23
 Geaney, L.E., 41
 Giannakopoulos, P.N., 48
 Giannini, F., 69
 Giovagnorio, F., 13, 17, 33, 45, 53
 Girishkumar, H., 5, 62
 Gitto, S., 31, 36, 45, 48, 54, 57, 61
 Giuffrè, B.M., 5, 42
 Givon, U., 5, 13, 62
 Godey, B., 49
 Golanó, P., 9
 Goldfarb, C.A., 48
 Gosens, T., 53
 Goto, H., 3
 Goto, T., 1, 10
 Granata, G., 5, 34, 50
 Granger, A., 63
 Grassi, R., 33, 56
 Gregoli, B., 5, 14, 17, 19, 34, 44, 45, 50, 54, 63, 66
 Gruber, L., 31
 Guegan, Y., 49

H

Haghighi, P., 5, 11, 13, 17, 19, 23, 24, 44, 61
 Halpern, E.J., 20, 31, 47, 53

Hamada, D., 1, 10
 Hansson, G.A., 53
 Hart, L., 48, 53, 57
 Harwood, M.I., 56
 Hausman, M., 17, 41
 Hay, B.A., 5, 13, 24, 62
 Hayes, C.W., 56
 Hay, S.M., 5, 13, 24, 62
 Higuchi, T., 1, 10
 Hodler, J., 5, 14, 17, 19, 45
 Hoffmann, R., 23, 24
 Hooper, A.W., 5, 44
 Hotchkiss, R.N., 44
 Hoy, G., 20, 47, 53
 Huber, J., 3
 Hunter, J.C., 44
 Husarik, D.B., 5, 14, 17, 19, 45

I

Iagnocco, A., 1, 3, 10, 41, 47, 53
 Introcaso, J.H., 53
 Iwanaga, J., 63

J

Jacob, D., 37, 48, 53
 Jacobson, J.A., 5, 13, 17, 23, 24, 33, 45, 56
 Jamadar, D.A., 56
 Jaovisidha, S., 17, 23, 24, 33, 45
 Jaschke, W., 31, 47
 Jaschke, W.R., 20, 31, 47, 53
 Jebson, P.J., 56
 Jost, B., 5, 14, 17, 19, 45

K

Kale, A.C., 11, 23, 50
 Kamineni, S., 5, 23, 62
 Kapoor, C., 50
 Ke, X.B., 69
 Khan, K.M., 31
 Khatol, M.H., 31
 Khine, H., 36, 56
 Khurana, B., 36
 Kilcoyne, K., 23, 24
 Kim, H.J., 11, 15, 49
 Kim, I.B., 70
 Kim, J.H., 70
 Klauser, A.S., 20, 31, 47, 53
 Klima, G., 20, 31, 47, 53
 Knutsen, E.J., 48
 Kocabiyik, N., 13, 23
 Kofler, J., 3
 Kohen, R.B., 44
 Konin, G.P., 1, 3, 10, 17, 31, 33, 41, 47, 49, 53, 61
 Korschake, M., 11, 18, 43

Krych, A.J., 44
 Kulkarni, R., 53
 Kusnezov, N., 23, 24
 Kutlu, C., 11, 23, 50
 Kwak, D.S., 70

L

Lai, Z.L., 69
 La Torre, G., 69
 Laulan, J., 23, 24
 Lecomte, F., 11, 15, 49
 Ledermann, H.P., 5, 23, 62
 Lee, T.Q., 9
 Lektrakul, N., 5, 44
 Leleup, G., 63
 Levin, D., 47
 Lewis, V.O., 36
 Li, A.E., 53
 Liang, B.S., 50
 Lill, S.R., 31, 47
 Lin, Q., 69
 Liotta, G., 5, 34
 Li, S., 70
 Liu, C.H., 69
 Liu, H.F., 70
 Li, Y.P., 50
 Loukas, M., 63
 Lui, T.H., 5, 45

M

Madani, A., 13, 14, 24, 25, 53, 55
 Maffulli, N., 5, 23, 62
 Mahan, M.A., 70
 Maharaj, M.M., 50
 Mallisee, T.A., 3, 10, 23
 Ma, Q., 70
 Martin, A., 23, 24
 Martini, A.K., 23, 24
 Martinoli, C., 5, 11, 13, 14, 17, 19, 23, 24, 33, 34, 35, 36,
 41, 45, 50, 53, 61, 63, 66, 68, 69
 Matsuura, T., 1, 10
 Mayerson, J.L., 36
 Mazzocca, A.D., 41
 McCauley, T., 31
 McNealy, S., 20, 47, 53
 McShane, J.M., 47, 56
 Mehlhoff, T.L., 3, 10
 Merlet, M.C., 63
 Michaud, J., 11, 17, 19, 41, 61
 Michelin, P., 63
 Micu, M.C., 1, 3, 10, 31, 41, 47, 53
 Miguel-Pérez, M., 11, 17, 41
 Milam, G.S., 3, 10
 Miletic, B., 11, 15, 49
 Miller, T.T., 47

Mirovski, Y., 5, 13, 62
 Mobbs, R.J., 50
 Mohammed, K., 44
 Mokhtee, D.B., 70
 Morag, Y., 5, 13
 Morandi, X., 49
 Moriggl, B., 11, 18, 20, 31, 43, 47, 53
 Morrey, B.F., 17, 41, 56
 Morris, C.D., 36
 Morris, H.J., 24, 53
 Morrison, W.B., 5, 23, 62
 Mruthyunjaya, P., 5, 62
 Muhle, C., 5, 44
 Mulligan, S.A., 56
 Murugappan, K.S., 44
 Musahl, V., 3

N

Natera Cisneros, L., 50
 Nazarian, L.N., 1, 3, 10, 17, 31, 33, 41, 47, 49, 53, 56, 61
 Negro, P., 11, 17, 19, 44
 Nestorova, R., 1, 3, 10, 31, 41, 47, 53
 Nichols, A.W., 31
 Nishida, Y., 44
 Nordander, C., 53
 Nucci, P., 61

O

Ohlsson, K., 53
 O’Kane, P.L., 47, 56
 Olecranon bursitis, J., 5, 23
 Orr, J., 23, 24
 Osei, D.A., 48
 Oskouian, R.J., 63
 Otsuka, T., 3
 Ould-Slimane, M., 63
 Ozan, H., 13, 23
 Ozturk, A., 11, 23, 50

P

Padua, L., 5, 34, 50, 69
 Padua, R., 69
 Pagani, C., 14, 34, 45
 Paletta, G.A. Jr., 56
 Palmieri, F., 61
 Palumbo, A., 5, 23, 62
 Pamminger, M., 20, 47, 53
 Pamminger, M.J., 31
 Pan, X.H., 5, 45
 Parker, L., 47
 Park, K.W., 48
 Pastore, D., 13, 23, 24, 61
 Patel, A., 48
 Patel, J., 5, 62
 Patel, K.I., 36
 Pazzaglia, C., 5, 34, 50
 Pérez-Bellmunt, A., 11, 17, 41

Perez, M.M., 11, 17, 19, 61
 Perkins, R., 34
 Petranova, T., 1, 3, 10, 31, 41, 47, 53
 Pfirrmann, C.W., 5, 14, 17, 19, 45
 Phan, K., 50
 Porta, F., 1, 3, 10, 31, 41, 47, 53
 Pracros, J.P., 36
 Preissler, P., 23, 24
 Propeck, T., 56
 Pryde, D., 20, 47, 53
 Pugliese, F., 13, 17, 23, 24, 33, 35, 45, 53, 66, 69

Q

Queenan, J.F., 44

R

Rabarin, F., 23, 24
 Rabiner, J.E., 36, 56
 Radunovic, G., 1, 3, 10, 31, 41, 47, 53
 Ramani, M.N., 24, 54
 Reichel, L.M., 3, 10
 Reilly, D., 5, 23, 62
 Resnick, D., 13, 23, 24, 61
 Resnick, D.L., 5, 11, 17, 19, 44
 Ricard, A., 36
 Riffaud, L., 49
 Riley, G.M., 1, 63
 Robotti, G., 37, 48, 53
 Rodeo, S.A., 44
 Rodriguez Miralles, J., 50
 Rotondo, A., 5, 62
 Ruangchaijatuporn, T., 5, 13
 Rubin, S., 23, 24
 Rupakumar, C.S., 5, 62

S

Safran, M.R., 53
 Sairyo, K., 1, 10
 Sanal, H.T., 11, 17, 19, 44
 Sardi, J.P., 63
 Sattari, A., 13, 14, 24, 25, 53, 55
 Saupe, N., 5, 14, 17, 19, 45
 Savoie, F.H., 17, 41
 Scarabin, J.M., 49
 Scharschmidt, T., 36
 Scheglmann, K., 23, 24
 Scheonberger, T.J., 44
 Schmidt, C.C., 17, 41
 Schwab, G.H., 56
 Schwartz, M.L., 56
 Schwerdtfeger, K., 23, 24
 Scudeller, L., 33, 56
 Sheehan, S.E., 36
 Shell, D., 34
 Shuttlewood, K., 23, 24, 69
 Sileo, C., 5, 14, 34, 44
 Simon, N., 50

Sitton, S.E., 3, 10
Sit, Y.K., 5, 45
Skaf, A.Y., 5, 44
Smidt, N., 48
Smith, C.D., 23, 24, 69
Sodickson, A.D., 36
Sotereanos, D.G., 17, 41, 48
Spinner, M., 13, 23
Steinbach, L.S., 1, 63
Steinmann, S.P., 17, 41
Stevens, M.A., 31
Stofferin, H., 11, 18, 43
Stoller, D.W., 53
Stroyan, M., 23
Sugimoto, K., 3
Sugiura, K., 1, 10
Suzue, N., 1, 10
Sztankay, J., 20, 31, 47, 53

T

Tagliafico, A., 11, 17, 19, 41, 61
Tagliafico, A.S., 13, 17, 19, 41, 50, 53, 61, 68
Takenaga, T., 3
Taljanovic, M.S., 20, 31, 47, 53
Taskara, N., 11, 23, 50
Tatar, I., 13, 23
Teefey, S.A., 56
Thornton, R., 1, 63
Tran, N., 1, 62
Trudell, D.J., 5, 11, 13, 17, 19, 23, 24, 44, 61
Tsuchiya, A., 3
Tsukushi, S., 44
Tsung, J.W., 36, 56
Tsutsui, T., 1, 10
Tubbs, R.S., 63
Tullos, H.S., 56

U

Urciuoli, L., 1, 5, 33, 56, 62

V

Vaishya, R., 50
Valle, M., 23, 24, 35, 66, 69
Van den Berghe, G.R., 44
Van der Windt, D.A., 48
Van Holsbeeck, M.T., 53

Vannet, N., 53
Varitimidis, S.E., 48
Vega, J., 9
Vijay, V., 50
Vlad, V., 1, 3, 10, 31, 41, 47, 53
Voloshin, I., 17, 41

W

Wada, K., 1, 10
Walz, D.M., 1, 3, 10, 17, 31, 33, 41, 47,
49, 53, 61
Wang, H.L., 69
Wang, J., 70
Wangwinyuvirat, M., 13, 23, 24, 61
Ward, S.I., 56
Warren, R.F., 44
Wasserstein, D., 44
Wavreille, G., 11, 15, 49
Weissengruber, G.E., 3
Wessels, K.D., 23, 24
Westkaemper, J.G., 48
White, L., 44
Wilk, K.E., 23
Wilson, T.J., 63
Winblad, J.B., 44
Wolf, J.M., 48
Won, H.S., 70
Woods, G.W., 56
Wu, S.Q., 69
Wu, Z.Q., 69

Y

Yablon, C.M., 5, 13
Yang, L., 63
Yang, M., 70
Yang, X., 70
Yoshida, M., 3

Z

Zacchino, M., 61
Zamorani, M.P., 35
Zanetti, M., 5, 14, 17, 19, 45
Zhang, D.F., 50
Zhang, W., 70
Zhong, W., 70
Zhuang, Z.Y., 69